EXPERIMENTAL STUDY AND OPTIMIZATION OF WELDING PARAMETERS OF V GROOVE JOINTS ON AISI4130 MATERIAL USING SHIELDED ARC WELDING

KORME YADETO ROBA

A Thesis Submitted to the Department of Mechanical Engineering

School of Mechanical, Chemical, and Materials Engineering

Presented in Partial Fulfillment of the Requirement for the Degree of Master's
in Manufacturing Engineering

Office of Graduate Studies
Adama Science and Technology University

January, 2026
Adama, Ethiopia

EXPERIMENTAL STUDY AND OPTIMIZATION OF WELDING PARAMETERS OF V GROOVE JOINTS ON AISI4130 MATERIAL USING SHIELDED ARC WELDING

Korme Yadeto Roba

Advisor: **Dr.Moera Gutu Jiru (Associate Professor)**

A Thesis Submitted to the Department of Mechanical Engineering
School of Mechanical, Chemical, and Materials Engineering

Presented in Partial Fulfilment of the Requirement for the Degree of Master's in Manufacturing Engineering

Office of Graduate Studies
Adama Science and Technology University

January, 2026
Adama, Ethiopia

DECLARATION

I hereby declare that this Master Thesis entitled "**Experimental Study and Optimization of Welding Parameters of V Groove Joints on AISI4130 Material Using Shielded Arc Welding**" is my original work. That is, it has not been submitted for the award of any academic degree, diploma or certificate in any other university. All sources of materials that are used for this thesis have been duly acknowledged through citation.

KormeYadeto Roba	______________	___________
Name of the students	Signature	Date

RECOMMENDATION

I, the major advisor of this thesis, hereby certify that I have read the revised version of the thesis entitled **"Experimental Study and Optimization of Welding Parameters of V Groove Joints on AISI4130 Material Using Shielded Arc Welding"** prepared under my guidance by **Korme Yadeto Roba** Submitted in partial fulfilment of the requirements for the degree of Mater's of Science in Manufacturing Engineering.

Therefore, I recommend the submission of revised version of the thesis to the department following the applicable procedures.

____________________	____________________	____________________
Major Advisor	Signature	Date

APPROVAL SHEET

I, the advisors of the thesis entitled **"Experimental Study and Optimization of Welding Parameters of V Groove Joints on AISI4130 Material Using Shielded Arc Welding"** and developed by **Korme Yadeto Roba** hereby certify that the recommendation and suggestions made by the board of examiners are appropriately incorporated into the final version of the thesis.

______________________	______________________	______________________
Major Advisor	Signature	Date

We, the undersigned, members of the Board of Examiners of the thesis by **Korma Yadate**have read and evaluated the thesis entitled **"Experimental Study and Optimization of Welding Parameters of V Groove Joints on AISI4130 Material Using Shielded Arc Welding"** and examined the candidate during open defense. This is, therefore, to certify that the thesis is accepted for partial fulfillment of the requirement of the degree of Master of Science in Manufacturing Engineering.

______________________	______________________	______________________
Chairperson	Signature	Date
______________________	______________________	__________
Internal Examiner	Signature	Date
______________________	______________________	______________________
External Examiner	Signature	Date

Finally, approval and acceptance of the thesis is contingent upon submission of its final copy to the Office of Postgraduate Studies (OPGS) through the Department Graduate Council (DGC) and School Graduate Committee (SGC)

______________________	______________________	______________________
Department Head	Signature	Date
______________________	______________________	______________________
School Dean	Signature	Date
______________________	______________	______________________
Office of Postgraduate Studies, Dean	Signature	Date

ACKNOWLEDGEMENTS

Above all, I want to thank Almighty God for providing me with the confidence and support I needed to complete this study endeavour. I'd like to gratefully thank my adviser, Dr.Moera Gutu, for her tremendous guidance, inspiration, moral support, and constant assistance during this project. It was an incredible honour and privilege to work and study under your supervision. I am extremely appreciative for everything you've done for me.

Furthermore, I am grateful to Dr.Birhane Assefa, an International Welding Federation-certified International Welding Practitioner and welding instructor, for his constant guidance, recommendations, and assistance during my time at the Centre of Excellence for Welding and Technology Manufacturing.

My one and only wife and children deserve my heartfelt thanks and love for their steadfast understanding and support. Throughout all, you have inspired me, and I have no doubt that you will be my rock for the rest of my life. I also want to thank my parents, sisters, and brothers for their love, prayers, and concern.

Finally, I'd like to thank the Centre of Excellence for Welding and Technology Manufacturing for helping to partially support my research.

CONTENTS

List of Figure

List of Table

LIST OF ABBREVATIONS

AC	Alternative Current
ANN	Artificial Neural Network
ANOVA	Analysis of Variance
BH	Brinell Hardness
BBD	Box-Behnken Design
CE	Carbon Equivalent
CYS	Compressive Yield Strength
DC	Direct Current
DCEN	Direct Current Electrode Negative
DCEP	Direct Current Electrode Positive
DoE	Design of Experiments
DoF	Degree of Freedom
DSS	Duplex Stainless Steel
EBSD	Electron Backscatter Diffraction
FDM	Fused Deposition Modelling
GA	Genetic Algorithms
GMAW	Gas Metal Arc Welding
GRA	Grey Relational Analysis
GTAW	Gas Tungsten Arc Welding
HAZ	Heat-Affected Zone
LFVW	Low-Frequency Vibration-Assisted Welding
MMAW	Manual Metal Arc Welding
PWHT	Post-Weld Heat Treatment
RSM	Response Surface Methodology
RWH	Rockwell Hardness Tests
SEM	Scanning Electron Microscopy
SMAW	Shielded Metal Arc Welding
TIG	Tungsten Inert Gas
UTM	Universal Testing Machine
UTS	Ultimate Tensile Strength
WEDM	Wire Electric Discharge Machining

ABSTRACT

Shielded metal arc welding (SMAW) is widely employed in heavy industries to join materials; however, it frequently ignores delicate connections that impair weld quality. AISI 4130 chromium-molybdenum alloy steel has unique weldability challenges, demanding a rigorous approach to welding parameter optimization with modern technologies. The objective of this study optimizes shielded arc welding parameters for V-groove joints in AISI 4130 alloy steel to maximize ultimate tensile strength (UTS), hardness, bending strength, and compressive strength. It also experimentally validates the predictive capability of Response Surface Methodology (RSM). The study result discovered that welding current is the most critical component in producing robust mechanical characteristics at RSM-optimized parameter values of 200 A, 2.5 mm, and 70°. The study also discovered complicated non-linear interactions, indicating that synergistic parameter combinations are the source of optimum features. Experimental validation showed the mechanical properties boosted capacity, with a 2% average improvement. RSM-optimized settings (200 A, 2.5 mm, 70°) resulted in strong mechanical characteristics (UTS: 1110 MPa, hardness: 112 HRB, compressive strength: 860 MPa, and bending strength: 840 MPa). The models' dependability is demonstrated by their low prediction errors (4.18% for RSM). In this work, the selection of SMAW parameters is moved from empirical approaches to a data-driven science. RSM integration creates a reliable and repeatable foundation for precision manufacturing. With this method, high-integrity AISI 4130 welds with customized, exceptional mechanical qualities that are appropriate for crucial structural applications can be produced. For AISI 4130 steel, welded V-groove joint integrity and durability in critical applications hinge on key mechanical properties—ultimate tensile strength, hardness, bending/compressive strength, and impact toughness—that guide RSM-optimized shielded metal arc welding parameters for ASTM-compliant, base metal-exceeding performance.

Keywords: SMAW; AISI4130; RSM; Parameter, Mechanical Property

CHAPTER ONE

INTRODUCTION

1.1. Background of the Study

Welding is a significant manufacturing procedure for combining joints of ferrous and non-ferrous metals to create complicated shapes. Shielded metal arc welding (SMAW) is a popular and effective technology utilized in a variety of sectors, including household appliances, automotive, and aerospace. SMAW employs a covered electrode to shield the molten weld pool from oxidation and contaminants [Groover,2010; Kumar et al.,2024; Ranjan & Jha, 2024]. The flux coating is critical for stabilizing the arc in SMAW equipment, which comprises the electrode, electrode holder, and power supply. Temperature, power input, travel speed, arc length, and electrode angle all have an impact on material characteristics. The electrode material is required for fusion welding of both comparable and dissimilar metals [Gupta et al.,2023].

The SMAW arc welding process, which creates an electric arc between an electrode and a base material, is commonly employed in educational settings due to its flexibility, inexpensive equipment costs, and minimum operator training [Haider et al.,2019]. Arc welding is a manual procedure that melts base metal surfaces using heat from an electric arc. SMAW creates heat between the workpiece and a flux-coated electrode. This approach is frequently utilized in educational settings because of its versatility, inexpensive equipment costs, and minimal operator training requirements [Baghel,2022].

The SMAW technique for mild steel welding encounters issues such as porosity, cracking, undercutting, and distortion. To address these challenges, meticulous workpiece preparation, electrode selection, and exact welding conditions are necessary [Davim, 2021; Chaturvedi & Vendan, 2022]. The SMAW procedure is widely used for welding iron and steel, aluminium, nickel, and copper alloys with thicknesses ranging from 1.6 mm to infinite, and it necessitates competent welders and small-diameter electrodes [Singh & Grover, 2015; O'Brien, 2007].

The SMAW technique provides flexibility, cost-effectiveness, and high-quality welds for fieldwork and remote sites, making it ideal for novices and tough situations such as overhead or vertical welding [Alkahla and Pervaiz ,2017]. SMAW welding uses V-groove connections to create strong, efficient welds in thicker materials. This design allows the welding electrode to penetrate deeper, and it is commonly used to combine heavy materials. Edge cleaning, electrode selection, and welding condition optimization are all part of the preparation process. The V-groove connection design increases weld strength and quality, and appropriate preparation, alignment, and electrode selection provide consistent welds ideal for a variety of applications [Marshall, 2013; Phillips, 2023].

Electric arc welding is a low-cost and often utilized welding process in the workplace. According to research on ASTM A36 steel, E6013 electrodes at 70 A yield 105 HRB and 34.697 MPa, whereas E7016 electrodes with a V 60° seam angle and 80 A current generate the maximum tensile strength [Rahangmetan et al.,2020]. The previous the study explored key welding factors like welding current, electrode type, root gap, voltage, arc length, and travel speed, which significantly impact weld characteristics. Various optimization methods were explored, including response surface methodology, the Taguchi technique, artificial neural networks, genetic algorithms, scatter search techniques, grey relational analysis, and fuzzy logic, to improve welding efficiency and quality [Lugade& Deshmukh, (2015); Bopaliya, (2016); Linger &Bogale, (2023)].

This thesis aimed to optimize shielded arc welding parameters for V-groove joints in AISI 4130 alloy steel. It focused on enhancing hardness, compressive, tensile, and bending strengths while investigating mechanical properties via Response Surface Methodology (RSM) to determine optimal parameters.

1.2. Statement of the Problem

Welding is crucial in construction and manufacturing, affecting structural integrity, performance and safety. AISI 4130 alloy steel is optimal for high-strength applications, while SMAW creates strong, long-lasting welds for thicker materials, emphasizing the importance of welding techniques and material properties. The SMAW process for welding AISI 4130 alloy steel faces issues like porosity, cracking, undercutting, and undesirable appearance due to gas bubbles, quick cooling, and heat deformation. This analysis suggests utilizing SMAW welding for AISI 4130 alloy steel plate owing to welded joint difficulties that cause leakage and breakage. Weld bead failure is caused by insufficient strength, hardness and ductility.

The mechanical qualities of V-groove joints made with SMAW in AISI 4130 alloy steel are critical due to their simplicity and cost-effectiveness. However, there is insufficient empirical information on how welding settings influence the mechanical behaviour of these junctions. Tensile strength, hardness, ductility, electrode type effects, and joint integrity are all potential challenges. Improving welding parameters is critical for performance enhancement. Porosity and lack of fusion are significant difficulties in organizations, accounting for 70% of faults. Poor welding quality lowers customer happiness, raises expenses, and weakens competitiveness. Improving welding techniques and understanding joint performance can lead to increased safety and dependability.

To address this, the study examines the impact of welding factors on hardness values, tensile strength, and bending strength on AISI 4130 alloy steel plate using response surface methods.

1.3. Objectives

1.3.1. General Objective

The general objective of this research was to experimentally studied and optimized shielded metal arc welding parameters for V-groove joints in AISI 4130 alloy steel, including mechanical testing and RSM-based process optimization.

1.3.2. Specific Objectives

- To prepare the SMAW welding setup and joint design.
- To investigate the mechanical properties (tensile strength, compressive strength, hardness, and bending strength) of V-groove joints in AISI 4130 alloy steel welded using SMAW.
- To analysis the influence of different welding parameters (welding current, electrode diameter, and electrode angle) on the mechanical behaviours of welded joints.
- To optimize shielded metal arc welding parameters using RSM for superior mechanical performance and quality of V-groove joints in AISI 4130 alloy steel.
- To experimentally validate optimal welding process parameters through rigorous investigations.

1.4. Significance of the Study

The thesis underlines the importance of SMAW in making high-quality welds, especially with AISI 4130-grade alloy steel. The work on mechanical testing of V-groove joints in RSM optimization techniqueswith SMAW has important significance for both industry and academics. By refining SMAW settings, the study hopes to improve the strength and dependability of welded joints, which are critical for structural integrity in industries such as construction, automotive, and manufacturing. This results in increased safety, product performance, cost savings, and customer pleasure. The findings were added the empirical data to welding engineering, enhance academic scholar, and direct future research into advanced welding processes.

1.5. Scope of the Study

This investigation of plate welding techniques focused on three SMAW welding parameters, each having three levels and one welding position. According to the selection criteria, the three key attributes had a higher impact on welding quality than the other welding parameters, and the single horizontal welding position was usually utilized on plate. The welding parameters chosen were welding current (150, 175, and 200 amps), electrode diameter (2.5 mm, 3.2 mm, and 4 mm), and welding electrode angle (70^0, 75^0, and 80^0). The following are the thesis scopes: The foundation metal for this optimization process is grade AISI 4130 alloy steel plate with dimensions of length, width, and thickness (L x W x T) of AISI 4130 alloy steel material plate samples of 200mm X 110 mm X 6mm, respectively. The RSM analysis approach is used in this experiment to investigate the optimization process factors and MINITAB 2023 software is used for the analysis and optimization of the parameters. `

1.6. Limitation of the Study

The study focuses on the mechanical properties of AISI 4130 alloy steel materials with horizontal position and butt joint designs. Although the research had achieved its objectives, there were certain inescapable limitations in the company's operations. Because this was an experimental study, each SMAW welding variable had to be evaluated in order to optimize; unfortunately, there was insufficient equipment to investigate every welding variable. The company lacks a high-speed camera, which is essential for investigating and inspecting welding defects traveling speed and determining arc length.

1.7. Organization of the Study

The thesis is organized into five sections. The first chapter introduction discusses the background of the study, the problem of the statements, the objectives of the study, the scope of the study, the limitations, and the significance of the study. The next chapter is a review of the literature, which covers quality control tools, the purpose and consequences of each SMAW welding parameter, welding techniques, welding processes, welding shapes, optimization tools and their applications, and welding parameter analysis tools. The third chapter discusses research procedures such as design of experiment (DOE), data validation strategies, and data collection methods. The third chapter addresses the data collection strategy, research design, data analysis procedure, and data analysis tools. The fourth chapter summarizes the outcomes of the investigation as well as the experimental analysis and interpretation of the DOE data. The proposed remedy and its outcome after execution are also offered based on the results obtained. Finally, the conclusion and recommendations were done in the fifth chapter.

CHAPTER TWO

LITERATURE REVIEW

2.1. Introduction

This chapter focuses on optimizing SMAW welding method variables on AISI 4130 alloy steel, focusing on weld bead form, mechanical features, process parameters, RSM technique, and mathematical modelling, using research to inspire and emulate previous findings.

2.2 Classification of welding types

Welding processes are classified according to their procedures and applications. Arc welding, which creates heat by using an electric arc, comes in a variety of forms, including Shielded Metal Arc Welding (SMAW), Gas Metal Arc Welding (GMAW), Gas Tungsten Arc Welding (GTAW), and Submerged Arc Welding. Gas welding, notably using oxy-acetylene, is a portable method of cutting thin metal. Resistance welding, a technique used in automotive assembly, creates heat via electrical resistance. Solid-state welding is appropriate for aeronautical parts. Laser welding uses focused beams to ensure precision, whereas electron beam welding employs high-energy electrons in a vacuum [Srinivasan et al.,2006]. Figure 2.1 Shown as the classifications of welding types. Table 2.1 display overview of principal benefits and application development

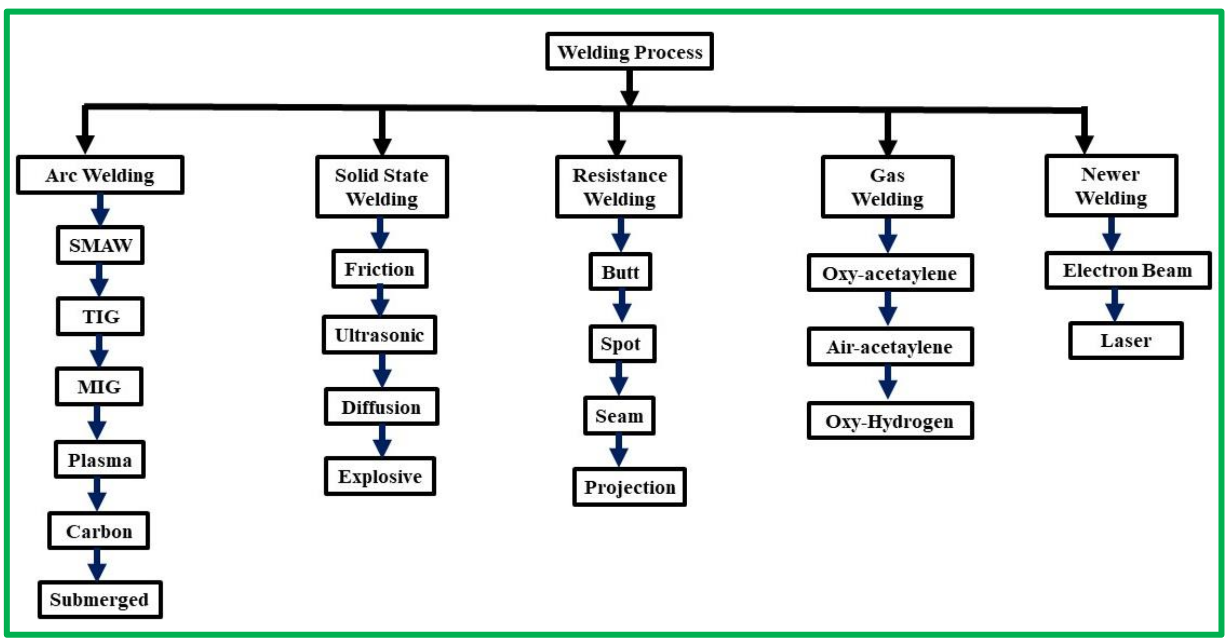

Figure 2.1 Classifications of welding types [Sunny and Muhammed,2023]

Table 2.2 Overview of principal benefits and application development [Lippold,2014]

S. N	Welding Process	Advantages	Typical Applications
1	Arc Welding	Efficient within several positions, portable, Versatile,	Automotive, maintenance, construction
2	Gas Welding	Versatile, portable and Simple	thin section material welding, brazing and cutting
3	Resistance Welding	Appropriate for mass Fabrication/production, efficient and Fast	Automotive, electronics, appliances
4	Solid-State Welding	Minimum distortion, Robust joints,	delicate assemblies, automotive and Aerospace
5	Laser Welding	Smaller heat input, High precision welding	Fine metalwork, medical devices and Aerospace

2.3. Shielded Metal Arc Welding (SMAW)

Shielded Metal Arc Welding (SMAW), also known as Manual Metal Arc Welding (MMAW) or stick welding, is a manual arc welding procedure that employs a consumable electrode coated with flux. An electric current generates an arc between the electrode and the workpieces, forcing them to melt and form a molten metal pool. This method reduces contamination and increases weld quality, making it widely employed in a variety of applications [Hariprasath et al.,2022].

SMAW is a flexible and straightforward welding technology utilized in maintenance and repair applications. It dissolves the electrode's flux coating, producing fumes that serve as a shielding gas and generating a protective slag layer. Despite its popularity, SMAW is still commonly employed in construction, notably for welding iron and steel, especially stainless steel, although it can also weld other alloys (Gowthaman et al.,2017; Baghel,2022; C. Arun, 2017).

2.4. Effects SMAW Welding Input Process Parameter

The welding properties of ferrous and nonferrous metals are governed by parameters such as amperage, flux, voltage, linear speed, and electrode size, all of which impact heat flow and solidification rate. Critical factors such as preheating, postheating, polarity, and interpass temperature all have an impact on these properties [Baghel,2022].

2.4.1 Welding Current

The welding current is an important element in the arc welding process, influencing things like electrode burn-off rate, depth of fusion, and weld shape. Shielded Metal Arc Welding (SMAW) employs direct current on the electrode negative to improve weld penetration and travel speed. Polarity selection influences heat distribution, with stronger currents facilitating material deposition but potentially generating spatter and overheating. Maintaining a constant arc current is critical for consistent performance, but voltage fluctuations might jeopardize stability. Effective welding current regulation is essential for delivering high-quality welds [Kah et al.,2014; Sumardiyanto& Susilowati, 2019].

Welding current is the electrical current used to generate an arc during welding, which is essential for heating and melting materials. It controls heat intake; greater currents generate more heat. A proper current level results in a homogenous weld structure. AC is often used for welding aluminium and magnesium, with currents of 150, 160, and 170 amps.
[Yu & Kim,2018].

2.4.2. Voltage

Arc voltage is critical in defining welding arc length, which impacts heating and melting processes. As the arc length rises, heat output reduces owing to more interaction with the environment, resulting in greater heat dissipation and cooler temperatures. A continuous welding current provides weld penetration without affecting heat input, allowing welders to alter parameters to achieve the appropriate weld quality while preserving penetration [Pauna et al.,2020].

2.4.3. Electrode Diameter

The electrode diameter is important in welding because it affects heat transfer and melting. A well-matched diameter promotes effective heat transmission, preventing weak welds and incomplete fusion. A small diameter can result in weak welds, whereas a big diameter can induce burn-through or distortion. Proper electrode size also enhances weld pool management, resulting in a more uniform and visually pleasing bead. Matching the electrode diameter to the gap is critical for achieving strong, high-quality welds while enhancing welding efficiency [Welding 1991; Phillips, 2023].

2.4.4. Polarity

Polarity is important in welding because it controls heat distribution between the electrode and the workpiece. There are two possible configurations: direct current electrode positive (DCEP) and direct current electrode negative (DCEN). DCEP focuses greater heat on the electrode, resulting in wear and inefficient melting of base materials. DCEN transfers 70% of the heat to the workpiece, boosting penetration while lowering the danger of burning the electrode. This quick heat transmission preserves the electrode's integrity while improving welding performance [Chaturvedi, 2022].

2.4.5. Welding Traveling Speed

Welding speed has a substantial influence on bead shape and microstructure. Higher speeds reduce heat input, resulting in inadequate penetration, whereas slower speeds allow grains to absorb more heat, resulting in nonuniform columnar forms [Kumar et al.,2024].

2.4.6. Groove Angle

The groove angle has a considerable impact on the quality and strength of the weld connection. A greater angle creates a bigger molten weld pool, which improves metal mixing and homogeneity. This also leads to a more controlled cooling rate during solidification, resulting in increased mechanical properties like as toughness and strength. A well-designed groove angle ensures complete metal penetration into the foundation materials, which improves joint integrity [Messler, 2019].

2.4.7. Electrode Angle

The electrode angle during welding has a considerable influence on the quality and efficacy of the resulting weld. It enables greater heat accumulation, faster melting of filler and base materials, and homogenous mixing of molten material. Controlling the electrode angle improves cooling rates during solidification, leading in better microstructure and mechanical properties. Adjusting the angle improves the weld connection's strength and longevity.
[Nath et al.,2022].

2.5. Influence of Welding Parameters on Macrostructure and Mechanical Properties

Tahir et al., (2018) investigated the mechanical characteristics of mild steel AISI 1020 and discovered that increasing heat input enhanced tensile strength and hardness when utilizing electrodes E7018 and E7016.

Shukla et al., (2018) discovered that the form and size of the weld bead greatly influence the mechanical characteristics of stainless steel 1020 plates. Higher currents resulted in larger heat-affected zones and worse performance. The ideal welding parameters for maximal penetration were DCEN polarity, 90° electrode angle, and 120 A current.

Sumardiyanto and Susilowati, (2019) discovered that welding current and electrode composition have a substantial impact on the mechanical properties of mild steel API 5L, whereas heat utilization affects weld characteristics.

Chowda et al., (2018) demonstrated that the ideal hardness for shielded metal arc welding may be attained under certain voltage and current conditions.

Patel et al., (2017) discovered that the Taguchi optimization technique was effective in regulating aspects such as penetration size, weld bead reinforcement, and reinforcement form factor on mechanical properties.

Jadoun et al., (2016) discovered that plate thickness and electrode diameter had a substantial impact on mechanical properties, with higher values producing better results, emphasizing the importance of material thickness.

Thakur and Chapgaon, (2017) observed that electrode diameter, current, and voltage have a substantial impact on the characteristics of duplex stainless steel as a workpiece material.

Mohammed et al., (2013) discovered that inter-pass temperature has a substantial influence on resistance to indentation and scratches in the weld fusion zone and heat-affected zone, although gas flow rate modifications had a minor impact.

Munawar, (2018) observed that the centre of the weld frequently had greater properties than the HAZ, which lowered hardness and tensile strength, resulting in a brittle structure.

Yadav et al., (2020) discovered that, while appropriate heat input can increase certain mechanical properties, it does not uniformly improve other characteristics, implying that welding parameters' effects on material attributes are complicated and multifarious.

Khamari et al., (2019) discovered that decreasing welding current, voltage, and speed minimizes warpage and deformation in structural steels, resulting in a smaller heat-affected zone (HAZ).

Chiong et al., (2019) discovered that welding current enhances hardness, microhardness, and impact toughness in mild steel, resulting in less deformation and a narrower HAZ. A refined grain structure, which includes ferrites and pearlite, improves properties. Welding conditions also influence the weld structure, which improves tensile and hardness properties. Reduced amperage and travel speed result in smaller HAZ widths and finer grains.

Baghel, (2020) research shows that arc welding process parameters influence the mechanical characteristics and microstructure of stainless steel. Increased heat induces microstructural deformation, whereas faster transit rates reduce heat, increase finer grain formation, and improve mechanical properties.

Dadi et al., (2018) discovered that SMAW parameters such as amperage, root width, and plate thickness had a substantial influence on mechanical properties, with finer grain sizes improving features.

Bodude and Momohjimoh, (2015) underlined the importance of grain size in mechanical performance, claiming that finer grains produce greater mechanical properties.

Mohammed et al., (2015) and Haider et al., (2019) discovered that heat input has a substantial influence on the microstructure and mechanical characteristics of mild steel. Increased heat input results in a wider heat-affected zone, but lower amperage reduces heat flow characteristics while increasing micro hardness and strength.

Sharma et al., (2014) discovered that magnetic and electrostatic fields influence the weld joint properties of AZ31B magnesium alloy, boosting reinforcement width while decreasing the penetration size factor.

Sidhu and Chatha,(2012) observed that E6013 electrodes provide excellent surface polish, smooth deposits, and resistance to corrosion and surface pollutants.

Niik and Reddy, (2016) discovered that electrode material had no effect on welding angular distortion, with duplex stainless steel producing less distortion during horizontal welding.

Bob and Gattani,(2013) study discovered that amperage had a substantial influence on weld bead geometry in mild steel, with higher amperage resulting in increased heat flow and heat-affected zone width.

Gupta et al., (2018) study on arc welding under electrostatic and magnetic fields discovered that raising the amperage causes changes in weld geometry parameters, such as increased transverse size and penetration size factor.

Nagesh and Datta, (2002) discovered that the most important parameters are arc length and travel speed, with arc length being directly proportional to bead size and inversely proportional to weld bead reinforcement height.

Kamra et al., (2015) discovered that combining E6010 and E6010 resulted in a finer grain microstructure, whereas Zoafakar and Hasan (2017) discovered that carbon content and chamfering angle had a substantial impact on tensile strength and ductility.

Ravikumar and Vijian, (2014) used Taguchi-based gray relational analysis to enhance weld quality in the SMAW process using low-carbon steel plates, identifying welding current and speed as critical variables.

Mohammed et al., (2015) discovered that the position and size of an electrode greatly affect weld quality, resulting in a finer grain microstructure.

Ali et al., (2014) used an artificial neural network to study how process factors such as temperature and cryo-treatment affect the mechanical and microstructural characteristics of low-carbon steel plates.

Hamaschi et al., (2015) investigated X70 HSLA steel in shielded metal arc welding with E6010 electrodes, identifying the formation of fine pearlite and alternating layers of ferrite in lamellar pearlite.

Gupta et al., (2018) investigated the effects of process variables on the metallurgical, microstructural, and morphological aspects of duplex stainless steel employing electrode E2595. The results showed that both low and high heat flow characteristics resulted in smaller HAZ widths.

Ranjan, (2014) used a factorial design approach to improve SMAW processes, concentrating on amperage, linear speed, and voltage.

Kumar and Vijayakumar, (2012) used Taguchi optimization on SMAW welded pipes to produce leak-free connections.

Sheikh and Kamble, (2018) employed the Taguchi L9 orthogonal array to increase welding outputs for ASTM A36 mild steel, eliminating defects caused by the molten weld pool.

Singh, (2014) study found that lowering heat input boosted cooling rates, leading in a finer grain structure and better mechanical characteristics.

Khamari et al., (2019) found that welding circumstances have a substantial influence on the mechanical and metallurgical characteristics of Ni steel welded connections.

Kumar et al., (2022) observed that various electrodes had a substantial influence on tensile strength and microhardness in high-Armor steel joints, with certain electrodes demonstrating greater strength and toughness.

Singh, (2019) observed that mechanical vibration during welding improves the characteristics of mild steel joints by churning the molten metal.

Talabi et al., (2014) discovered that increasing heat input in low carbon steel welding results in enhanced hardness but also brittleness, needing post-weld heat treatment.

Asibeluo and Emifoniye, (2015) discovered that greater amperage SMAW welding current on A36 carbon steel increased weld temperature, resulting in decreased toughness and hardness.

Rohit and Jha, (2014) discovered that 120 A amperage improves tensile strength in mild steel joints by restricting grain growth and generating a refined microstructure.

According to Bang et al., (2015), increasing heat input enhances impact toughness in low carbon steel welds but decreasing tensile strength due to coarse grain structures.

2.6. Process for SMAW Welding Output Response Optimization

SMAW is a manual welding method that employs a consumable electrode covered with flux to provide a protective gas shield. It includes characteristics such as welding current, arc length, travel speed, and electrode type. Optimisation entails experimentation, data collecting, and statistical techniques. Response Surface Methodology, Taguchi, Artificial Neural Networks, Genetic Algorithms, and Machine Learning are used to find the best settings. Validating changes, developing standard operating procedures, and providing continuing training are critical to success. The technique employs Grey Relation Analysis, Response Surface Methodology, the Taguchi Method, Artificial Neural Networks, and Genetic Algorithms to optimize SMAW process parameters for maximum UTS, bending strength, hardness, wear strength, corrosion resistance, and compressive strength [Gonfa et al. (2022); Kavimani et al. (2020)] confirmed the efficacy of these approaches.

2.6.1. Ultimate Tensile Strength

Addamani et al. (2018) discovered that appropriate welding circumstances have a substantial impact on the ultimate tensile strength (UTS) and hardness of steel pipes. They discovered that the ideal settings for maximal UTS were 65 amps current, 14 LPM gas flow, and 110 mm/min wire feed rate, whereas the optimal settings for maximum hardness were 60 amps current, 12 LPM gas flow, and 120 mm/min wire feed rate. Gas flow rate was discovered to be the second most critical factor influencing UTS and hardness.

According to Ranjan and Jha, (2024), research on low-frequency vibration-assisted welding (LFVW) demonstrates that using vibrations during the Shielded Metal Arc Welding (SMAW) process greatly enhances the mechanical properties of welded parts. Ideal parameters include a current of 135 amps, a vibration frequency of 250 Hz, and a duration of 30 seconds. The mechanical properties of vibrated mild steel plates differ from those of traditionally welded ones, with frequency having the greatest influence. Under ideal conditions, LFVW may reach a hardness of 123.99 VHN and a UTS of 605.16 MPa, minimizing the requirement for post-weld heat treatment.

Sharma et al., (2019) investigated the effect of an additional electromagnetic field on the weld quality of magnesium alloy AZ31B, with a focus on tensile strength. They discovered that increasing the external magnetic field dramatically lowers yield strength, with an ideal yield strength of 138 MPa at 120 Gauss. The micro-hardness of the weld zone varies with yield strength, reaching 98 to 100 HV compared to 70 HV for the base metal.

Patil and Kadam, (2021) investigated how welding current, speed, electrode angle, and root gap affected performance parameters such as welding strength, metal deposition rate, and microstructure in stainless steel 304 and mild steel 1018. The best welding settings were 85 A current, 8 mm/sec speed, 30° electrode angle, and 0.75 mm root gap. This resulted in a welding strength of 403 N/mm² and a metal deposition rate of 9.3 grams.

Esabunor et al., (2025) investigated the mechanical characteristics of welded mild steel SAE10XX joints using Shielded Metal Arc Welding (SMAW). To investigate welding speed, welding current, and arc voltage, they applied the Central Composite Design of Response Surface Methodology (RSM). A quadratic model best fit the experimental data, yielding optimum values for 165.628 BHN for hardness, 551.090 N/mm² for tensile strength, and 0.90 J/mm² for impact strength at a current of 103.396 A, a speed of 246.019 mm/min, and a voltage of 221.696. The resultant weldment has great tensile strength, hardness, and impact resistance, making it ideal for robustness and resilience applications.

Pratiwi et al., (2023) employed a grey-based Taguchi technique to improve shielded metal arc welding (SMAW) parameters for SS316 and ASTM A36. They investigated various welding elements using a L9 orthogonal array, and the optimal conditions were an E309 electrode, 100 A welding current, 14 V arc voltage, and 4 cm/min welding speed, which resulted in a 23.0% performance boost and 272 HBW hardness, 408.91 MPa tensile strength, and 684.96 MPa flexural strength.

Abima et al., (2022) enhanced TIG-MIG hybrid welding for AISI 1008 mild steel joints by employing gray relational system theory and the Taguchi approach. The gas flow rate had a considerable influence on answers, accounting for 39.77% of the total. The optimization enhanced the Gray relational grade by 0.0489, and response surface plots revealed the interaction effects of process parameters. The investigation obtained a UTS of 872.27 MPa and a yield strength of 688 MPa.

Pathak et al., (2020) investigated the SMAW process, which is a low-cost way of welding low-carbon steel plates. They discovered that increasing the welding current from 95 to 125 A while keeping the electrode angles between 650 and 850 improved weld strength. Tensile strength was higher with direct current electrode negative (DCEN) compared to DCEP. Tensile strength rose from 514 MPa to 529 MPa as electrode angles were changed, and from 540 MPa to 588 MPa as current increased.

2.6.2 Hardness Strength

Sada, (2018) utilized the Response Surface Methodology to optimize weld strength parameters in gas tungsten arc welding 10mm thick mild steel plate. The model's performance was validated by analysis of variance, which revealed that welding current and gas flow rate considerably impact tensile strength, whereas gas flow rate and filler rod diameter significantly influence hardness. The best circumstances were 170.12 amps, 19.84 volts, 23.92 l/min, and 2.4 mm filler rod diameter, yielding 497.555 N/mm^2 and 192.556 BHN.

Ranjan et al., (2024) investigated the application of vibration-assisted welding for producing high-quality welds with outstanding mechanical properties. Using the Taguchi Methodology, they employed low-frequency vibration while shielded metal arc welding 5mm thick mild steel plates. Microstructural examinations found that the optimum hardness performance was attained with a modest heat input of 80 Amps, a 100 Hz vibration frequency, and a 100-second period, resulting in a maximum hardness of 97.1643 RHN, indicating that vibration frequency is the most significant factor influencing hardness.

Assefa et al., (2022) improved parameters in tungsten inert gas (TIG) welding of dissimilar steels, achieving a tensile strength of 502 MPa, with welding current being important. The ideal combination of parameters, which included 110A welding current, 10 L/min gas flow rate, 2.5 mm root spacing, and ER-309L filler wire, resulted in a minimum weld width of 6.21 mm, a maximum hardness of 90 HRB, and a flexural strength of 692 MPa. This modification improved the composite's overall strength and attractiveness.

According to Pagare et al., (2020), these welding parameters, such as welding filler, current, and electrode diameter, all have a substantial effect on the tensile strength and hardness of welded metal. Increased electrode diameter enhances deposition; however, low current levels diminish weld strength. The ideal parameters for maximal tensile strength in Shielded Metal Arc Welding (SMAW) are 110A current, E7016 filler, and 3.15mm electrode diameter. Hardness investigations reveal a significant relationship between tensile strength and weld hardness, with the fusion zone reaching 92 HRB, requiring low hydrogen-coated compositions for optimal welding quality.

2.6.3. Bending Strength

Pratiwi et al. (2023) used a grey-based Taguchi approach to optimize SMAW operating parameters between SS316 and ASTM A36, resulting in a 23.0% performance increase and enhanced mechanical properties such as 275 HBN hardness, 410MPa ultimate tensile strength, and 700MPa bending strength.

Van Huong et al. (2024) investigated the effects of welding parameters on MIG welding in SUS 304 stainless steel and S20C steel. They discovered that both base metals had ferrite, pearlite, and austenite phases, whereas the weld bead zone contained martensite and bainite microstructures. The best tensile strength was attained with a 15 V welding voltage, 500 mm/min speed, 12 mm stick-out, and 110 A current, resulting in a UTS of 469.4 MPa. The ideal settings for flexural strength were comparable, resulting in a phenomenal strength of 1937.45 MPa.

Matin et al. (2024) found that while the base metal remained largely unchanged, larger current fluctuations during the welding process significantly affected the microstructure of the weld metal and heat-affected zone (HAZ). These variations also affect the weld zone's macrostructure, which improves its mechanical qualities. With increasing current, the tensile strength reaches 596.66 MPa (115, 100, 70A), 633.84 MPa (130, 120, 70A), and 715.40 MPa (130, 125, 70A). Bending strength also increases, reaching 1289.01 MPa for (115, 100, 70A), 1293.01 MPa for (130, 120, 70A), and 1417.93 MPa for (130, 125, 70A).

Yodianto's 2023 study looked into the effects of current strength variations and groove types on defects and bending strength in ASTM A36 steel butt joints. The study discovered flaws such as splatter and undercut, with the specific faults altering with current strength. At 90 A, the single V and double V grooves had the maximum bending strength (1069.44 MPa).

Baghel (2022) explains the adaptability of SMAW, a low-cost, portable, and durable welding method for both ferrous and non-ferrous metals. The review investigates its viability for copper-stainless steel, as well as the economic and environmental ramifications and appropriate electrodes. SMAW has bending strengths of up to 2150 MPa, exhibiting its adaptability across metal kinds.

Laschke (2012) investigated improving tungsten inert gas (TIG) welding process settings to improve the hardness and bending strength of butt joints. MINITAB software was employed in the investigation, as was the Taguchi approach and Grey relational analysis. The results indicated that welding current has a substantial influence on hardness and bending strength. TIG welding is suited for joining reactive materials and may be used to a variety of metals. Bending strength was tested with a three-point bend fixture.

2.7. Heat Affected Zone

Widyianto et al., (2021) discovered that orbital pipe welding, a popular approach for piping systems, presents issues owing to torch location. A research of SS 316L square butt joints found maximal distortions at 120 A with four sequences, resulting in a 51% drop in ultimate tensile strength and microhardness values. The heat-affected zone was austenite with big grains, and the microstructure varied among sequences.

Baghel, (2022) discovered that the heat-affected zone (HAZ) on the copper side softens, resulting in increased structural heterogeneity. Kar et al. (2016) discovered that putting copper filler in joints increases homogeneity, resulting in a more uniform copper structure. The study also looked at beam movement in radial and circular patterns on ferrous and non-ferrous joints, and discovered that beam oscillation with a constant diameter enhances impact strength and percentage elongation by churning the molten metal and increasing copper mixing in stainless steel.

According to Arora et al., (2018), heat input during welding thermal cycles has a considerable influence on the parent material's microstructure, resulting in fusion and heat-affected zones. Post-welding microstructural features such as austenite grains, bainite, and martensite phases reduce HAZ toughness, particularly at low temperatures. The polarity of the electrode influences penetration depth and microstructural changes. The fusion zone is divided into two phases: hard and soft. Lower welding currents promote martensite and bainite formation, while higher currents produce softer ferrites and pearlite.

Sim et al., (2022) investigated the microstructures of as-welded duplex stainless steel (DSS) samples and discovered two-phase structures. Austenite was more readily formed after post-weld heat treatment (PWHT) than ferrite. Solution annealing at 1050°C produced many intra-granular austenite grains and a considerable reduction in ferrite. The dilution of the DSS weld overlay was 32.87% for as-welded samples, with slight variations following PWHT. Solid solution annealing produced low hardness values and big granules.

2.8. Influence of welding parameters on HAZ properties

Weld metal microstructure necessitates careful consideration of welding settings since numerous variables, such as base metal, filler metal, flux, and cooling rate, all have an influence on the joint's microstructure. Heat input, alloy chemistry, and weld pool form are all important elements in determining cooling rate, which impacts the microstructure and mechanical properties of the weld joint. Adjusting these factors is critical for achieving the desired weld characteristics [Omale, 2016].

2.8.1. Effect of heat input on HAZ

The study demonstrates that numerous elements impact the microstructure of weld metal, including the chemical composition of the base metal, filler metal, flux, and weldment cooling rate. These parameters, together with heat input, alloy chemistry, and weld pool shape, influence the microstructure and mechanical properties of the weld joint, making adjustments critical for obtaining the required weld characteristics [Omale, 2016]. It is calculated from equation 2.1 below

$$H = \frac{60EI}{1000s} \qquad \text{Equ 2.1}$$

H = Heat input (kJ/inch or kJ/mm)

E = Arc voltage in Volts

I = Current (Amps)

S = Travel speed (inch/min or mm/min)

Analytical models of heat conduction in welding have been developed using the universal differential equation (Eq. 2.2), which describes the influence of both momentary and moving heat sources on the solid materials being welded. These models provide light on how heat distribution impacts the welding process, providing for a better understanding of the thermal behaviour and subsequent microstructural changes in welded materials.

$$\frac{\partial T}{\partial t} = \alpha \left(\frac{\partial^2 T}{\partial x^2} + \frac{\partial^2 T}{\partial y^2} + \frac{\partial^2 T}{\partial z^2} \right) \qquad \text{Equ 2.2}$$

α – coefficient of thermal diffusion m2/s.

The equation in question is a second-order homogeneous partial linear differential equation of parabolic type, which establishes a relationship between the rate of temperature change at a specific point and the surrounding temperature distribution. When a workpiece is subjected to a heat source F(x,y,z,t)F(x,y,z,t)F(x,y,z,t) while also experiencing heat transfer to its environment, the heat conduction equation takes on a specific form that accounts for both the heat input and the thermal losses to the surroundings.

$$\frac{\partial T}{\partial t} = \alpha \left(\frac{\partial^2 T}{\partial x^2} + \frac{\partial^2 T}{\partial y^2} + \frac{\partial^2 T}{\partial z^2} \right) + \frac{1}{\rho . c} . F(x, y, z, t) - b . t \qquad \text{Equ 2.3}$$

Whereas: c, λ, ρ - material's physical properties; b - coefficient of temperature drop intensity due to heat transfer from the object into the environment, s-1. The differential Eq. (2.3) resulted in solutions for cooling upon the action of a fixed momentary (impulse) heat source for common combinations of solid shape and the shape of fixed heat sources.

2.8.2 Effect of cooling rate on HAZ

Weldments' cooling rate is determined by heat input from the welding arc, which is controlled by current, voltage, and speed. Higher heat input causes quicker cooling, solidifying the weld pool and bringing it to room temperature. The heat is transported to the base metal, resulting in the heat-affected zone (HAZ). The cooling rate is critical in defining the ultimate metallurgical structure of the weld and HAZ. Heat loss is a significant aspect in determining cooling pace. The microstructure and microhardness of the weld are affected by the cooling rate, with higher rates often reducing transformation start temperatures from austenite to ferrite. Understanding cooling rates is critical for determining ferrite stability during multi-pass welding or high-temperature applications [Krasnykh et al.,2013].

2.9. The Metallurgy of Welding

The weldment is separated into three sections: the fusion zone (FZ), the heat-affected zone (HAZ), and the unaffected base material. The microstructure and features of these locations have a considerable influence on the strength of welded connections. Rapid heating and cooling, along with local structural changes, result in large spatial variations in composition, microstructure, and residual stress within these zones [David &DebRoy, 1992]. Figure 2. 2 shown the three distinct regions in the weldment: the fusion zone, HAZ and base metal zone

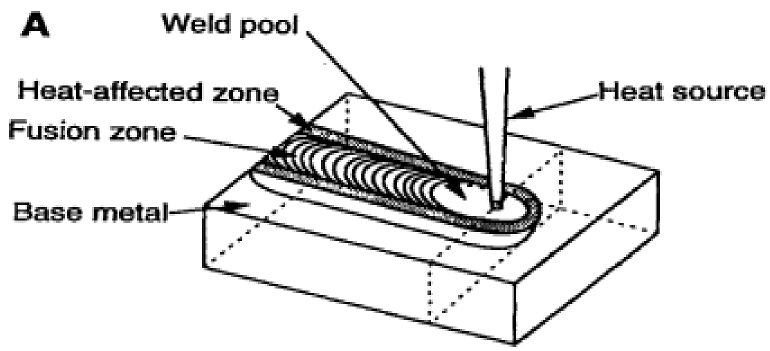

Figure 2.3 Three distinct regions in the weldment: the fusion zone, HAZ and base metal zone [David and DebRoy,1992]

The welding heat input determines the breadth of the heat-affected zone and its areas, with excessive inputs resulting in sluggish cooling rates and potentially influencing the final transformation products. The hardness of the zone is affected by the base metal carbon concentration, as seen in Figure 2.3 for 0.30% carbon steel.

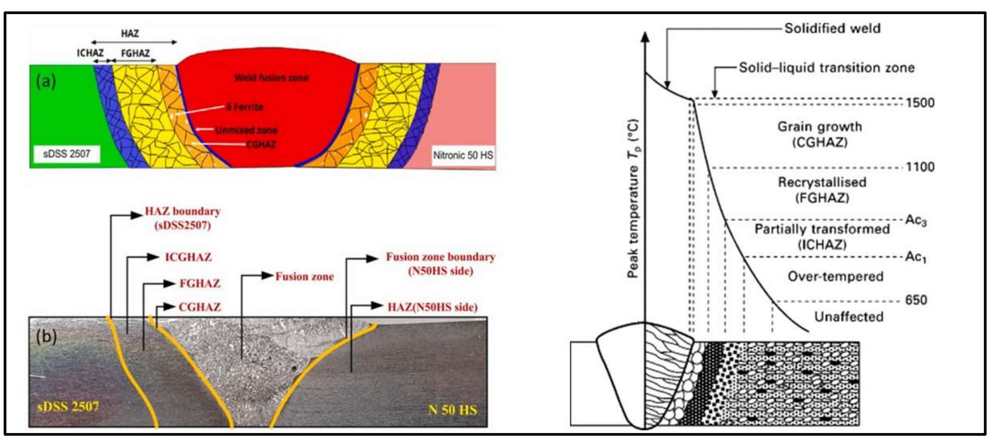

Figure 2.4 Schematic illustration of various regions in a fusion-weld zone and the corresponding phase diagram for 0.30% C steel [Cornu,2013]

2.9.1. Weldability

Weldability refers to a metal's ability to be welded into solid connections while maintaining structural integrity or mechanical qualities. Weldability is influenced by factors such as hardenability, which examines a metal's ability to harden after heat treatment, and cracking susceptibility, which analyses joint failure under stress. Higher carbon concentration improves hardenability but increases cracking risk, necessitating careful balancing. Alloying elements like as nickel and chromium can increase hardenability without increasing fracture susceptibility. The carbon equivalent (CE) formula predicts weldability by analysing carbon and alloy concentration; lower values indicate greater weldability. The carbon equivalent (CE) formula is as follows [Lippold, 2014]:

$$\mathrm{CE} = \%\mathrm{C} + \frac{\%\mathrm{Mn}}{6} + \frac{\%\mathrm{Mo}}{4} + \frac{\%\mathrm{Cr}}{5} + \frac{\%\mathrm{Ni} + \%\mathrm{Cu}}{15} + \frac{\%\mathrm{P}}{3} \quad \text{Equation 2.4}$$

Yurioka,(2001) analysis emphasizes the significance of carbon equivalency in determining steel weldability, although a simple sum of carbon content does not adequately measure heat-affected zone (HAZ) hardness, which is influenced by both parameters.

Zhou et al. (2000) discovered that aluminium and brass are simpler to resistance weld than copper because to their higher electrical resistance and lower thermal conductivity. Resistance weldability is governed by a variety of physical features, and some metals necessitate particular procedures. Cast iron is often weldable, whereas lead is easier to weld. Magnesium alloys require protective shielding, whereas nickel and stainless steels may be welded using a variety of ways. High-alloy steels are weldable under regulated circumstances, whereas low-alloy steels are fair to good. Plain-carbon steels have great weldability in low-carbon variations but inferior performance in high-carbon steels. Other metals, such as tantalum, titanium alloys, and zirconium, can be welded with the correct procedures.

2.10. Welding Defect

Shielded Metal Arc Welding (SMAW) is a welding process that can result in faults that affect weld quality and structural strength. Common faults include porosity, slag inclusion, undercutting, incomplete fusion, cracking, overlap, a lack of penetration, and burn-through. These problems can be caused by poor welding technique, inadequate shielding, excessive temperatures, and contamination. To avoid these defects, welders should follow established processes, store electrodes correctly, prepare surfaces, adjust settings, and do post-weld tests

[Cornish et al.,2019; Singh & Grover, 2015]. Figure 2. 5 shown as cross-sections of welds containing typical defects

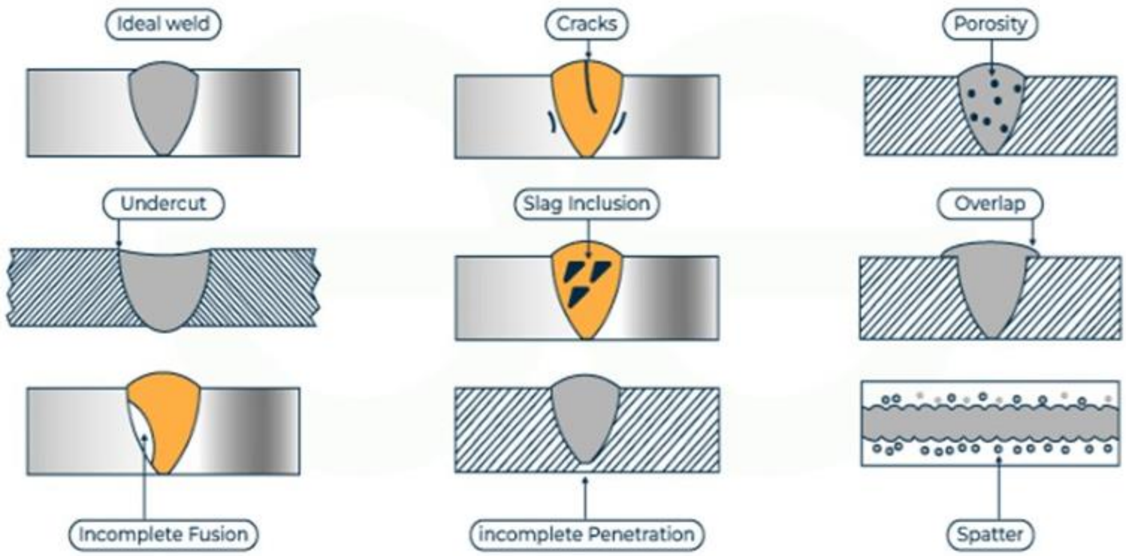

Figure 2.6 Cross-sections of welds containing typical defects [Madhvacharyula et al.,2022]

Trahair et al.'s 2017 research of damaged rail welds in Japan between 1985 and 2001 discovered three major variables affecting their integrity: absence of fusion and centreline shrinkage, suggesting welding problems, and solder fractures, indicating a specific failure mechanism. The research also discussed the vulnerability of enclosed arc welds to fatigue failure owing to liquation cracks and a lack of fusion. The study underlines the need of using rigorous welding processes and identifying specific causes of rail weld failures in order to enhance welding techniques and railway infrastructure safety.

2.11. Steel

Mild steel, a low-carbon steel with a carbon content ranging from 0.05% to 0.50%, is appropriate for applications that demand strength, ductility, and weldability. It is divided into three categories: low-carbon steel (excellent ductility and weldability), medium-carbon steel (increased strength and hardness), and high-carbon steel (extremely hard, used for tools and high-wear components). It is known for its ease of machining, good weldability, and inexpensive cost, although it is corrosive if not protected by coatings. Its versatility makes it widely used in construction, automotive, manufacturing, and residential products [Rashid,1980].

Mild steel is a low-carbon steel that has 0.05% to 0.25% carbon and is mostly composed of iron. It has advantages such as increased ductility, machinability, and weldability, but it cannot be fully hardened by heating and quenching. Its low tensile strength is owing to a lack of carbon and alloying materials. Mild steel is magnetic due to its high iron and ferrite content and is employed in industries such as gas and oil pipelines, vehicle production, building, and forging [Latifi,2012].

AISI 1045 is a medium-carbon steel that is strong, robust, and wear resistant, making it appropriate for a wide range of industrial applications. It contains 0.43% to 0.50% carbon, 0.60% to 0.90% manganese, and up to 0.40% silicon, with iron being the primary component. Its tensile strength, hardness, and ductility make it suitable for machining and manufacturing. Although welded, caution is required to prevent cracking. Heat treatments like as quenching and tempering improve the hardness and grain structure [Vieira et al., 2021].

Mild steel is essential for manufacturing machine components due to its machinability, strength, ductility, and weldability. It is resistant to induction, flame hardening, and nitriding because of its low carbon content. Carburization can enhance case hardness in smaller sections, but it diminishes as the section size grows. Carbon nitriding is feasible and has advantages over conventional procedures. Arc welding, which includes SMAW, MIG, and TIG, is the most versatile method for mild steel [Da Costa Pepe,2010].

2.12. Optimization

Engineering optimization is critical for resource utilization and reducing environmental effect in fields such as design, maintenance, and production. It calculates function maximum and minimum values, guiding software to peak performance. Robust optimization aids in the prediction of uncertainty and complicated interactions in nonlinear systems, ultimately contributing to optimum engineering outputs [Jaisankar, 2018; Kakandikar&Nandedkar, 2018; Krishnaiah &Shahabudeen, 2012].

2.12.1. Taguchi Approach

Taguchi techniques to manufacturing experiment design seek to generate long-lasting goods and processes by taking into account environmental influences, component variability, and reducing departure from goal values. This strategy improves knowledge of variance and its economic impact by merging system, parameter, and tolerance design [Nalbant et al., 2007]. The Taguchi Method use a patented orthogonal array to evaluate output responses based on signal-to-noise ratio (S/N) and determine the optimal parameter combinations. The Degree of Freedom (DoF) determines the number of trials required to evaluate observable qualities; lower values suggest better quality [Haq et al., 2008]. Table 2.4 shown as the problem types and signal-to-ratio functions

Table 2.3 Problem types and signal to ratio functions [Ashebir et al., 2022].

S/N function	S/N formula	Usage when the goal
Smaller the better	$\frac{S}{N} = -10\text{Log}\left[\frac{1}{3}\sum_{i=1}^{3} Xi^2\right]$	Minimizing the response: For example, in this inquiry, minimize the output outcome.
Larger the better	$\frac{S}{N} = -10\text{Log}\left[\frac{1}{m}\sum_{i=1}^{m} \frac{1}{Xi^2}\right]$	Maximized response: for instance, through investigation, maximized the final result.
Nominal the better	$\frac{S}{N} = 10\text{Log}\frac{\mu^n}{\sigma^n}$	Target the result and compute the S/N ratio using means and variances by standard deviation.

2.12.2. Grey Relational Analysis (GRA)

Grey Relation Analysis (GRA) is a data analysis technique that ranks characteristics according to pre-determined scores or ratings to determine the significance of variables. It enables multi-response optimizations while emphasizing overall findings, and is especially relevant for social preference research. GRA may evaluate partial and constrained data while retaining result credibility, making it a useful method for multi-objective parametric optimization [Prakash et al., 2021; Gerus-Gosciewska&Gosciewski, 2022].

2.12.3. Response Surface Methodology

The Response Surface Method (RSM) is a technique for assessing reliability in complicated engineering systems with implicit limit state functions. It employs factorial techniques and ANOVA to optimize for maximum or minimum values, yielding comprehensive results from a limited number of trials. RSM is especially beneficial for studying primary effects and how they interact with responses, and it is optimized using the RSM Box-Behnken Design or Central Composite Design [Elsen& Ramesh, 2015; 2016].

2.12.4. Artificial Neural Network and Genetic Algorithm

Frank Rosenblatt developed the Perceptron in 1958, the first artificial neural network (ANN) that mimicked human visual processing and object recognition. Since then, ANNs and deep learning algorithms have been used to study human cognition and predict outcomes, particularly in assessing outputs of SMAW welding processes. The researchers used MATLAB's ANN toolkit to design and evaluate various neural network architectures, focusing on optimal configurations, training methods, and activation functions (Koopialipoor et al., 2019; Sheelwant et al., 2021). Backpropagation neural networks are commonly used in engineering applications due to their simplicity and efficiency. Genetic Algorithms (GAs) are an evolutionary computation method that uses natural selection to solve optimization problems, making them popular in conjunction with ANNs for multi-objective optimization [Chandrasekhar & Prasad, 2020; Pandey et al., 2020, Sheelwant et al., 2021].

2.12.5. Comparison of Optimization Methods

Research investigates and compares four commonly used optimization techniques: the Taguchi Method, Response Surface Methodology (RSM), Artificial Neural Networks (ANN), and Genetic Algorithms (GA), each with its own set of characteristics, benefits, and drawbacks suitable for a wide range of material optimization applications. The technique chosen is decided by the study's specific objectives, the nature of the problem, and the available data. The Taguchi Method is suitable for simple, sturdy designs that seek to reduce unpredictability, whereas RSM is excellent for examining nonlinear relationships and optimizing circumstances. ANN is good at modelling complex patterns and relationships, but GA is great at traversing complex optimization landscapes. A hybrid strategy that combines these tactics can enhance their strengths while minimizing their weaknesses, resulting in more effective optimization outcomes. Table 2.4 shown as the comparison of several optimization methods

Table 2.4 Comparison of several optimization methods [Paney et al.,2020; Qazi et al.,2020; Hussain et al.,2024]

No	Criteria	Taguchi Method	Response Surface Methodology (RSM)	Artificial Neural Networks (ANN)	Genetic Algorithms (GA)
1	Outline	The emphasis is on resilient design and quality enhancement via experimental design.	Statistical tools are used to model and evaluate connections between variables and responses.	Learn from data using a computational model that mimics human brain activity.	A natural selection-inspired search heuristic for optimization issues.
2	Benefits	Simple to carry out and comprehend. - Needs lesser experimentation. Resilient against noise and unpredictability.	Enables graphical representations. Capability of modelling multidimensional interactions. The predictive power of consequences.	Excellent for complicated, nonlinear interactions. Adaptive learning abilities. Handles huge datasets with various inputs and outputs.	Effective in highly complicated optimization settings. Flexible and adaptable to a variety of issues. Can be used with other techniques.
3	Drawback	Primarily suitable for linear issues. A restricted analysis.	Needs more experimentation. Results may be influenced by preconceptions about normalcy.	Training requires a large amount of data. The black box nature hampers interpretation.	Large populations require a significant amount of mathematical computation. Highly sensitive to variable selection.
4	The most effective, suitable for	Fundamental designs that prioritize durability and quality.	Examining linkages and optimizing circumstances pertaining to complicated systems.	Modelling complicated, nonlinear interactions via adaptive data processing.	Complicated problems with optimization involving numerous objectives and restrictions.

2.13. Identification of Gaps

Research using an BBD experimental design has identified that key SMAW variables—welding current, electrode type/angle, joint design, and travel speed—critically impact weld quality. Inadequate settings for these parameters lead to common defects like lack of fusion, slag inclusion, and overlap, which result in poor mechanical properties such as weak tensile strength and low ductility. The study of literature reviews concludes that maintaining a proper electrode work angle is essential for prevention and highlights a need for future research to precisely quantify how each factor individually affects weld strength. The findings demonstrate that suboptimal parameter selection directly compromises mechanical properties, resulting in weak tensile strength, low hardness, and reduced ductility, which collectively elevate the risk of weld bead failure. These deficiencies are primarily attributed to three root causes: inappropriate material selection, such as electrode mismatch; suboptimal joint configuration and preparation; and improper welding parameters, notably excessive current and incorrect travel speed. Furthermore, the study delineates common defects and their mechanisms: lack of fusion, arising from non-uniform electrode positioning and inadequate penetration; slag inclusion, where entrapped flux residue creates detectable flaws; and overlap, caused by an excessive work angle that forms a stress-concentrating notch susceptible to cracking. A pivotal preventive measure identified is the maintenance of a correct electrode work angle and position, which is fundamental to mitigating lack of fusion and slag inclusion. Despite these insights, the research underscores a significant knowledge gap, noting that a quantified understanding of each factor's specific impact on mechanical properties remains under-explored, thereby necessitating future studies employing advanced analytical and microstructural analysis techniques to precisely delineate these cause-effect relationships.

CHAPTER THREE

MATERIAL AND METHODS

This chapter describes a systematic strategy for improving SMAW parameters for AISI 4130 alloy steel that combines experimental and computational approaches. It employs ASTM standards for tensile testing, hardness measuring, bend testing, and compressive strength assessment. This methodology employs a two-phase optimization framework, beginning with experimental trials using a BBD within RSM, followed by a more complex mathematical model optimization strategy. This method simulates complicated interactions between factors and determines optimal setups. The technique combines experimental and computational aspects through structured data collecting, model construction, optimization, experimental validation, and comparative assessment, therefore improving existing methods by combining statistical design and algorithmic intelligence.

3.1 Experimental Work

This study conducts a thorough examination of welding materials and procedures, employing rigorous research methodology to discover the ideal design elements impacting robust, high-quality welding. It also includes Figure 3.1 workflow diagrams, which demonstrate the research procedures and provide a detailed overview of welding techniques.

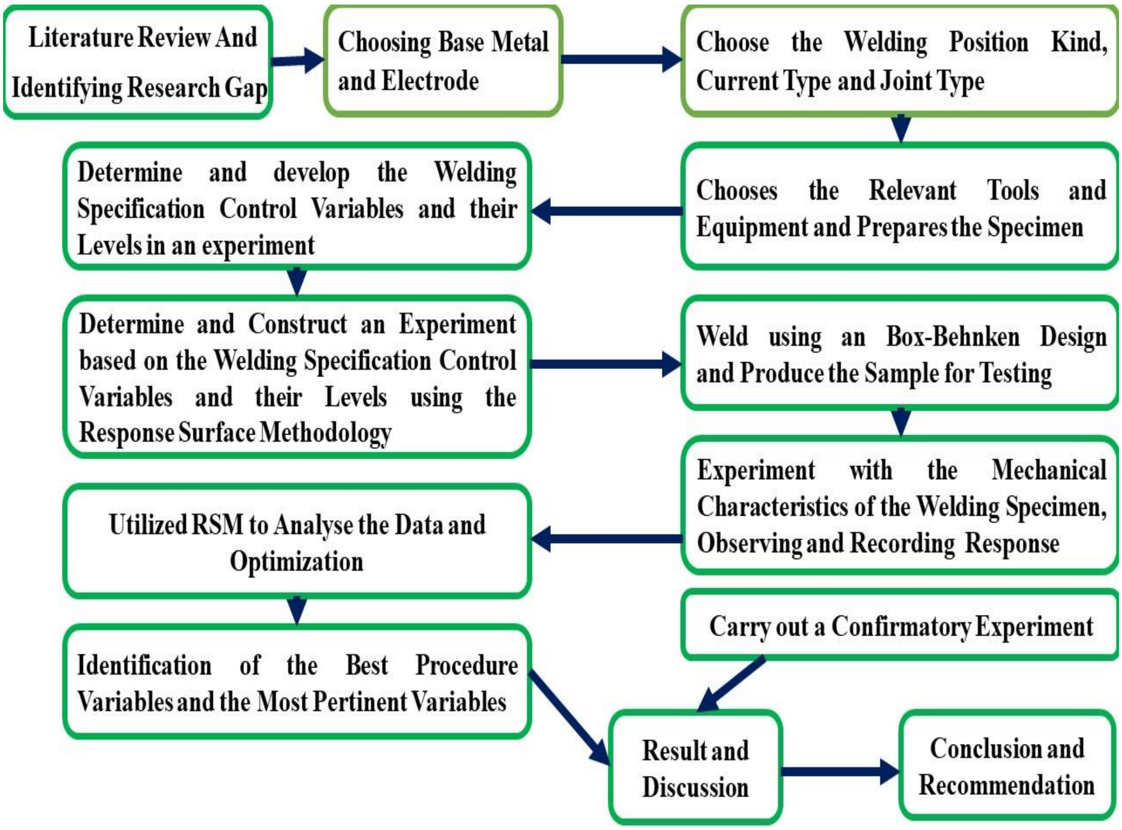

Figure 3.1 Exponential workflow diagram

3.2. Materials and Equipment

The research used an AISI 4130 alloy steel plate measuring 200mm X 110mm X 6mm for plate welding testing using butt joint designs, as illustrated in Figure 3.2. The E6013 basic electrode is used to weld AISI 4130 workpieces. The joint is intended to link the edges of the components, and its nature is defined by their structural configuration. Some connections may require edge preparation to guarantee proper welding and inspection.

3.2.1. Alloy Steel of AISI 4130 Plate Base Material

The chemical composition of AISI 4130 alloy steel plate is critical for determining its weldability, as determined by the American Welding Society. AISI 4130 is highly weldable and may be welded using any technique, providing a balance of toughness, strength, and ductility. Tables 3.1 and 3.2 describe mechanical, thermal, and physical parameters for AISI 4130.

Table 3.1 Chemical composition of the AISI 4130 specimen weight percentage of alloying elements [Zaman et al.,2019;2022]

Alloy	C	Mn	P	S	Si	Cr	Mo
Wt %	0.28 – 0.33	0.40 – 0.60	0.04	0.05	0.2.-0.35	0.80-1.10	0.15-0.25

Table 3.2 Mechanical characteristics for AISI 4130 at room temperature [zaman et al.,2019; De Carvalho,2023]

Mechanical Property	Metric (Unit)
Brinell Hardness (BH)	163
Rockwell Hardness (HR)	84
Ultimate Tensile strength	565MPa
Yield Strength	310MPa
Modulus of Elasticity (E)	200GPa
Bulk Modulus (K)	140GPa
Poisson Ratio (v)	0.29
Shear Modulus (G)	80GPa

3.3. Research Approach

In this research experimental research approaches were utilized to investigate the effects of weld parameters on the mechanical properties which is utilized with SMAW joint specimen.

3.4. Sampling Methods

Sampling is a technique for selecting representative pieces of a material to assess its properties. This study employed box Behnken design methods for AISI 4130 alloy steel plates to investigate the influence of welding parameters on the SMAW process. This experiment requires alloy steel material samples.

3.4.1. Sample Size

The experimental investigation focused on the AISI 4130 alloy steel plate material, with fifteen samples chosen based on thickness, breadth, and length. The base material was 200mm X 110mm X 6mm, and the study used Figure 3.2 to depict the sample size measurements and their perspectives on the material.

Sample Size

The experimental investigation focused on the AISI 4130 alloy steel plate material, with fifteen samples chosen based on thickness, breadth, and length. The base material was 200mm X 110mm X 6mm, and the study used Figure 3.2 to depict the sample size measurements and their perspectives on the material.

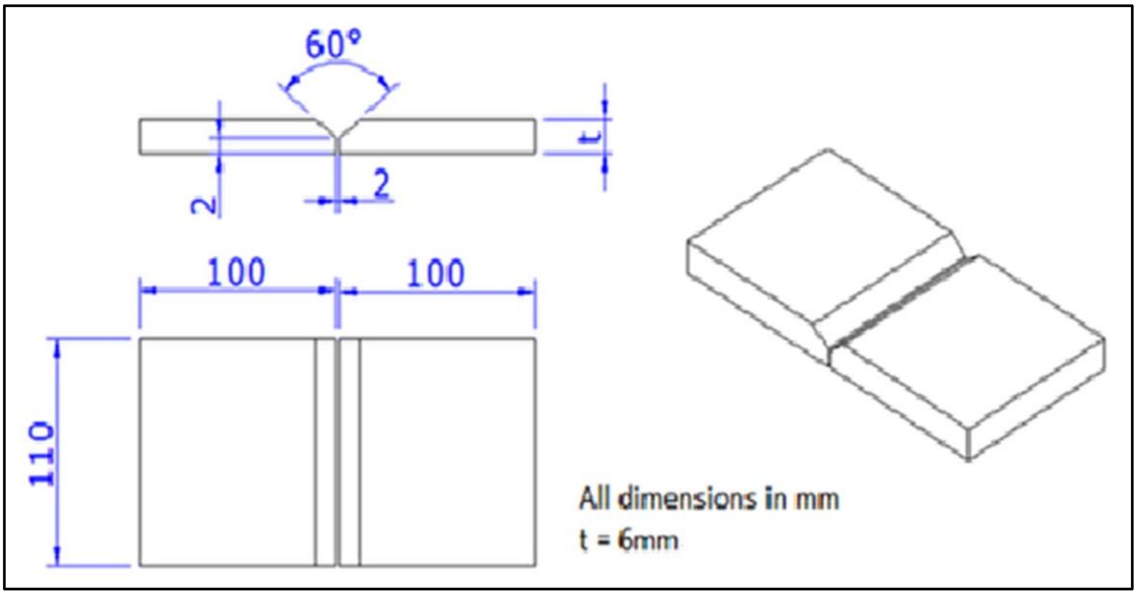

Figure 3.2 Sample joint design preparation

The study focuses on the usage of edge preparation in welding samples in vertical upward positions, using the ISO symbol flat position. Following ISO 9692 joint preparation standards, a butt joint with a wide root spacing was used. The workpiece was cut with a groove angle of 60°, root spacing of 2mm, and root face of 2mm. The SMAW procedure called for an air gap/arc length of 2.5mm. Plates were secured to the welding jig or work piece holding mechanisms to prevent misalignment, movement, and thermal distortions when welding. Surfaces were mechanically cleaned and polished to accommodate a vertical butt joint at 60 degrees.

3.5. Data Collection Methods

The study used an experimental approach to acquire data on a research problem. Primary data was collected from laboratory equipment following welding samples, including UTS, hardness, compressive and bending strength readings from the UTM testing machine, as well as hardness data from the hardness testing machine. The data obtained is given in tabular format.

3.6. Tools and Equipment

In this experimental research work variety of tools and equipment were used, like PICO 300 CEL welding machine, SMAW rutile electrodes, portable grinding machine, safety materials, measuring tools (steel rule, vernier calliper, try square), testing machines (UTM and hardness) and wire brush. Table 3.3 shown as fixed parameters used in this research investigations.

Table 3.3 Fixed parameters used in this research investigations

S. N	Fixed parameters	Value
1	Base metal material	AISI 4130
2	Electrode	E6013
3	Base metal thickness	6 mm
4	Welding condition	Dry
5	Welding joint type	BUTT
6	Current type	DC
7	Welding position	Horizontal
8	Welding groove	V type
9	Groove angle	600
10	weld pass	Multi pass
11	Type of welding position	Flat

3.6.1. Welding Machine

Shielded Metal Arc Welding (SMAW) is a versatile and popular welding technique that includes creating an arc between a covered metal electrode and a workpiece. It is an efficient and cost-effective way of connecting metals. The PICO 300 CEL Welding Machine was employed for this particular task. Figure 3.3 Welding machine with accessorise used for these experiments.

Figure 3.3 PICO 300 CEL Welding Machine with Accessories, Used in These Experiments

PICO 300 CEL is a versatile SMAW inverter welding machine. The machine work perfect with all types of electrodes. They are well suited for both workshop and outdoor working conditions. Easy to use with one-knob operation with welding data display. Table 3.4 shown specification of the welding machines.

Table 3.4 Specification of the welding machines

Version	Pico 300 cel
Setting range for welding current	10 A - 300 A
Duty cycle 40 °C	300 A / 25 %
	220 A / 60 %
	170 A / 100 %
Open circuit voltage	107 V
Mains voltage (ex-works)	3 x 400 V
Mains tolerances (ex-works)	-25 % up to +20 %
Mains frequency	50 Hz / 60 Hz
Recommended generator power	16.3 kVA
Efficiency	88 %
Protection classification	IP23
EMC class	A
Dimensions (L x B x H)	490 mm x 186 mm x 350 mm
Weight	16.5 kg
Standards	IEC 60974-1 and -10 CL. A

3.6.2. Electrode

The study utilized electrodes of varying diameters for 6mm butt joints, with weld conditions set at 22 volts and currents of 150, 175, and 200 amps. The welding current was manually adjusted for each specimen to investigate the effect of SMAW welding on chosen 6mm material thickness specimens. The experiment showed that carbon steel welding electrodes are suitable for all situations, have outstanding welding technical features, and produce a steady arc with a nice look. Due to this feature, AWS E6013 steel welding electrodes are used. Table 3.5 shown as mechanical properties of electrode of E6013; Table 3.6 Chemical composition of filler electrode of E6013 and Table 3.**7** shown as electrode used specification conditions.

Table 3.5 Mechanical properties of electrode of E6013

Electrode	Minimum yield strength (MPa)	Minimum tensile strength (MPa)
E6013	345	425

Table 3.6 Chemical composition of filler electrode of E6013

Element	C	Mn	S	P	Si	Fe
Weight (%)	0.06 - 0.15	0.3 - 0.6	≤ 0.035%	≤ 0.035%	≤ 0.03%	≈98.5%

E6013's rutile-potassium flux coating blends rutile (30-50%, TiO_2) for smooth slag and beads, potassium compounds (15-30%, e.g., K_2SiO_3) for AC arc stability, cellulose (5-15%) for moderate gas shielding, silicates (10-20%) for slag support, carbonates (5-10%) for CO_2 shielding, ferromanganese (5-10%) and ferrosilicon (0-5%) as deoxidizers, and trace moisture controls—delivering all-position capability, easy striking, and medium penetration without low-hydrogen properties.

Table 3.7 Electrode used specification conditions

S. N	Variables	Specification
1	Electrode type	E 6013
2	Electrode diameter	2.5, 3.2 and 4mm
3	Electrode extension	250 mm
4	Work angle	70^o-80^o from vertical

3.7. Welding Material Preparations

The study investigated the effect of SMAW process parameters and mechanical qualities on AISI 4130 alloy steel plates with vertical up butt joint, employing a multiple-pass welding method and welding bead as input and output variables.

3.7.1. Pre weld surface cleaning

Plates were cut at the proper angle for butt joint preparation, as shown in figure 3.3, and the samples were welded in v according to the ISO symbol flat position. Plates measuring 100 mm x 110 mm x 6mm were cut and welded in v using the ISO symbol flat position. The test plates were placed flat, and surfaces were prepared by removing pollutants such as dirt, metal particles, oil grease, paint, and moisture with a wire brush and an alkaline cleanser.

3.8. Data Analysis Method

This thesis employed a variety of data analysis techniques, including the response surface methodological method of box Behnken design and experimental analysis using bending, compression, tensile, and hardness tests. It sought to investigate the impact of welding parameters on SMAW process parameters and devise suitable combinations for higher-quality weld products with enhanced mechanical qualities. The researchers wanted to enhance the mechanical behaviours of SMAW weld products.

3.9. Experimental Testing Method

This research focuses on improving welding settings for weld bead quality with manual arc welding technique. Three important welding factors - welding current, electrode diameter, and electrode welding angle have been recognized as critical to welding quality. The system is designed to provide the best welding current and travel speed for the experiment sample. The workpieces are secured to a working bench, and test samples are made of AISI 4130 alloy steel plate and AWS E6013 electrode. The study's goal is to research the features of heat-affected zones and optimize welding conditions for improved weld bead quality.

3.9.1. Hardness Testing

Hardness is a material's capacity to withstand penetration, abrasion, scratching, or cutting. It is a trait that protects against permanent deformation. Rockwell Hardness Tests (RWH) are frequently used in the industrial sector, with diamond/steel indenters producing scales such as HRA, HRB, HRC, and HRN. Micro hardness measurement testing was performed using a Digital Rockwell microhardness type HRS-150 from Beijing United Tester Co., LTD in China, which was chosen owing to problems in integrating evaluation procedures on other machines. The RWH scale was used to compute sample hardness values using ASTM E18 and 28 standard testing techniques. The hardness number was calculated by averaging the findings of three trial specimen indentations from each weld specimen's Rockwell hardness/RWH/type "B" test at room temperature. Before testing, the specimens were polished and ground. Hardness test was carried out through experimental circumstances are listed in Table 3.8. Figures 3.4–3.5 show the HRS-150 digital Rockwell hardness tester and a schematic of specimens for mechanical property evaluation.

Table 3.8 Hardness test parameters

S. N	Parameter	Operating conditions
1	Scale Type	Rockwell B
2	Indenter Load	100 kgf
3	Indenter Material	Steel
4	Dwell Time	15 seconds
5	Overall Diameter (Inch)	3/8"
6	Specimens’ preparation	400, 800 and 1200 grit SiC sand paper
7	Overall Length (Inch)	29/32"

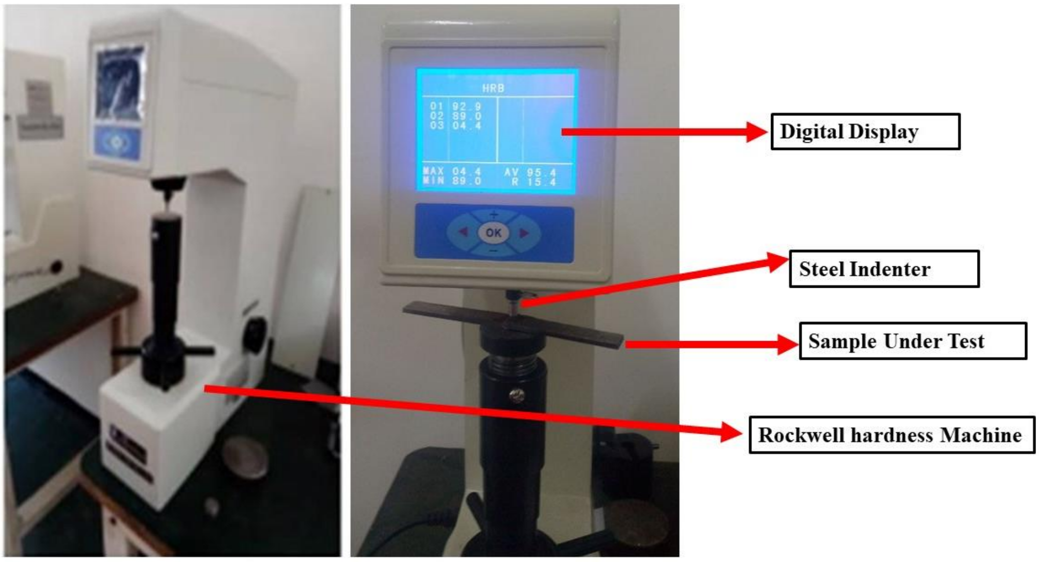

Figure 3.4 Rockwell hardness tester machine model HRS-150 series

The sample specimen was placed with the surface on the anvil, and slowly turning the hand wheel until the specimen was raised to touch the indenter.

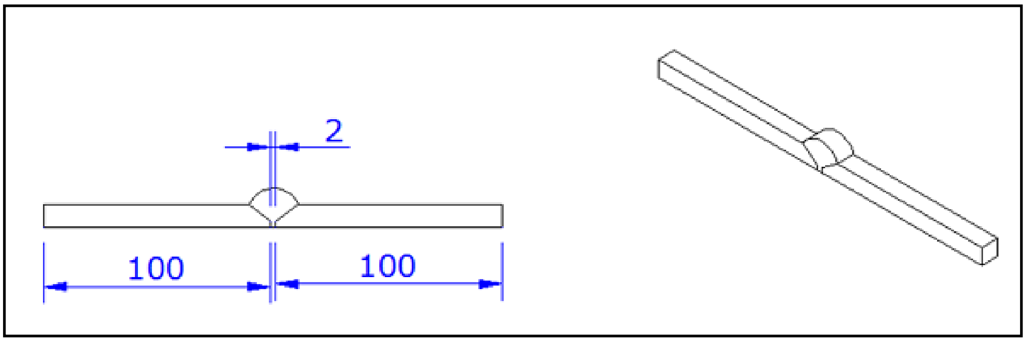

Figure 3.5 Hardness testing sample design

The analysis indicates that the weld bead is not flush with the material, and the surface to be evaluated for hardness is ground down so that it fits flat on the base area of the testing machine. The surface must be level, perpendicular to the indenter, and with a fine surface polish. RWH hardness measurements are taken on a metallographically prepared surface to minimize tempering during grinding and work-hardening during polishing. Two primary factors will be tested: the change in hardness in the weld heat affected zone and the breadth of the heat affected zone in response to variations in hardness value as the weld bead travels to the parent metal.

3.9.2. Ultimate Tensile Strength, Compressive strength and Bending Strength Testing

Tensile strength is the maximum stress that a material can sustain in tension. In other words, we can say the amount of applied load per cross sectional area that a material can withstand before failure. Mathematically it is calculated as the ratio of maximum tensile load to the original cross section area. One of the most common ways to test a material's strength is by using tensile testing. Tensile tests measure the stress over the strain of a material under uni-axial loading conditions. Because testing is done under one stress state (only one direction), it can be concluded from the test that the strengths in this test are the maximum a specimen at a certain thickness and temperature can withstand. Tensile test was conducted on sub size the sample made as per ASTM E8/E8M cut from Adjacent to the weld bead using a hydraulic extensometer with prepared machined specimen dimensioned 200mm X 110 mm X 6mm Tensile samples were prepared by milling of the top and bottom surfaces to remove flashing and other surface irregularities. The standard shape is obtained using UTS testing dimension as shown in the figure 3.6.

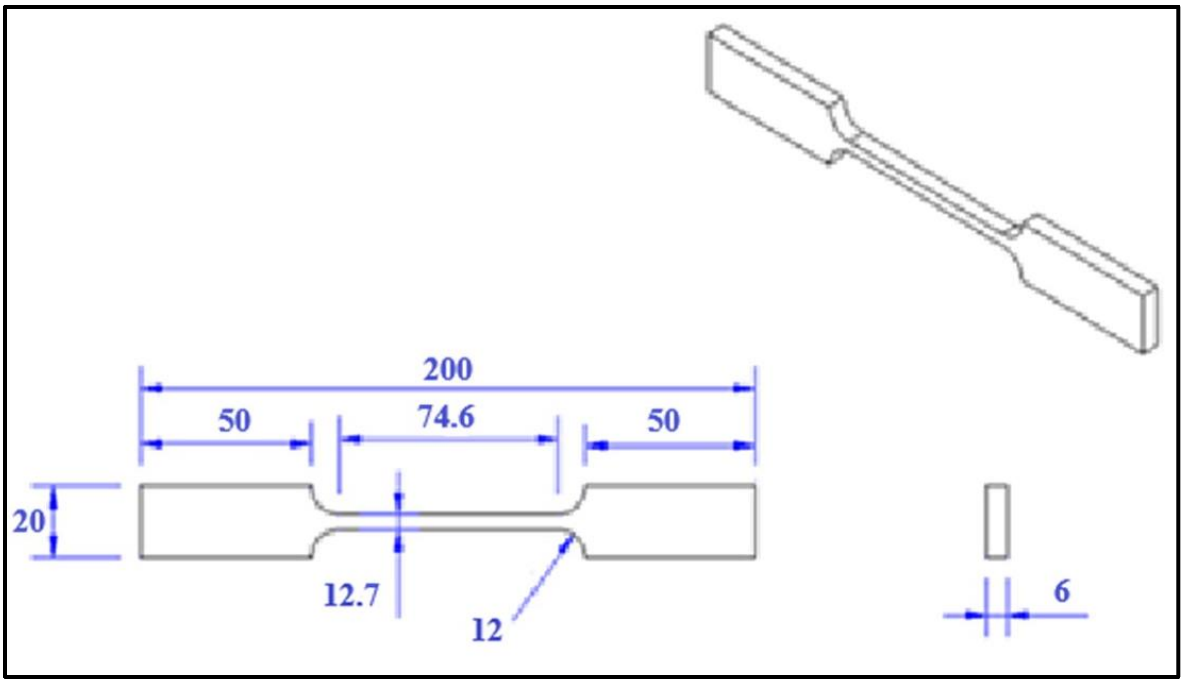

Figure 3.6 UTM testing sample design

The ultimate tensile strength of the machined specimens measured on a calibrated Control lab testing machine. Tensile test was carried out according to ASTM A370-14 standard, which is the "Destructive tests on welds in metallic materials-Transverse tensile test". During uni-axial tensile testing, the upper head or grip moves upward hydraulic force, while the lower head or grip stays stationary.

The compressive strength testing of AISI 4130, a low-alloy chromium-molybdenum steel recognized for its strength, fracture toughness, and fatigue resistance, must comply with ASTM E9 standards to ensure accurate and reproducible compressive property data. Additionally, these properties must be validated against regulatory requirements like AMS 6350 and ASTM A29 to confirm material conformance and performance integrity in critical applications.

The ASTM E290 and EN 910 standards govern bend testing for metal ductility. This test examines the ductility of the material using a jig and fixture on a universal testing machine. The jig and fixture have a span of 54mm and an internal length of 34mm. Tensile, compression, and bending tests are performed on both metallic and non-metallic materials using servo-hydraulic testing devices. Figure 3.**7** shown as Bairoe HUT-600 model computer-controlled electro-hydraulic universal testing machine.

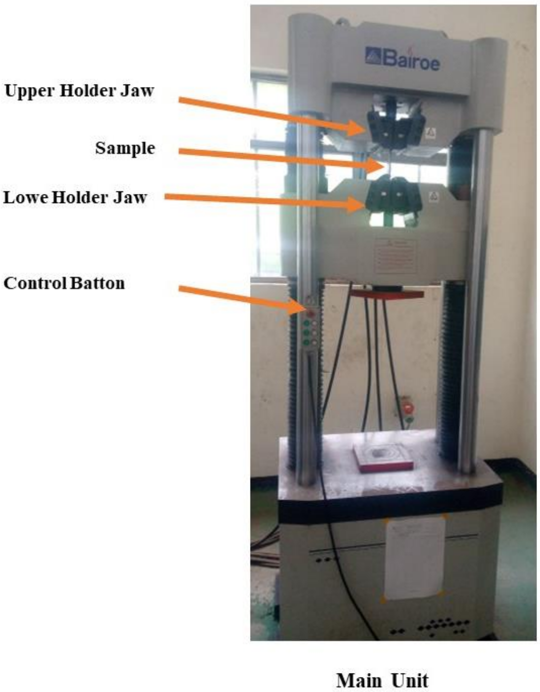

Figure 3.7 Bairoe HUT-600 Computer-Controlled Electro-Hydraulic Universal Testing Machine

For tensile testing, it is considered a “static” test, meaning the force is to be applied slowly. Applying the load too fast may result in skewed results, therefore a slow speed is chosen to best represent static loading. Once all the parameters have been specified, the test begins to run and the lower head begins to drop at a constant rate. The force required to keep the head continuing upward at the constant speed is recorded as a function of displacement. After the specimen breaks, the test is stopped and the digital screen displays the load in KN and elongation in mm.

3.10. Methodology

This research established its methodological foundation through a comprehensive literature review, enabling the selection of optimally effective parameters and approaches. The investigation employed two sophisticated optimization techniques: Response Surface Methodology (RSM) implemented through MINITAB 2023a software.

Experimental specimens consisted of AISI 4130 steel plates with dimensions of 110mm width × 200mm length × 6mm thickness. All welding surfaces underwent rigorous preparation involving chemical cleaning to eliminate contaminants including corrosion, scale, oil, and grease, followed by mechanical edge preparation using power hacksaws and grinders to ensure optimal weld integrity.

The study specifically examined flat and horizontal welding positions for single V-groove butt joints, focusing on how workpiece orientation and positioning enhance operational efficiency and welding speed. The joining sequence initiated with precise tack welding according to the prepared joint geometry, followed by complete joint penetration using Shielded Metal Arc Welding (SMAW). All welding parameters were systematically controlled and documented according to experimental requirements.

3.11. Multi objective Response Optimization

For novel welding initiatives, engineers traditionally determine optimal parameters by drawing upon existing experience or conducting costly and time-consuming experimental tests. To overcome these limitations, researchers increasingly employ computational optimization methodologies. The techniques outlined in this work are specifically suitable for optimizing the SMAW process for AISI 4130 materials. In general, the fundamental goal of these optimization methods is to identify the set of variable values that maximize or minimize a multivariate objective function while adhering to a defined set of constraints. These constraints establish a bounded search space, often termed the feasible region, which must contain the optimal solution for the process. This overview provides a summary of these optimization methodologies, with a particular focus on their applications in engineering.

3.11.1. Response Surface Methodology

The RSM offers a powerful statistical approach for optimizing complex engineering processes operating within defined constraints. Integrating factorial design and ANOVA, this methodology enables efficient optimization of multiple parameters to achieve specific target responses (Elsen& Ramesh, 2016). RSM yields significant insights from a limited experimental dataset, facilitating comprehensive analysis of both individual parameter effects and their interactive influences on output variables. By implementing three distinct levels for each independent variable, the method effectively captures nonlinear relationships and interaction effects, while consistent parameter variation enables identification of optimal operational conditions.

This study employed a BBD to investigate the effects of welding current, electrode diameter, and electrode angle on the mechanical properties of SMAW joints. The BBD configuration was selected for its capability to efficiently generate second-order response models through strategically positioned centre and axial points, allowing precise quantification of quadratic effects. The three input parameters were configured as a multifactorial system with explicitly defined upper and lower limits, as detailed in Table 3.9. The experimental matrix presented in Table 3.10 documents the parameter combinations and their corresponding mechanical property measurements within the RSM framework, establishing a systematic approach for enhancing weld quality through optimized process parameter selection. Figure 3.3 shown as RSM-BBD Procedure flow diagram.

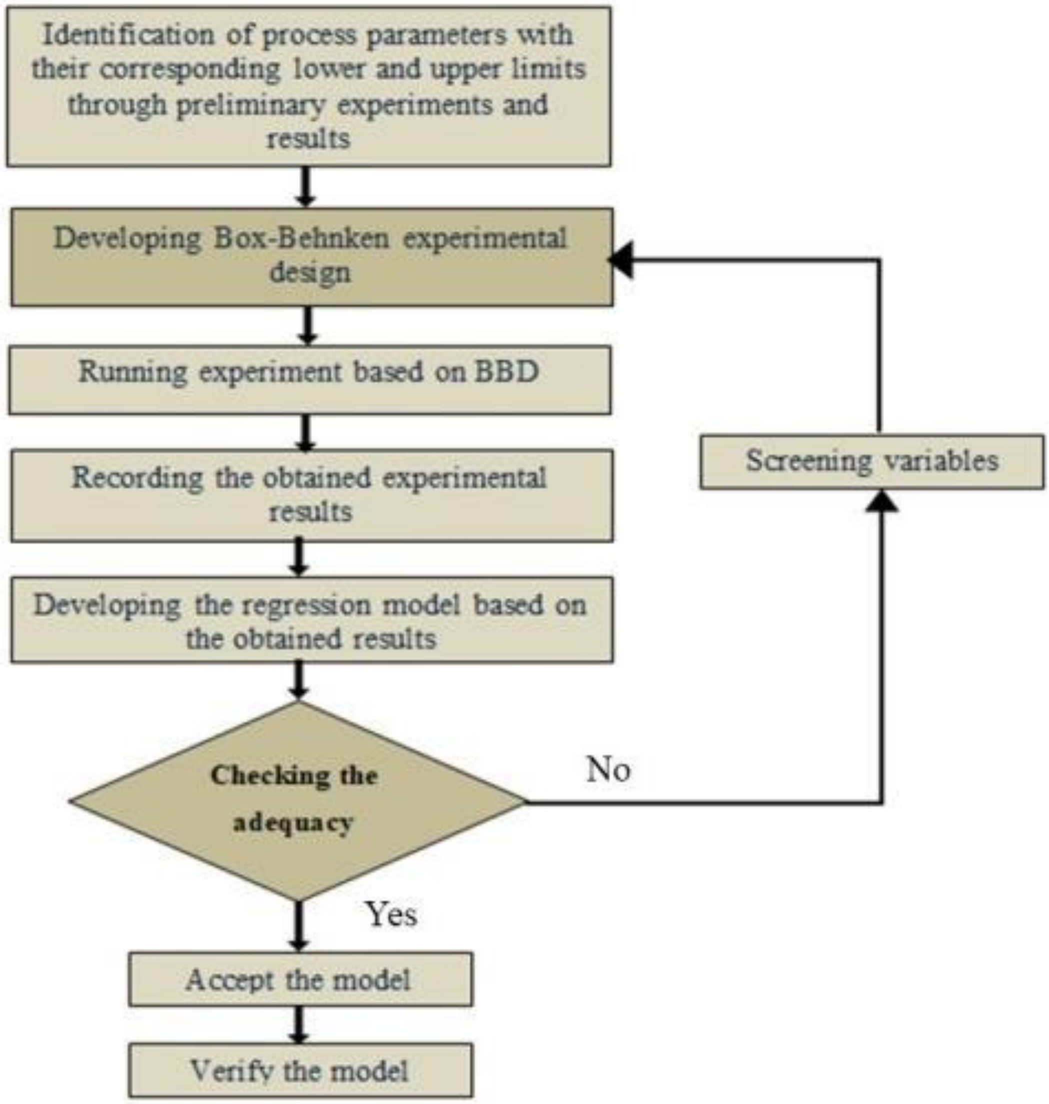

Figure 3.8 RSM-BBD Procedure [Palanikumar and Davim,2013]

Table 3.**9** DoE BBD experimental factor

S. N	**Process parameters**	**code**	**Units**	**Type of Groove: Single V joint**		
				Level 1	**Level 2**	**Level 3**
1	Welding current	A	Amperes (A)	150	175	200
2	Welding electrode Angle	B	Degrees (°)	70	75	80
3	Electrode diameter	C	Millimetres (mm)	2.5	3.2	4

The BBD array matrices of the experimental setup and design of experiments are shown in table 3.10, which was generated with the MINITAB 23 program. And the experiment will be carried out based on the values of the provided variables.

Table 3.10 BBD generated list of experiments

S. N	Welding current (A)	Welding electrode Angle (0)	Electrode Diameter (mm)
A1	175	80	4.0
A2	175	70	2.5
A3	175	75	3.2
A4	175	75	2.5
A5	200	80	3.2
A6	150	80	3.2
A7	150	75	2.5
A8	200	75	2.5
A9	200	70	3.2
A10	175	80	2.5
A11	200	75	4.0
A12	200	75	3.2
A13	150	70	3.2
A14	150	75	4.0
A15	175	70	4.0

The entire investigation was carried out in accordance with the specifications and mechanical parameters such as tensile strength, weld hardness, and bending strength were tested by obtaining a sample from the weld products. An BBD is a set of variables (input parameters) over the parameters of the output that provides the best configuration of process control variables.

CHAPTER FOUR
RESULTS AND DISCUSSION

4.1. Experimental Works

All plate was cleaned with a polisher disc before to welding to remove any pollutants such as rust, dust, or oil, and the edge was prepared according to the design using a steel grinding disc. The welding experiment was carried out with the Box-Behnken design shown in Table 3.10. Figure 4.1 shown Welding experimentation of welded specimen according DOE of BBD experiment list.

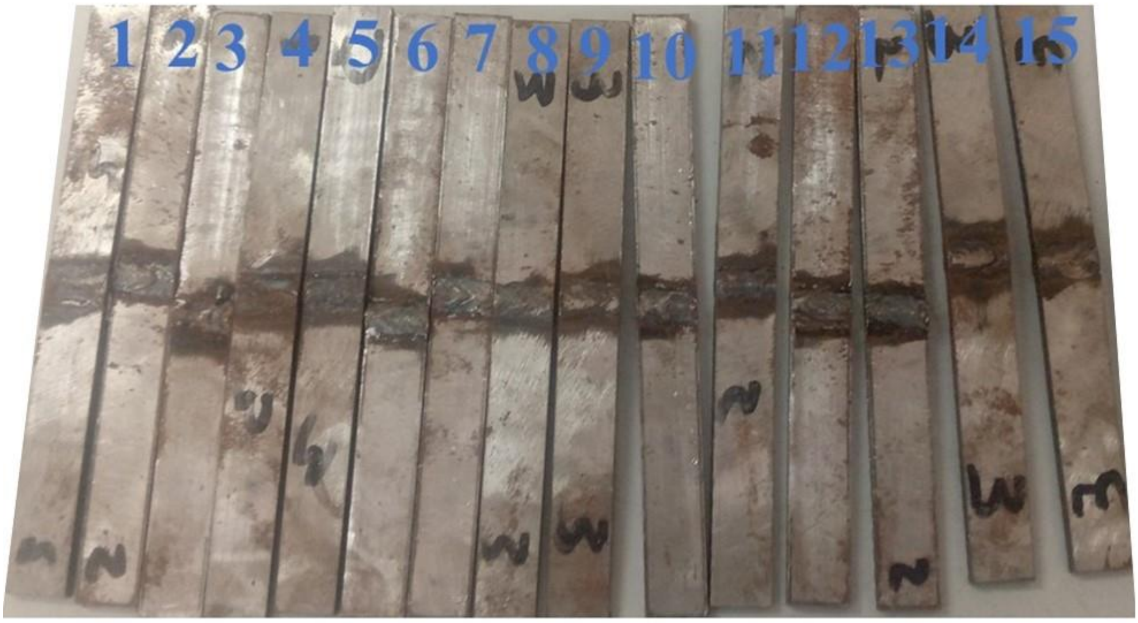

Figure 4.1 Welding experiments work of welded samples

4.2. Validation of the AISI 4130 Base Metal Composition

Spectroscopy is a key analytical method used to identify, quantify, and analyse the molecular and structural properties of materials. It operates by measuring how substances interact with light at specific wavelengths, providing an accurate means of determining the elemental composition of unknown materials.

Optical emission spectrometry (OES) was employed to verify the chemical composition of AISI 4130 alloy steel. The material was vaporized and excited in an argon atmosphere, allowing for the measurement of emission spectra. The results confirmed that the composition matches the standard AISI 4130 grade. Figure 4.2 shown as the composition analysis of AISI 4130 alloy steel through spectroscopy. Figure 4.3 shown as the result of the chemical composition of weld base metal of AISI 4130 alloy steel analysis

Figure 4.2 Composition analysis of AISI 4130 alloy steel through spectroscopy

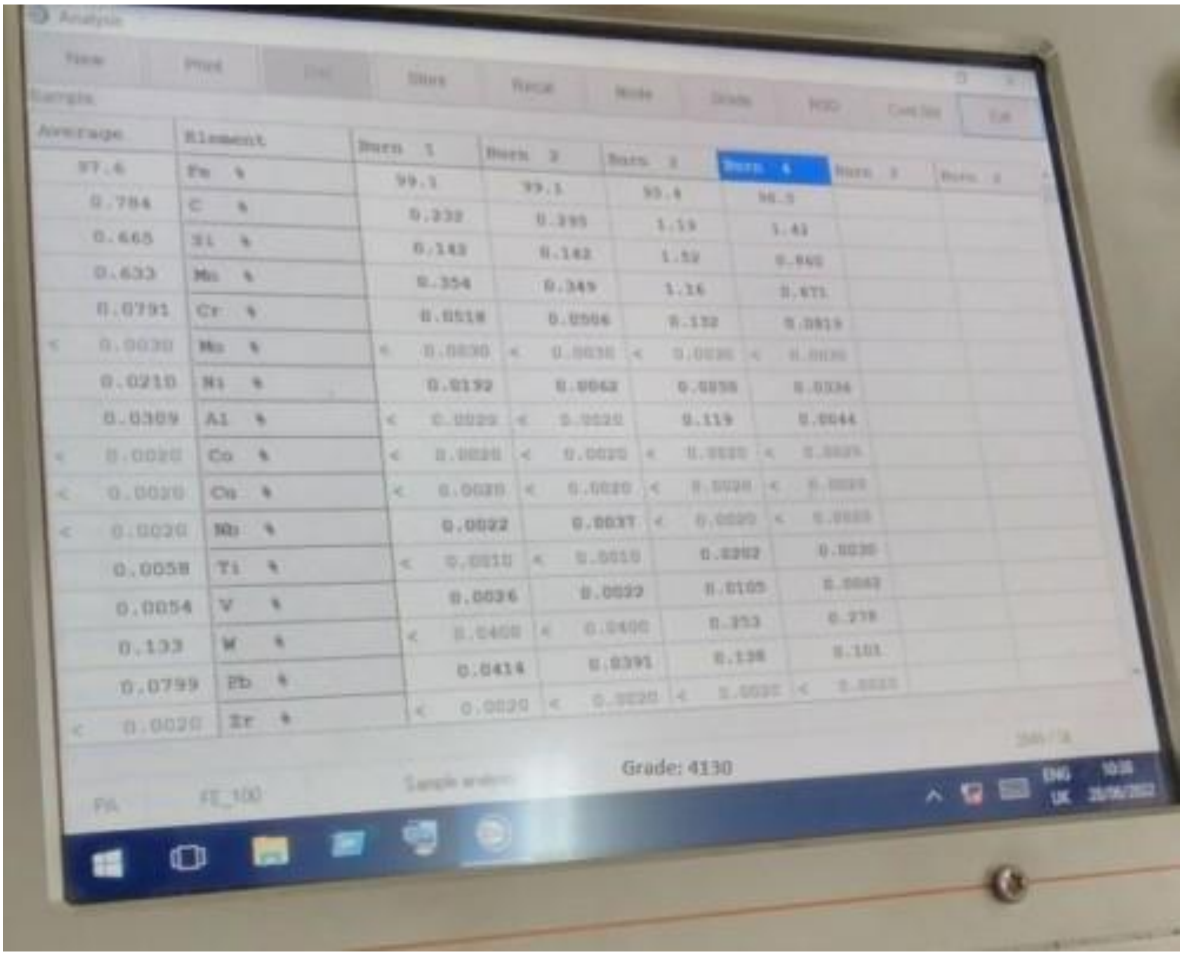

Figure 4.3 The result of the chemical composition of weld base metal of AISI 4130 alloy steel analysis

4.3. Hardness Analysis

Hardness is a key material property in metallurgy and engineering, indicating resistance to indentation and wear. It is assessed through standardized tests, including Rockwell, Brinell, and Vickers methods, with the Rockwell method being particularly popular (Committee, 2000). This method measures hardness by evaluating the permanent depth of an indentation created under specific stress. The Rockwell B scale uses a steel ball indenter. Accurate testing requires specimens to be polished to a defined size prior to assessment. Figure 4.4 shown the hardness testing specimen prepared. Table 4.1 shown as experimental Rockwell hardness result. Figure 4.5 shown as graph of hardness specimen result analysis.

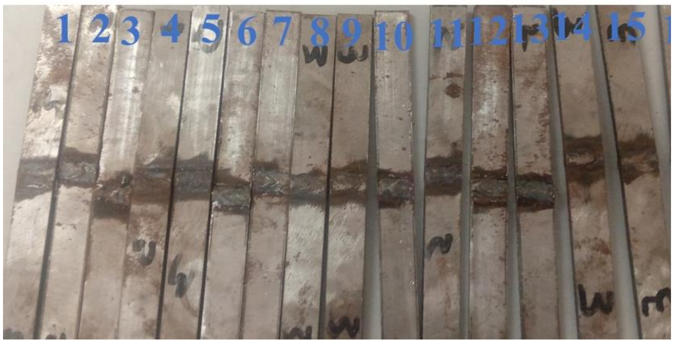

Figure 4.4 Hardness testing specimen prepared

Table 4.1 Experimental Rockwell hardness result

S. N	Welding current (A)	Welding electrode Angle (0)	Electrode Diameter (mm)	Average Hardness (HRB)
A1	175	80	4.0	99.7
A2	175	70	2.5	101.5
A3	175	75	3.2	112
A4	175	75	2.5	99.8
A5	200	80	3.2	96.4
A6	150	80	3.2	109.4
A7	150	75	2.5	110.9
A8	200	75	2.5	107.5
A9	200	70	3.2	103.2
A10	175	80	2.5	108.1
A11	200	75	4.0	101.2
A12	200	75	3.2	101.7
A13	150	70	3.2	105.8
A14	150	75	4.0	105.3
A15	175	70	4.0	101

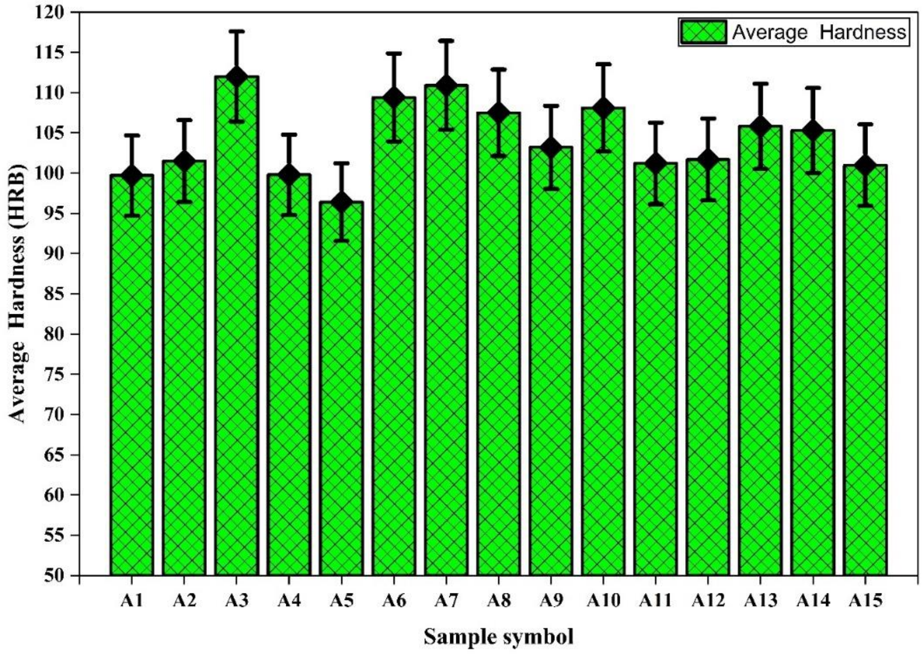

Figure 4.5 Graph of hardness specimen result analysis

This investigation explored the impact of key SMAW parameters—welding current, electrode angle, and electrode diameter—on the hardness of weld metal. Statistical analysis revealed a strong correlation between these parameters and hardness outcomes, with electrode diameter and welding current identified as the primary influencing factors. The electrode angle had a negligible effect within the tested range. The mechanism behind these results is rooted in thermal dynamics: using a smaller diameter electrode (2.5 mm) and a lower current (150A) increases current density and reduces heat input, which promotes faster cooling and the formation of a finer microstructure, thereby enhancing hardness. In contrast, larger diameters and higher currents lead to increased heat input and slower cooling, resulting in a coarser grain structure and reduced hardness. The higher parameters for achieving maximum hardness, demonstrated by a peak value of 112 HRB in sample 3, are a current of 175A, an electrode diameter of 3.2 mm, and an electrode angle of 75°. The lower parameters for achieving minimum hardness, demonstrated by a peak value of 96.4 HRB in sample 5, are a current of 200A, an electrode diameter of 3.2 mm, and an electrode angle of 80°. These findings establish a scientific basis for optimizing SMAW techniques, transitioning from empirical methods to precision-based manufacturing. This study extends recent research on weld property enhancement, particularly the work of Haider et al. (2019) and Abdelsalam et al. (2023). It identifies electrode diameter and welding current as key factors influencing weld metal hardness in SMAW. By establishing optimal settings for peak hardness, the study promotes precision-based production in SMAW while aligning with established standards.

4.4. Ultimate Tensile Strength

Tensile testing is a crucial method for evaluating key mechanical properties like strength and ductility under stretching stresses, providing vital information for material selection and design (Joseph et al., 2016). In this study, specimens were machined according to ASTM E8-04 standards, featuring a shortened centre gauge section to reduce distortion and breakage. Two specimens were extracted transversely to a weld bead and tested under increasing stress, with average mechanical parameters summarized in a table. Figure 4.6 shown as UTS test samples prepared: (a) Before test and (b) After test. Table 4.2 shown as UTS testing result analysis. Figure 4.7 shown as graph of Average UTS specimen result analysis.

(a) Before test

(b) After test

Figure 4.6 UTS test samples prepared: (a) Before test and (b) After test

Table 4.2 UTS testing result analysis

Test no	Welding current (A)	Welding electrode Angle (^{0})	Electrode diameter (mm)	Ultimate tensile strength (MPa)
A1	175	80	4.0	865.57
A2	175	70	2.5	930.21
A3	175	75	3.2	1007.98
A4	175	75	2.5	856.48
A5	200	80	3.2	817.09
A6	150	80	3.2	1000.91
A7	150	75	2.5	1003.94
A8	200	75	2.5	941.32
A9	200	70	3.2	947.28
A10	175	80	2.5	979.7
A11	200	75	4.0	905.97
A12	200	75	3.2	884.76
A13	150	70	3.2	859.51
A14	150	75	4.0	937.28
A15	175	70	4.0	889.81

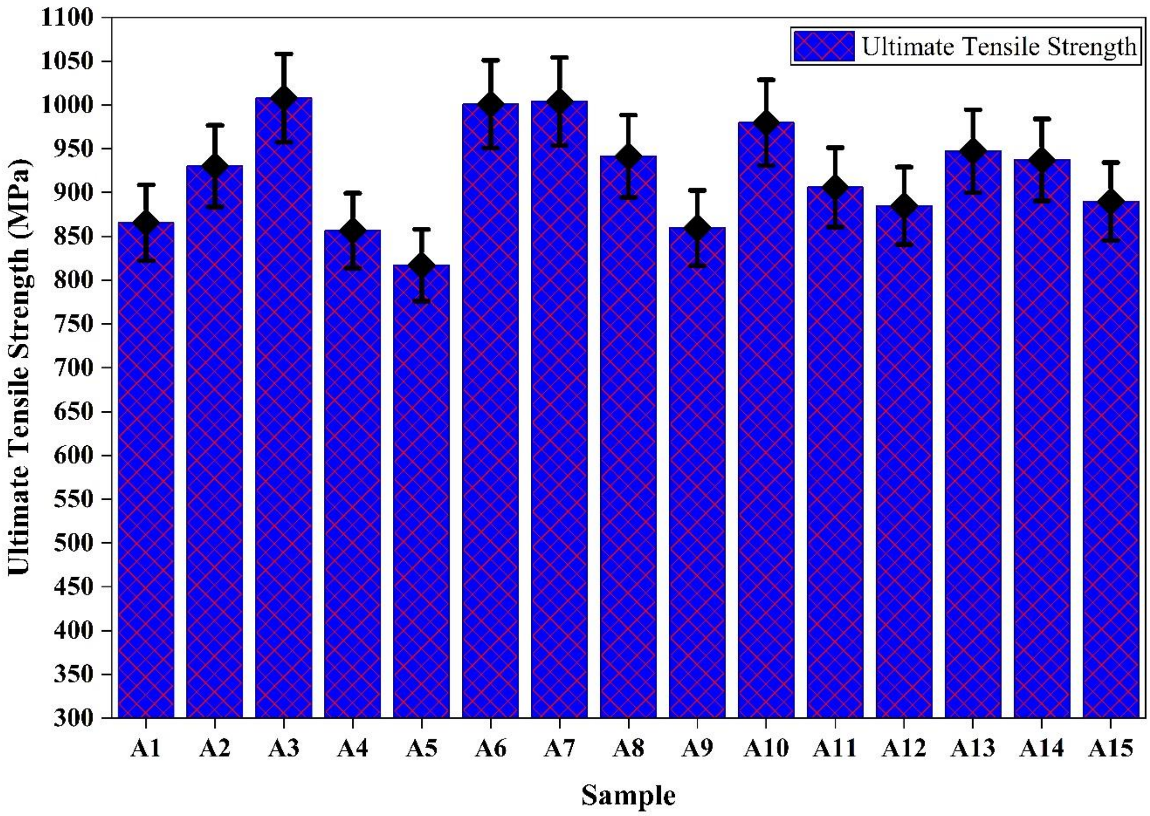

Figure 4.7 Graph of Average UTS specimen result analysis

This study employed the Design of Experiments (DoE) technique to enhance Shielded Metal Arc Welding (SMAW) settings for improved Ultimate Tensile Strength (UTS). Through rigorous experimentation and analysis, it identified welding current, electrode angle, and electrode diameter as critical factors affecting mechanical performance. The researchers found that a combination of 175A current, 75° electrode angle, and a 3.2 mm diameter electrode yielded the best results by increasing penetration through higher current density while maintaining controlled arc dynamics and minimum heat affect zone. The higher parameters for achieving maximum UTS, demonstrated by a peak value of 1007.98MPa in sample 3, are a current of 175A, an electrode diameter of 3.2 mm, and an electrode angle of 75°. The lower parameters for achieving minimum UTS, demonstrated by a peak value of 817.09MPa in sample 5, are a current of 200A, an electrode diameter of 3.2 mm, and an electrode angle of 80°.These findings provide a robust foundation for precision welding manufacturing, facilitating a shift from traditional trial-and-error methods to optimal parameter selection, thereby enhancing structural reliability and tensile strength. This investigation builds on recent advancements in improving the mechanical properties of weld joints and aligns with earlier research in welding technology by Liu et al. (2023) and Yaacob et al. (2024).

4.5. Bending Strength Analysis

Bend testing determines the ductility and strength of a material by bending it over a radius. It assesses weld plastic deformation as well as flaws such as sidewall fusion, root fusion, and joint penetration. Bend testing is an important method for evaluating the modulus of elasticity and bending strength of a material. Two face bend samples have been bent 180° in welding investigations using a 20 mm (4T) mandrel diameter ASME section IX mandrel [Joseph et al., 2016] as shown in figure 4.10. The samples are gently and gradually bent from the center in a circle of a given radius as shown in figure 4.9. Due to strain during bending, certain samples develop exterior surface cracks, rendering them undesirable for use in technical applications. High bend strength is permitted if there are no apparent cracks on the exterior surface [Kumar et al., 2017]. Figure 4.8 shown bending strength testing specimens prepared before and after testing. Figure 4.9 shown mandrel diameter vs length of span with prepared jig. Table 4.3 shown bending strength tested result analysis. Figure 4.10 shown the graph Average bending strength specimen result analysis.

Before test

After test

Figure 4.8 Bending strength testing specimens prepared before and after testing

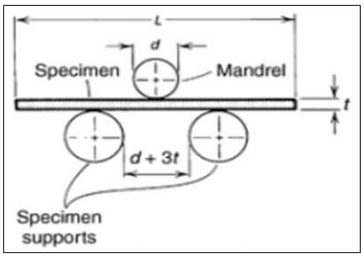

Figure 4.9 Mandrel diameter vs length of span with prepared jig

Table 4.3 Bending strength tested result analysis

S. N	Welding current (A)	Welding electrode Angle (0)	Electrode diameter (mm)	Bending strength (MPa)
A1	175	80	4.0	964.7
A2	175	70	2.5	844
A3	175	75	3.2	913
A4	175	75	2.5	996
A5	200	80	3.2	979
A6	150	80	3.2	956
A7	150	75	2.5	818.8
A8	200	75	2.5	947.5
A9	200	70	3.2	861
A10	175	80	2.5	930
A11	200	75	4.0	810
A12	200	75	3.2	700
A13	150	70	3.2	928
A14	150	75	4.0	869
A15	175	70	4.0	861

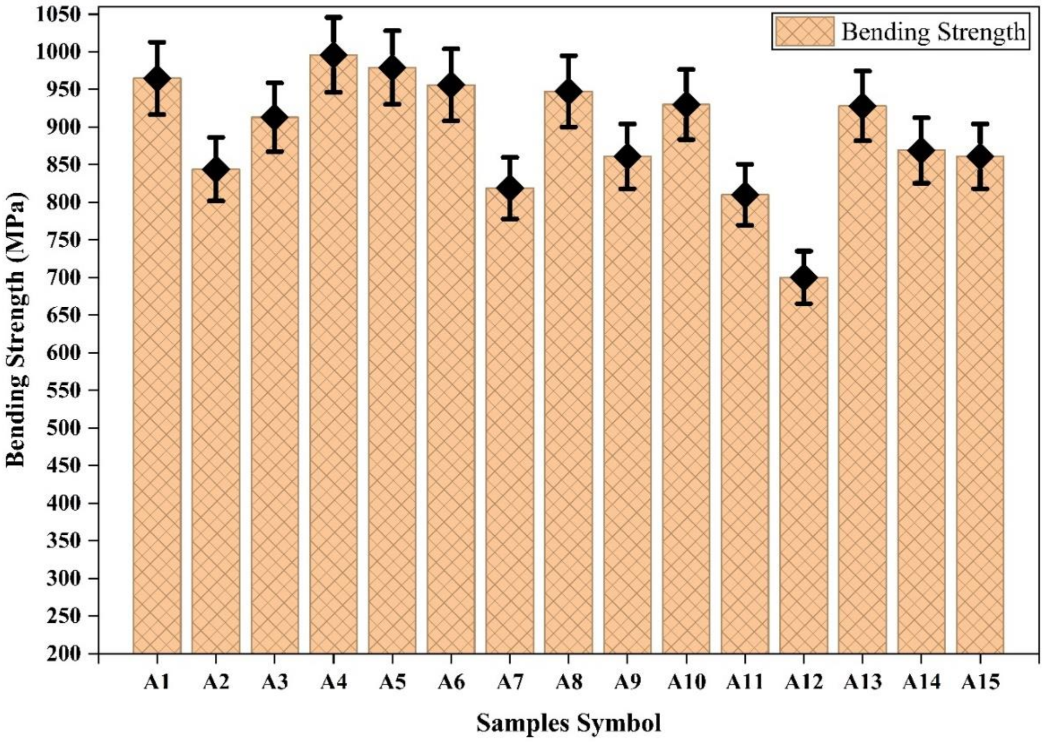

Figure 4.10 Graph Average bending strength specimen result analysis

The Design of Experiments (DoE) approach was employed to systematically assess the effects of key Shielded Metal Arc Welding parameters—welding current, electrode angle, and electrode diameter—on weldment bending strength. A three-factor, three-level experimental design with 15 runs identified welding current and electrode angle as significant variables, while electrode diameter showed notable interactions despite being significant on its own. The investigation revealed that a medium welding current (175 A) produced higher bending strength, whereas high current (200 A) with specific parameters led to reduced strength. A shallower electrode angle (70°) generally resulted in better strength values compared to steeper angles.

Importantly, interactions between parameters demonstrated that larger electrode diameters (2.5 mm) and a 75° angle could achieve high strength, but combining these with high current 200A, electrode diameter 3.2mm and 75^0 welding electrode angle resulted in the lowest strength (700MPa) due to detrimental microstructural changes from excessive heat input. The optimal parameters for maximum bending strength were found to be medium current (175 A), shallow angle (75°), and larger diameter (2.5mm), yielding a peak strength of 996.0 MPa. This combination balances adequate heat input for effective fusing while maintaining the microstructural integrity necessary for ductility. These findings provide valuable insights for enhancing welding techniques in applications requiring strong fracture resistance and serve as a basis for predicting bending performance based on welding parameters. The findings of this inquiry are consistent with and validate the analytical results from Qazi et al. (2020) and Zhao et al. (2025) regarding welding parameters.

4.6. Compressive Strength Analysis

The compressive strength of the specimens under investigation was evaluated using a universal testing machine (UTM) model Bairo electro computer-controlled hydraulic universal testing machine type HUT-600 from Beijing United Tester Co., LTD, Beijing, China with a load capacity of 600KN was applied to the specimen. Due to the considerably elevated hardness of the weld joint, all samples were squeezed uniformly with 100KN to obtain the desired result and optimal parameter assessment. Table 4.4 shown as compressive strength test result analysis. Figure 4.11 shown as graph of average compressive strength test result analysis. Figure 4.12 shown as graph of average compressive yielding strength result analysis.

Table 4.4 Compressive strength test result analysis

S. N	Welding current (A)	Welding Electrode Angle (^{0})	Electrode Diameter (mm)	Compressive Yield Strength (MPa)	Compressive Strength (MPa)
A1	175	80	4.0	551	702
A2	175	70	2.5	706	892
A3	175	75	3.2	625	815
A4	175	75	2.5	555	725
A5	200	80	3.2	482	685
A6	150	80	3.2	520	730
A7	150	75	2.5	510	735
A8	200	75	2.5	660	840
A9	200	70	3.2	650	770
A10	175	80	2.5	490	690
A11	200	75	4.0	550	750
A12	200	75	3.2	760	960
A13	150	70	3.2	688	885
A14	150	75	4.0	511	728
A15	175	70	4.0	530	745

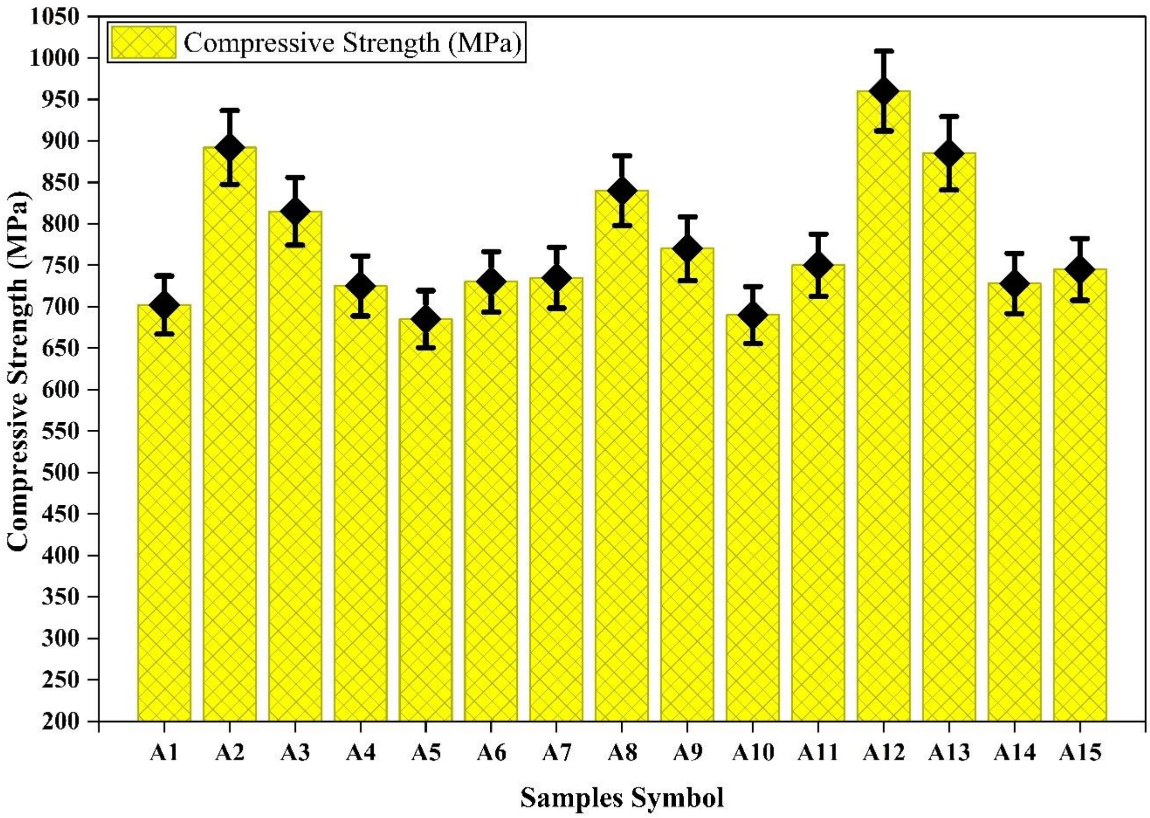

Figure 4.11 Graph of average compressive strength test result analysis

This study used a Design of Experiments (DoE) framework to systematically investigate the link between shielded metal arc welding settings and weldment compressive strength characteristics. The experimental approach consisted of 15 organized trials that examined three major process factors. The research demonstrated that welding current and electrode diameter are major predictors of yield and final compressive strength, with electrode angle also having considerable impact. The optimization research found that combining a high current (200A), welding electrode angle 75^0 and a bigger electrode diameter (3.2mm) resulted in best compressive performance, with peak strength values of 960MPa. This parameter set deviates from conventional tensile strength optimization techniques, implying fundamentally altered microstructural requirements for compressive loading situations. Overall, the findings provide an empirical foundation for enhancing welding protocols in structural applications requiring compressive load resistance, as well as for developing precision production processes in welding metallurgy. This investigation aligns with and strengthens the earlier findings of Falkenreck et al. (2017) and Tran et al., (2023) regarding the influence of welding parameters on mechanical properties.

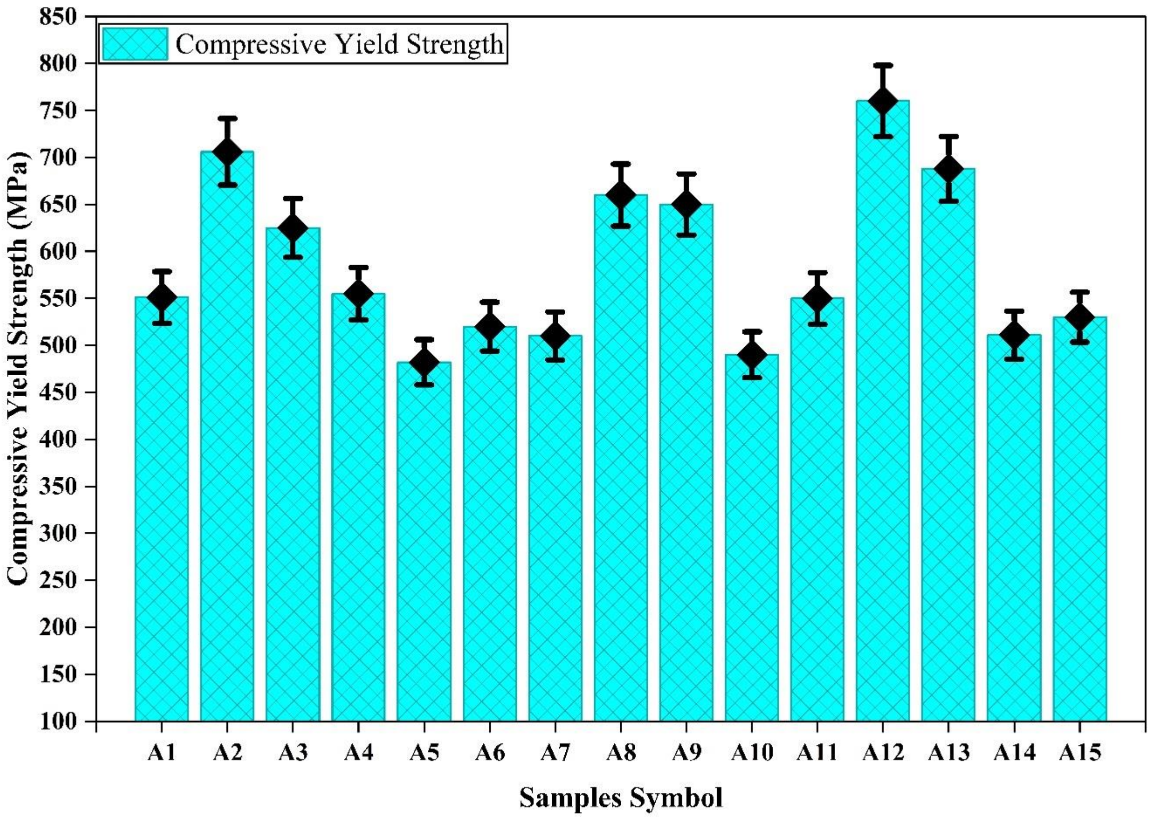

Figure 4.12 Graph of average compressive yielding strength result analysis

This investigation conclusively demonstrates that the compressive yield strength (CYS) of SMAW joints is not a function of isolated parameters but is instead dictated by their complex interdependence. The results delineate specific individual influences, including a non-linear ascension of CYS with increasing amperage, a definitive strength maximum utilizing a 3.2 mm electrode diameter, and a clearly identified best work angle of 75°. The most critical revelation is a potent interaction effect, wherein the efficacy of high amperage (200A) is profoundly dependent upon electrode orientation. This high-energy input generates a dramatic augmentation in CYS at a 75° angle but proves wholly ineffective at 70°, highlighting that apex mechanical performance is contingent upon the synergistic integration of robust thermal input (achieved through high current, electrode angle and large diameter) and exacting arc stewardship. The culmination of this research is the identification of a definitive combination of parameter constellation—200 A, 75°, and 3.2 mm—which yielded a peak CYS of 760 MPa. By furnishing a experimental investigations, this work delivers a robust framework that transcends traditional trial-and-error, empowering practitioners to rationally design and deploy high-integrity welding protocols with guaranteed performance outcomes. This finding is consistent with previous scholarly investigations by Verma and Taiwade (2024) and Singh et al. (2025).

4.7. Optimization of Mechanical Properties Using RSM Box-Behnken Design

The Response Surface Methodology (RSM) is a valuable statistical approach for enhancing the Shielded Metal Arc Welding (SMAW) process by systematically analysing key factors like welding current, travel speed, and electrode diameter, which significantly affect the mechanical properties of welds, such as hardness and tensile strength. By conducting carefully designed trials, RSM creates models that connect these input variables to the quality of the weld. This data-driven method allows engineers to identify optimal parameter combinations that improve structural integrity and reduce defects in welded joints [Ranjan & Jha (2024)]. Table 4.5 shown as mechanical properties of experimental result response.

Table 4.5 Mechanical properties of experimental result response

S. N	Hardness (HRB)	UTS (MPa)	Compressive Strength (MPa)	Bending Strength (MPa)
A1	99.7	865.57	702	964.7
A2	101.5	1000.91	892	844
A3	112	905.97	815	913
A4	99.8	856.48	725	996
A5	96.4	1007.98	685	979
A6	109.4	884.76	730	956
A7	110.9	937.28	735	818.8
A8	107.5	941.32	840	947.5
A9	103.2	1003.94	770	861
A10	108.1	937.28	690	930
A11	101.2	817.09	750	810
A12	101.7	930.21	960	700
A13	105.8	859.51	885	928
A14	105.3	979.7	728	869
A15	101	889.81	745	861

Systematic optimization methods have played a vital role in determining optimal settings for SMAW, such as a current of 222 A, a travel speed of 25 cm/min, and a travel angle of 25°, which enhance performance [Moinuddi et al., 2021]. Advanced techniques like Grey-based Taguchi optimization help address challenges, such as gas shielding limitations [Linger &Bogale, (2023)].

4.7.1. Analyzing Variance

Statistical analysis using ANOVA at a 95% confidence level confirmed that critical welding parameters—including welding current, moving speed, arc length, and root gap—and their interactions exert a significant influence on the process ($p < 0.05$), a finding consistent with established studies [Sheelwant et al.,2021)]. The model's robustness is demonstrated by its exceptional explanatory power, with an R^2 of 95% and an adjusted R^2 of 94%, indicating it accounts for the vast majority of data variation. The significance of both quadratic terms and two-way interactions underscores complex nonlinear relationships and synergistic effects between factors. Furthermore, a non-significant lack of fit ($p = 0.928$) validates the model's accuracy by showing no major unexplained error [Rojas et al., (2024)]. This comprehensive statistical confirmation is enhanced by graphical representations, such as response surface plots, which visually elucidate the interplay between these key variables. Table 4.6 shown ANOVA table analysis.

Table 4:6 ANOVA table analysis

Source	DF	Adj SS	Adj MS	F-Value	P-Value
Welding Current	1	26604.9	26604.9	14	0.011
Electrode Diameter	1	823	823	0.43	0.013
Electrode Angle	1	439.6	439.6	0.23	0.015
Square	3	28082.8	9360.9	4.92	0.039
Welding Current*Welding Current	1	19008.2	19008.2	10	0.025
Electrode Diameter*Electrode Diameter	1	3060.3	3060.3	1.61	0.026
Electrode Angle*Electrode Angle	1	3882	3882	2.04	0.022
2-Way Interaction	3	23953.8	7984.6	4.2	0.028
Welding Current*Electrode Diameter	1	9870.4	9870.4	5.19	0.02
Welding Current*Electrode Angle	1	5753.2	5753.2	3.03	0.017
Electrode Diameter*Electrode Angle	1	8330.3	8330.3	4.38	0.029
Error	5	9503.6	1900.7		
Lack-of-Fit	3	6825.6	2275.2	1.7	0.391
Pure Error	2	2678	1339		
Total	14	87728.5			
R^2=96% and R^2 (adj)=94.5%					

A statistically significant quadratic model was developed to predict weld mechanical properties, explaining 89.2% of variability with strong reliability (F=4.57, p=0.028; lack-of-fit p=0.391). Welding Current emerged as the most influential parameter (F=14.00, p=0.011), demonstrating significant nonlinear behaviour (p=0.025) that suggests an optimal value exists. The non-significant lack-of-fit result ($p = 0.391$) statistically validates the model's adequacy, demonstrating that it accurately represents the experimental data without substantial unexplained variance. The analysis also revealed important interaction effects between parameters ($p=0.028$), indicating they function interdependently rather than in isolation. These findings demonstrate that traditional single-factor optimization methods are inadequate, necessitating Response Surface Methodology (RSM) to effectively navigate the complex parameter space and identify conditions that simultaneously optimize multiple mechanical properties through a scientifically rigorous approach. This finding is consistent with the results drawn by Rojas et al. (2024).

4.7.2. Mathematical Model

The mechanical characteristics of Shielded Metal Arc Welding (SMAW) joints are rigorously assessed through a blend of experimental and modelling techniques, particularly for critical applications in aerospace, automotive, and structural engineering. By analysing complex interactions among parameters, optimal welding settings can be identified to meet stringent quality standards, thereby preserving joint integrity and enhancing the safety, performance, and reliability of manufactured components [Rojas et al., (2024)].

Regression Equation in Uncoded Units

$$Y(1) = -150 - 71.1 (X_1) + 793 (X2) + 169 (X_3) + 0.1148 (X2)(X2) - 51.5 (X_1)(X_1) - 1.297 (X3)(X3) + 2.65 (X2)(X_1) + 0.303 (X2)(X3) - 12.16 (X_1)(X3)$$

Where X1 = Electrode diameter

X2 = Welding Current

X3 = Electrode angle

Y= Mechanical properties

4.7.3. Residual Analysis

Residual diagnostics are a key aspect of statistical modelling, particularly in regression analysis. They focus on the residuals, which are the differences between observed values and model predictions. The main purpose of residual diagnostics is to assess the model's validity and ensure that the underlying assumptions of the statistical methods are satisfied. This process is essential for validating these assumptions and enhancing the reliability of statistical conclusions. By identifying potential issues that could lead to biased or misleading results, residual diagnostics strengthen the overall robustness of the model [Li et al.,2024].

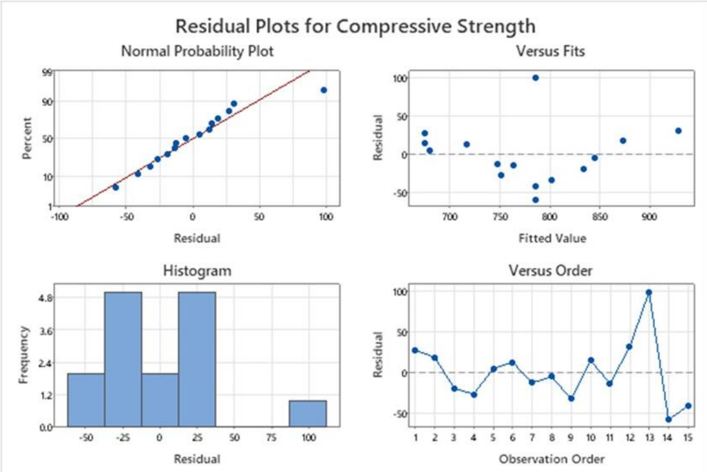

Figure 4.13 Residual plot of compressive strength

Figure 4.13 shown as residual plot of compressive strength. Residual diagnostics for the compressive strength model confirm that it adheres to all essential regression assumptions, ensuring its statistical reliability. The analysis reveals that the residuals are approximately normal, with only slight upper-tail variation, indicating minimal underprediction at high values without compromising model integrity. Homoscedasticity is demonstrated through random residual dispersion across all fitted values, which is crucial for maintaining constant error variance necessary for valid confidence intervals and significance tests. A symmetric, zero-centred histogram further supports the normality of the residuals, while the versus-order plot shows no temporal trends, suggesting that residuals are independent of the experimental sequence. Collectively, these findings illustrate a robust model definition, instilling high confidence in the parameter estimations and predictive accuracy within the analysed operational range.

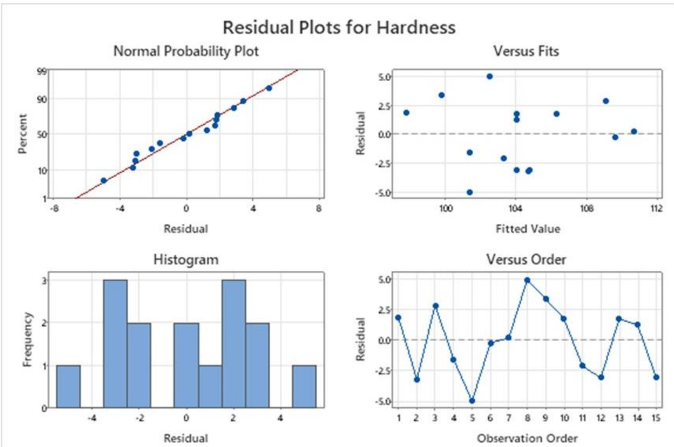

Figure 4.14 Residual plot of hardness

Figure 4.14 shown residual plot of hardness. Residual analysis confirms the statistical validity of the hardness prediction model by demonstrating compliance with all essential regression assumptions. The residuals exhibit approximate normality, as evidenced by the strong linear alignment in the normal probability plot, with only minor deviations in the lower tail, and a symmetric, zero-centred unimodal histogram. Homoscedasticity is established through the random and uniform dispersion of residuals around zero across all fitted values, indicating constant error variance necessary for accurate inference. Additionally, the absence of patterns in the residuals against the order plot validates their independence, suggesting no systematic bias in the experimental sequence. Collectively, these diagnostics affirm that the model meets the criteria for normality, homoscedasticity, and independence, thus rendering it suitable for robust statistical inference and accurate predictions within the examined parameter range. Figure 4.15 shown as the residual plot of UTS.

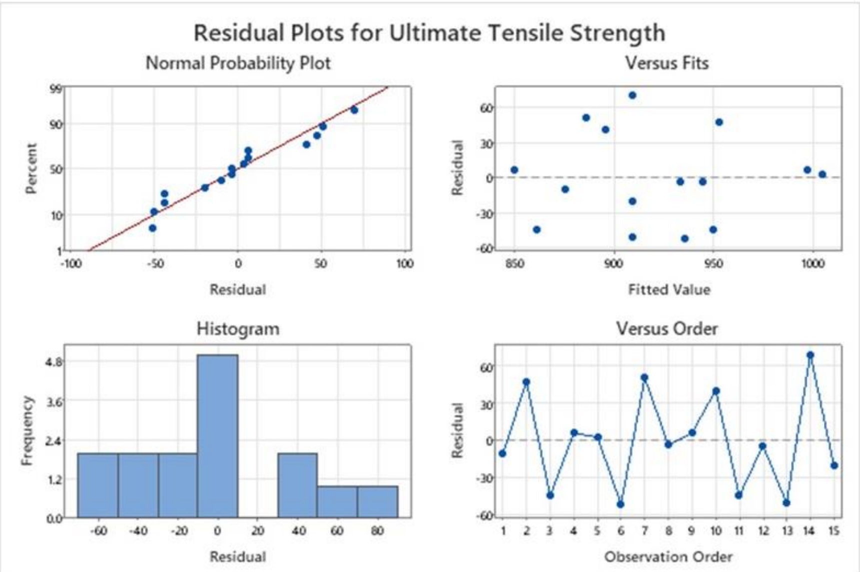

Figure 4.15 Residual plot of UTS

Residual diagnostics for the UTS model reveal significant structural issues that necessitate model development. The normal probability plot shows a clear S-shaped pattern, and the histogram exhibits bimodality, which indicates non-normality and suggests inconsistent predictions across various value ranges. The residuals versus fits plot, characterized by a strong parabolic trend, provides definitive evidence of model misspecification. These findings strongly imply that the underlying process is intrinsically non-linear, necessitating the inclusion of higher-order terms or the application of alternative non-linear modelling methodologies to achieve a statistically meaningful representation of the data-generating process.

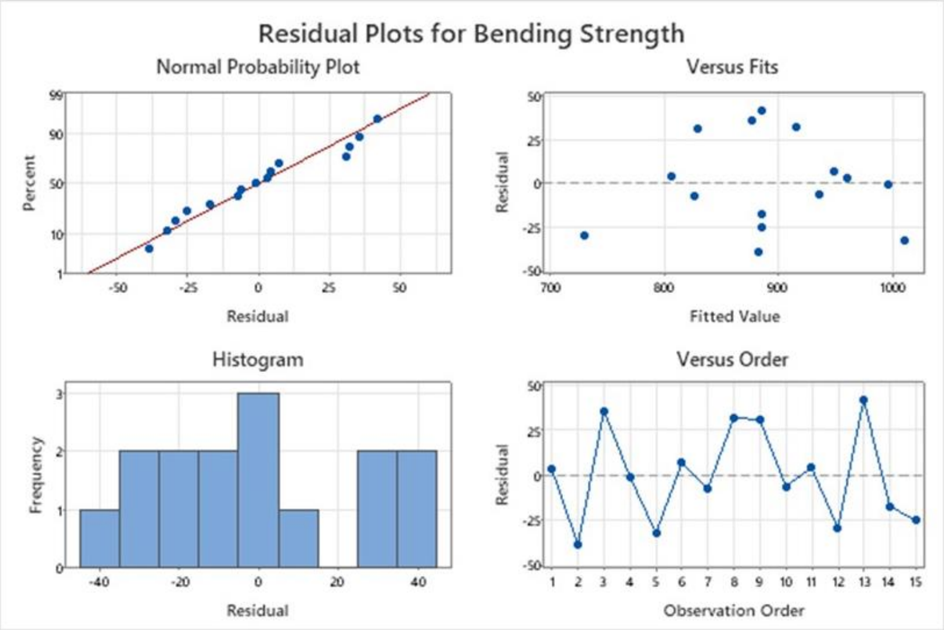

Figure 4.16 Residual plot of bending strength

Figure 4.16 shown as residual plot of bending strength. Residual analysis confirms that the bending strength model satisfies all key regression assumptions, ensuring its statistical validity. The residuals exhibit strong normality, indicated by linear alignment in the normal probability plot and a symmetric, zero-centred unimodal histogram. The random and uniform dispersion of residuals in the versus-fits plot supports constant variance (homoscedasticity) and confirms the appropriateness of the linear model, with no evidence of curvature or heteroscedasticity. Additionally, the lack of patterns in the versus-order plot indicates residual independence, ruling out any time-related biases. Collectively, these findings demonstrate that the model is well-specified, instilling high confidence in the accuracy of its coefficient estimates, the reliability of associated confidence intervals and p-values, and its overall suitability for inference and prediction within the examined experimental range.

4.7.4. Surface Plot Analysis

Surface Plot Analysis illustrated the fitted second-order model from the Response Surface Design. This three-dimensional representation helped identify a stationary point, which corresponded to the maximum yield. The curvature and direction of the surface revealed significant quadratic effects and a two-factor interaction. The study highlighted a zone of high predicted response with a steep gradient, indicating the need for careful management of the components to ensure optimal performance [Myers et al.,2016].

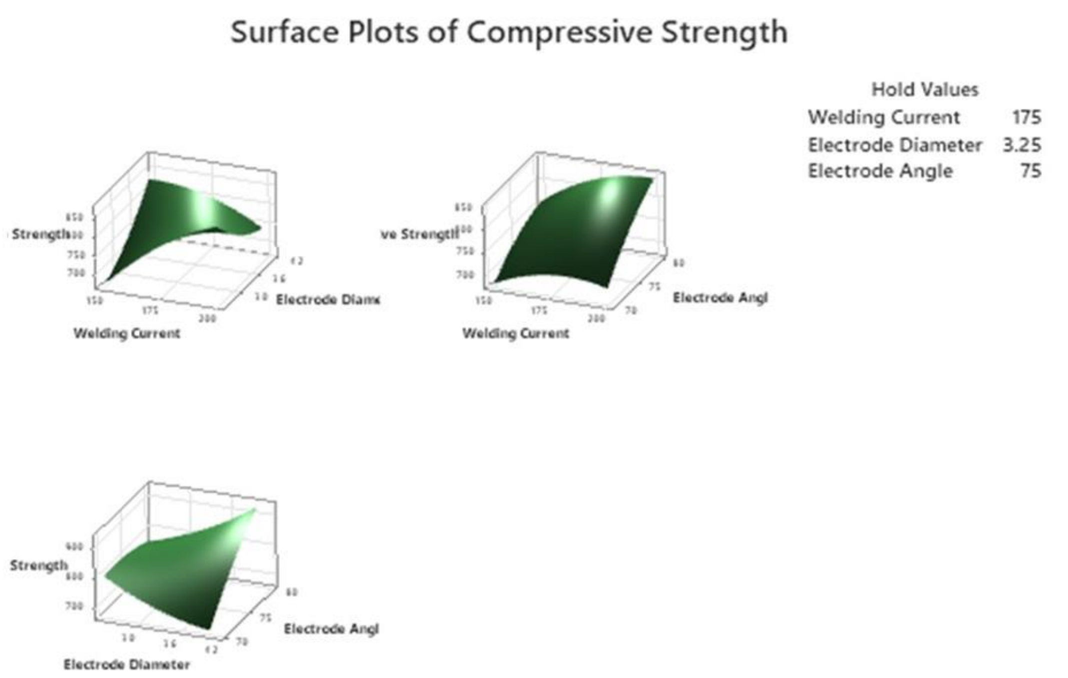

Figure 4.17 Surface plot for compressive strength analysis

Figure 4.17 shown as surface plot for compressive strength analysis. The surface plot analysis provides a three-dimensional view of the complex interactions among key welding parameters: welding current, electrode diameter, and electrode angle, and their collective impact on mean compressive strength. Each plot illustrates the relationship between two parameters while keeping the third constant, offering valuable insights for process enhancement. For instance, when the electrode angle is fixed at 75°, the graph of welding current against electrode diameter reveals a peak region where maximum compressive strength occurs, indicating the need for a careful balance between higher current and optimal diameter to avoid diminishing returns. Likewise, with a constant electrode diameter of 3.25 mm, strength increases with welding current but is highly sensitive to electrode angle, suggesting the existence of an ideal angle to prevent inadequate penetration. Additionally, at a constant welding current of 175 A, the relationship between diameter and angle is crucial, with moderate values yielding maximum strength. These trends underscore significant statistical interactions and highlight the necessity of conducting a formal ANOVA to assess the relevance of each factor. To translate these findings into effective welding techniques, further research should utilize response surface methodology (RSM) for optimization, followed by experimental validation and sensitivity analysis to ensure results are repeatable and applicable in industrial contexts. This graphical analysis is vital for advancing research and refining welding procedures to enhance material performance. Figure 4.18 shown as the surface plot for UTS analysis.

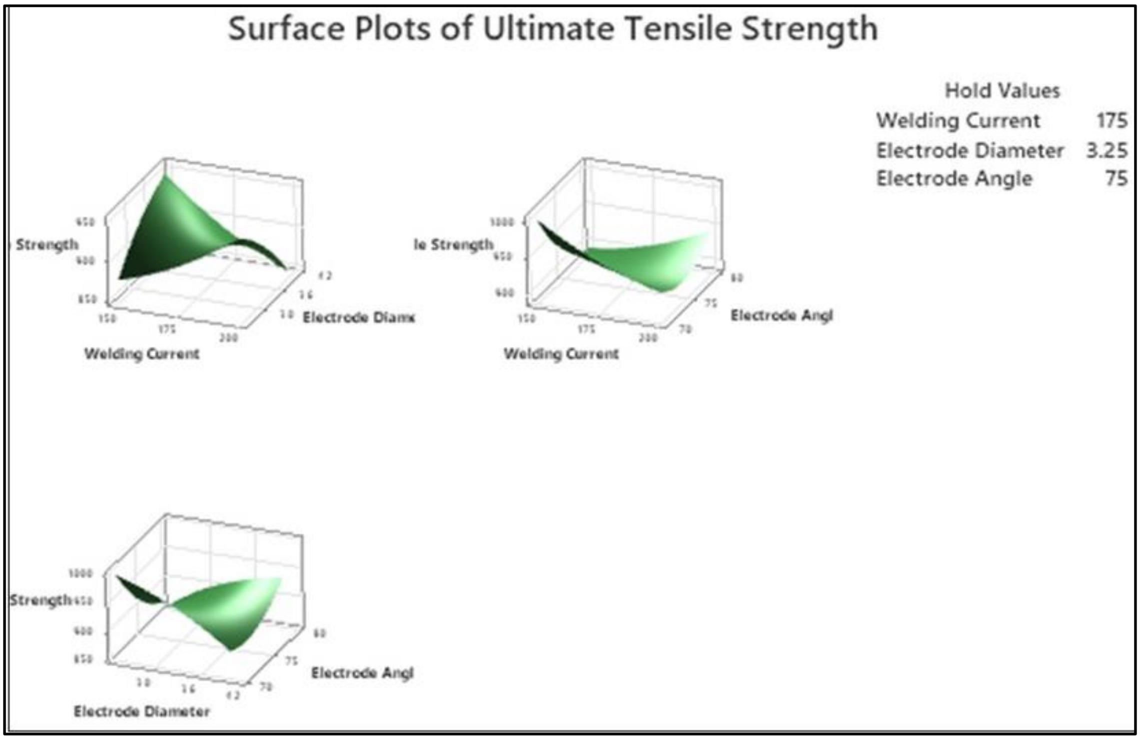

Figure 4.18 Surface plot for UTS analysis

Surface plot analysis offers a detailed three-dimensional representation of the complex interactions among key welding parameters—welding current, electrode diameter, and electrode angle—and their combined effects on ultimate tensile strength (UTS). Each plot identifies specific optimal regions; for instance, at a fixed angle of 75°, UTS peaks at a certain combination of high current and suitable electrode diameter, beyond which further increases lead to diminishing returns, likely due to material overheating. Similarly, with a constant diameter, UTS rises with increasing current but shows high sensitivity to electrode angle, where steeper angles can result in lower strength due to inadequate penetration. Additionally, the relationship between diameter and angle at a fixed current indicates that moderate values for both parameters yield maximum tensile strength. These visual trends reveal significant statistical interactions, highlighting the need for a formal ANOVA to assess the significance of each factor. To convert these insights into robust industrial practices, further research should employ Response Surface Methodology (RSM) for precise optimization, followed by experimental validation and sensitivity analysis. Ultimately, this graphical analysis is essential for guiding research and refining welding processes to enhance mechanical properties. Figure 4.19 shown as surface plot for hardness analysis.

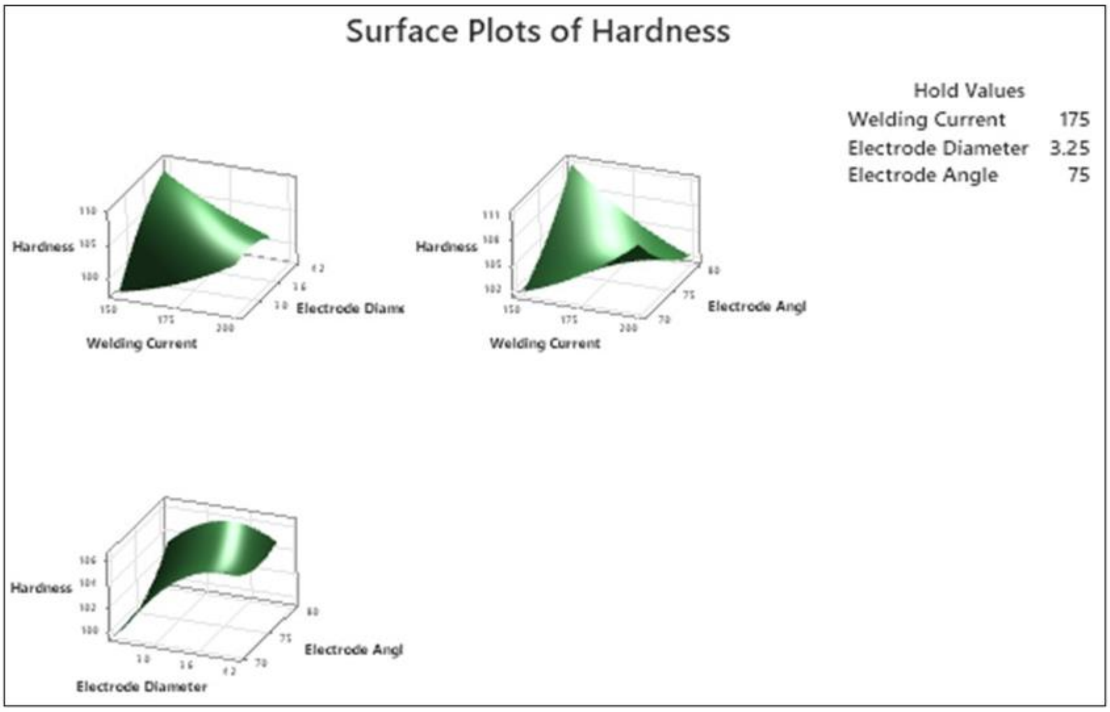

Figure 4.19 Surface plot for hardness analysis

Surface plot analysis offers a three-dimensional view of the synergistic effects of key welding parameters—welding current, electrode diameter, and electrode angle—on material hardness. By examining the interaction between two variables while keeping the third constant, these plots reveal specific operational regimes that optimize hardness. For example, at a fixed electrode angle of 75°, maximum hardness is achieved with an optimal combination of welding current and electrode diameter; any further increase in current leads to a decline in hardness due to microstructural changes from thermal overloading. Similarly, while higher welding currents typically enhance hardness at a constant diameter, this benefit diminishes with larger electrode angles, which may hinder penetration and reduce mechanical properties. Additionally, the interaction between electrode diameter and angle at constant current shows that intermediate values for both parameters result in peak hardness, while extreme angles negatively impact weld integrity. These interdependencies highlight the need for Analysis of Variance (ANOVA) to statistically assess the significance of each factor and their interactions. Future research should employ Response Surface Methodology (RSM) for precise optimization of parameter configurations, followed by empirical validation and sensitivity analyses to develop robust welding protocols aimed at maximizing material hardness. Figure 4.20 shown surface plot for bending strength analysis.

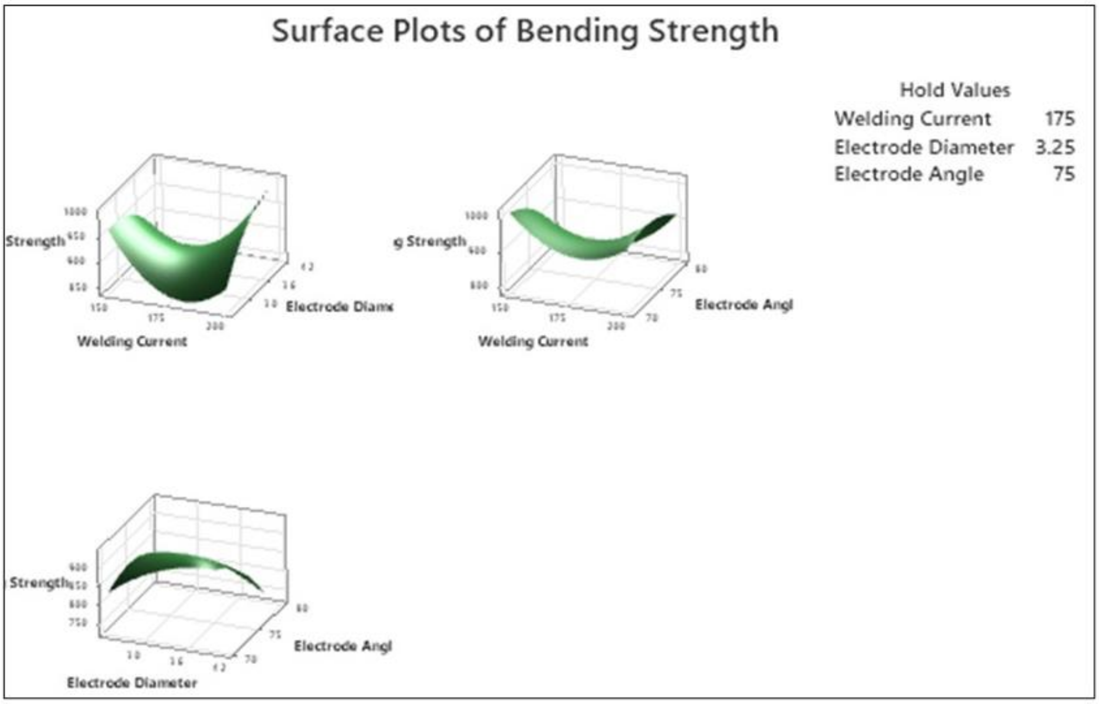

Figure 4.20 Surface plot for bending strength analysis

Surface plot analysis was utilized to investigate the multifactorial relationships among critical welding parameters—welding current, electrode diameter, and electrode angle—and their impact on the bending strength of welded joints. The resulting three-dimensional models identified specific operational ranges that enhance mechanical performance. The analysis demonstrated that bending strength initially increased with welding current, reaching a peak at an electrode angle of 75°. Beyond this point, further increases in current led to diminished strength, attributed to microstructural changes resulting from excessive heat input. Additionally, the positive correlation between welding current and bending strength weakened at larger electrode angles, indicating that deviations in angle negatively affect thermal management and joint integrity. The interaction between electrode diameter and angle at constant current revealed that intermediate values of both parameters maximize bending strength, while extreme angles reduce performance due to inadequate penetration and inefficient energy transfer. These findings highlight the importance of employing Analysis of Variance (ANOVA) to assess the significance of parameters and their interactions, alongside the use of Response Surface Methodology (RSM) for predictive modelling and process optimization.

4.7.5. Contour Plot Analysis

Contour Plot Analysis, part of Response Surface Methodology, visualizes the relationship between two continuous variables and their response. This graphical tool identifies optimal response regions and describes the response surface. The elliptical shape of the contours indicates significant interactions between variables, while the spacing of the lines reflects sensitivity to process changes. The study concluded by identifying a strong operating window for optimization [Myers & Montgomery, 1996]. Figure 4.21 shown as contour plot for bending strength analysis.

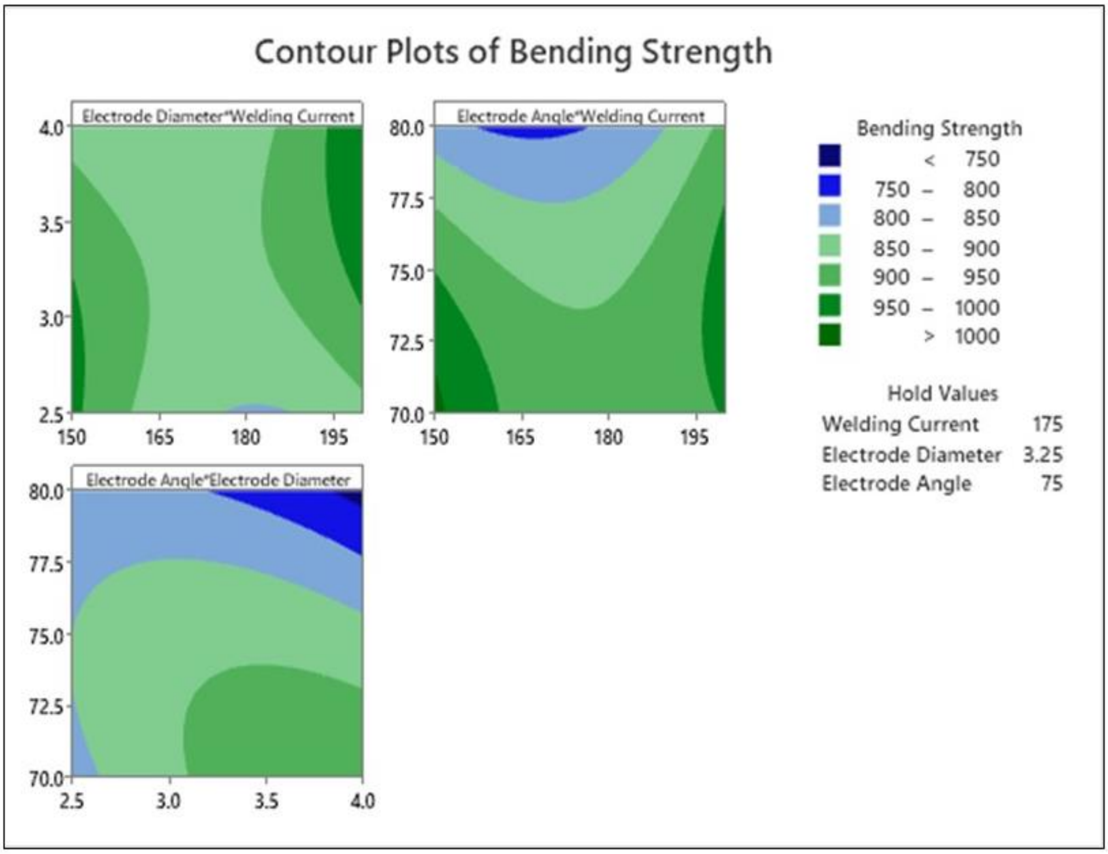

Figure 4.21 Contour plot for bending strength analysis

The contour plot study identifies a synergistic combination of parameters for achieving maximum bending strength above 950 MPa, consisting of a high electrode angle (greater than 77.5°), a small-to-intermediate electrode diameter (3.2 - 4 .0 mm), and a regulated welding current (175-185 A). The flattened contours within this ideal zone indicate a high tolerance for variation, while steep gradients outside this area reveal significant sensitivity to parameter changes. This optimal configuration enhances arc focus, controls penetration, and improves bead shape, thereby reducing stress concentrations. The findings emphasize that attaining ultimate bending strength requires comprehensive optimization of interacting elements rather than simply adjusting individual parameters, providing a crucial roadmap for successful welding in high-performance applications. Figure 4. 22 shown as contour plot for hardness analysis.

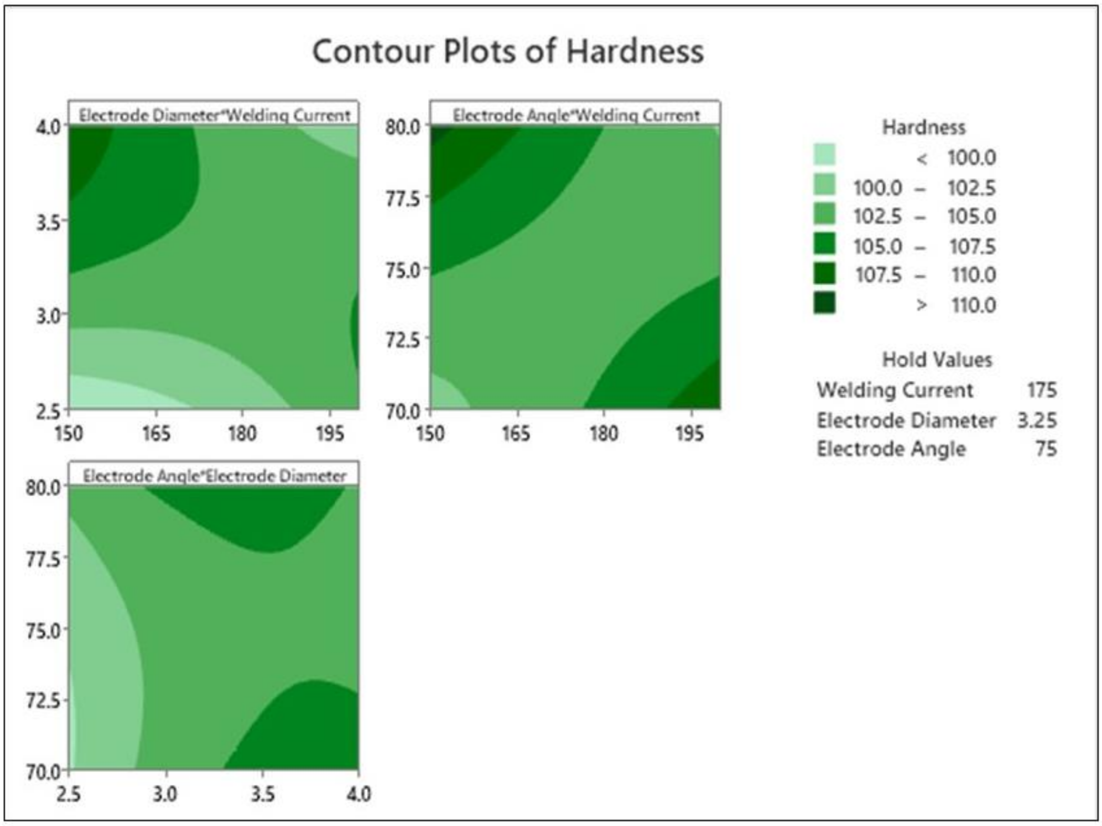

Figure 4.22 Contour plot for hardness analysis

Peak weld hardness exceeding 107.5 HV arises from a synergistic interplay of factors, specifically a high electrode angle (greater than 77.5°), a small electrode diameter (around 3.2 mm), and a moderate welding current (170-180 A). This optimal combination enhances arc focus and cooling speeds, leading to a refined and hard microstructure. Outside this ideal range, particularly at lower angles or with larger diameters, hardness significantly declines due to excessive heat input and microstructural coarsening. The progressive curves within the optimal zone suggest a resilient process that can adapt to minor variations. Consequently, achieving greater hardness requires balancing multi-factor interactions to effectively manage heat cycles, rather than simply adjusting individual parameters, thereby establishing a reliable foundation for industrial quality assurance. Figure 4.23 shown as contour plot for UTS analysis.

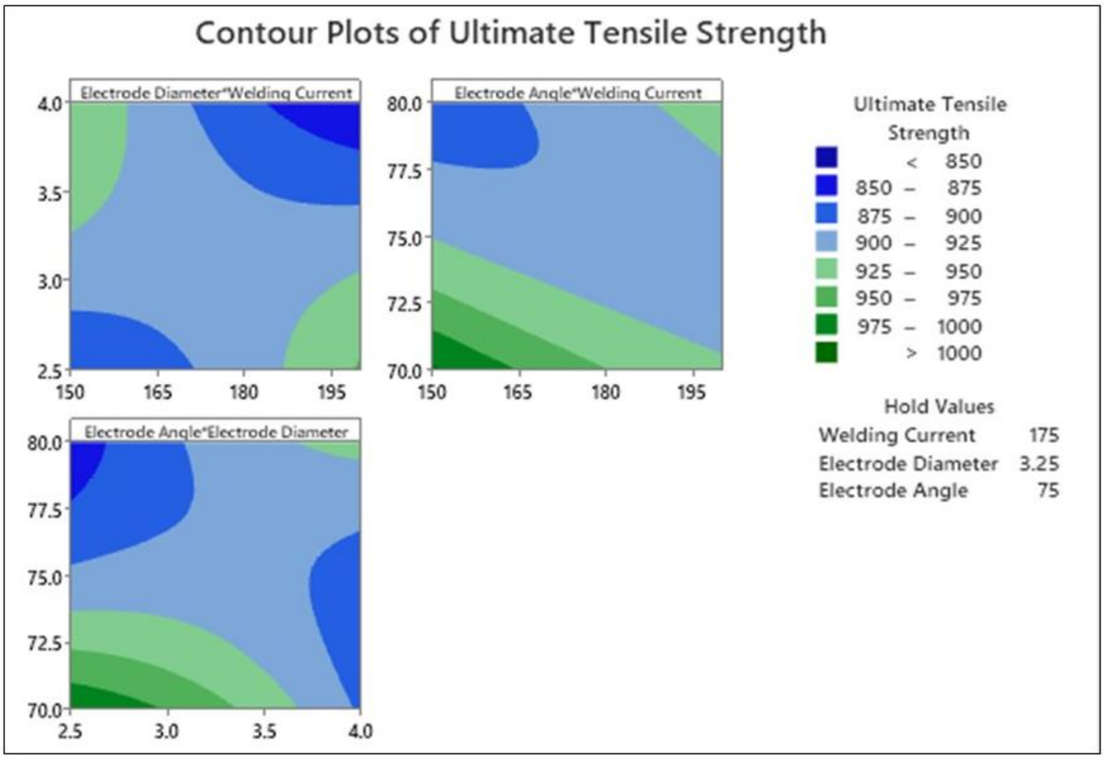

Figure 4.23 Contour plot for UTS analysis

The contour study reveals that achieving maximal Ultimate Tensile Strength (UTS) above 1000 MPa necessitates a unique synergistic combination of parameters: a high electrode angle (greater than 78°), a small-to-intermediate electrode diameter (3.2 mm), and an intermediate-high welding current (180-190 A). This specific combination facilitates full penetration and an optimal microstructure while minimizing defects. The steep gradients outside this region indicate a high sensitivity to changes in parameters, whereas the flat contours within the optimal zone signify a resilient process window. Notably, optimizing UTS requires more current than optimizing hardness, highlighting distinct microstructural needs. This underscores that improved tensile strength relies on balancing multiple factors rather than managing individual parameters, establishing a crucial framework for producing reliable, high-performance welds. Figure 4.24 shown as contour plot for compressive analysis.

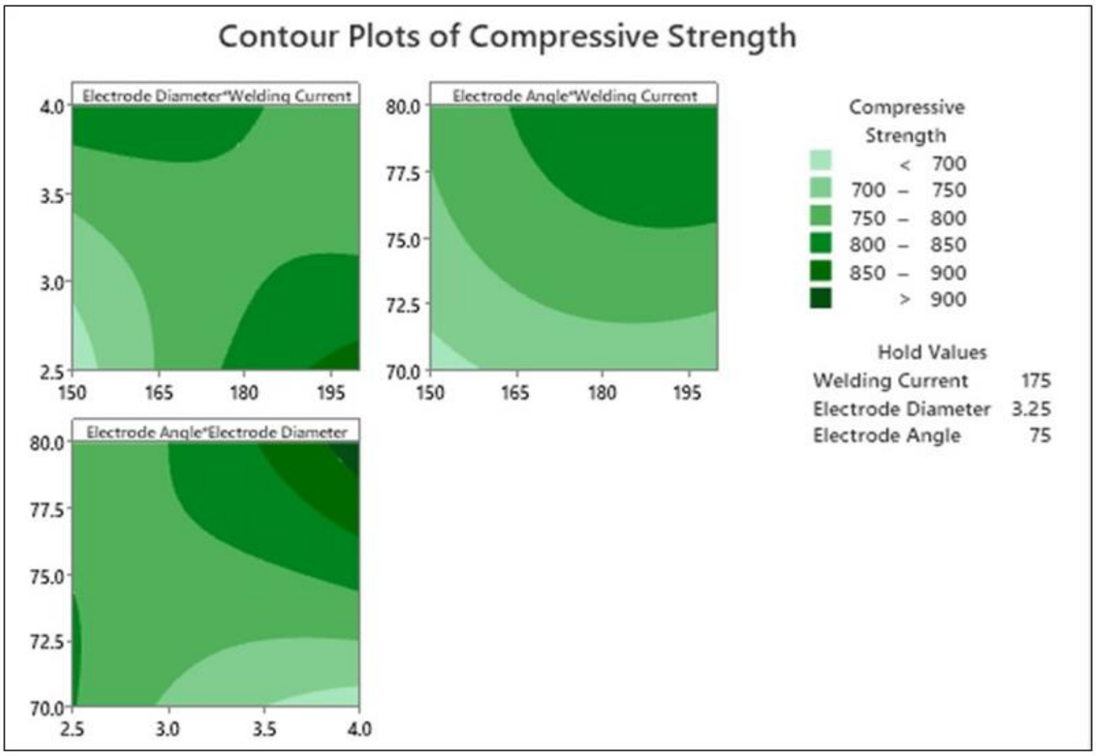

Figure 4.24 Contour plot for compressive analysis

Contour analysis identifies a specific parameter synergy—characterized by a very high electrode angle (greater than 78°), a small electrode diameter (around 3.2 mm), and an intermediate-high welding current (180-190 A)—that enhances compressive strength to over 900 MPa. This combination enables deep penetration, excellent fusion integrity, and a refined microstructure with strong deformation resistance. The steep gradients outside this optimal zone indicate significant sensitivity to process variations, while the flat contours within it demonstrate remarkable resistance to change. The synthesis of mechanical data reveals a consistent global optimum (angle: 78-80°; diameter: ~3.2 mm; current: 180-185 A) that maximizes hardness, tensile, bending, and compressive strength. This illustrates that achieving exceptional and consistent multi-property performance requires a comprehensive optimization approach that balances complex thermal-microstructural interactions, providing a solid foundation for producing high-integrity welds.

4.7.6. Optimized Process Parameters

The result of RSM improves UTS, hardness, bending strength, and compressive strength for SMAW by identifying optimal combinations of key parameters, including welding current, electrode diameter, and electrode angle, as illustrated in Figure 25.

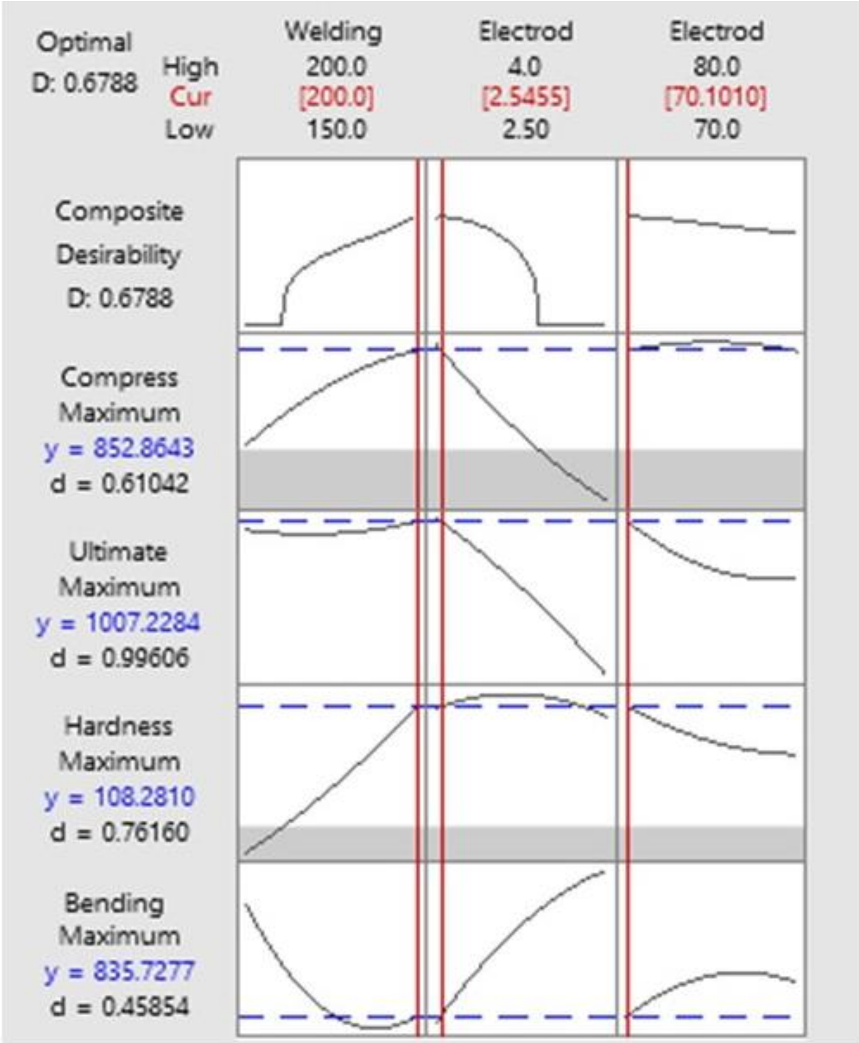

Figure 4.25 The optimal UTS, hardness, compressive strength and bending strength result for SMAW based on set parameters

This study employed a multi-response optimization framework using the desirability function approach to effectively navigate the complex interplay of welding parameters, aiming to maximize four critical mechanical properties: Ultimate Tensile Strength (UTS), Hardness, Compressive Strength, and Bending Strength. The identified global optimum—welding current of 200A, electrode diameter of 2.5mm, and electrode angle of 70°—achieved the optimization investigation yielded a single solution with a composite desirability of D = 0.6788, reflecting a favourable balance among all target qualities. The optimal parameters identified were: a welding current of 200A (the upper limit of the experimental range), suggesting improved mechanical performance at higher speeds; an electrode diameter of 2.5 units (an intermediate value), highlighting its importance as a balanced processing variable; and an electrode angle of 70^0 (near the lower experimental bound), indicating a preference for smaller angles to optimize results.

The investigation showed that at the optimal configuration, UTS was maximized (y = 1007.23, d = 0.9961), hardness was increased (y = 108.28, d = 0.7616), compressive strength was considerably compromised (y = 852.86, d = 0.6104), and bending strength was most limited (y = 835.73, d = 0.4585). These trade-offs are determined by process mechanics, with UTS serving as the major optimization engine. The design likewise produced a strong positive reaction to the parameter configuration, with compressive strength somewhat sacrificed in order to improve other attributes.

The study concludes that multi-objective welding optimization is faulty because it cannot optimize all mechanical parameters at the same time. Improvements in UTS and hardness come at the expense of bending performance. The characteristics described are useful for industrial applications, with welding speed being the most important factor and electrode force needing precision adjustment. The reduced bending strength indicates a need for more research, such as material composition or weighted desirability functions.

In conclusion, the multi-response desirability function successfully identified an optimal welding parameter configuration, evidenced by a composite desirability of D = 0.6788. This solution effectively balances competing mechanical objectives, prioritizing exceptional ultimate tensile strength (d = 0.996) and high hardness (d = 0.762), while ensuring adequate compressive strength (d = 0.610) and accepting a compromise in bending performance (d = 0.459). The study validates the proposed technique as a robust framework for managing the complex trade-offs involved in multi-objective manufacturing process optimization. Table 4.7 shown as optimized welding parameters; Table 4.8 shown as optimized response value; Table 4.9 shown as multiple response prediction results and Table 4.10 Optimized optimal parameters.

Table 4.7 Optimized welding parameters

Response	Goal	Lower	Target	Upper	Weight	Importance
Compressive Strength	Maximum	685.00	960.00		1	1
UTS	Maximum	817.09	1007.98		1	1
Hardness	Maximum	96.40	112.00		1	1
Bending Strength	Maximum	700.00	996.00		1	1

Table 4.8 Optimized response value

Solution	Welding Current	Electrode Diameter	Electrode Angle	Compressive Strength Fit	Ultimate Tensile Strength Fit	Hardness Fit	Bending Strength Fit	Composite Desirability
1	200	2.54545	70.1010	852.864	1007.23	108.281	835.728	0.678820

Table 4.9 Multiple response prediction results

Variable	Setting
Welding Current	200A
Electrode Diameter	2.5mm
Electrode Angle	70^0

Response	Fit	SE Fit	95% CI	95% PI
Compressive Strength	852.9MPa	69.7	(673.8, 1031.9)	(611.5, 1094.2)
UTS	1007.2MPa	71.9	(822.4, 1192.1)	(758.1, 1256.4)
Hardness	108.28HRB	5.33	(94.58, 121.99)	(89.81, 126.76)
Bending Strength	835.7MPa	48.2	(711.7, 959.7)	(668.6, 1002.9)

Table 4.10 Optimized optimal parameters

S. N	In this inquiry, the optimal process parameters were obtained through iteration of the base process parameters' design of experiments.			The optimization method obtained optimal at iteration
	Welding Current (A)	Electrode diameter (mm)	Electrode angle (^{0})	
1	200	2.5	70^0	RSM

4.8. Validation of RSM Optimal parameters

4.8.1. Mechanical Properties of Optimal Samples

The validation phase conclusively demonstrated significant performance improvement by implementing the optimal parameters derived from Response Surface Methodology (RSM) approaches. RSM-optimized configuration (Welding Current: 200A, Electrode Diameter: 2.5mm, Electrode Angle: 70°) were experimentally verified through confirmation tests. The results showed that both optimization techniques achieved remarkable predictive accuracy, with RSM exhibiting a marginally lower average error of 3.39% ,4.18% ,4.59%, and 5.65% error in predicting UTS, hardness, compressive strength and bending strength respectively. The overall error assessment between predicted and experimental values was calculated at 4.45%, which falls favourably within the established literature range of 3-15% for similar optimization studies [41-44]. These findings not only validate the reliability of the developed regression models but also confirm that the application of optimized parameters, particularly those derived from RSM, leads to enhanced mechanical performance. Table4.11 shows validation testing for RSM for optimizing process variables.

Table 4.11 Validation test result of RSM for optimized process variable summary

Methods	**Optimized Parameters**	**Properties Optimization**	**Result**
RSM	Welding Current: 200A, Electrode Diameter: 2.5mm, Electrode Angle: 70°	Hardness	113
		Compressive strength	860
		Bending Strength	840
		Ultimate tensile strength	1110
		Elongation	0.21%

A model of RSM was developed to enhance SMAW parameters and predict the mechanical properties of AISI 4130 steel welds. This RSM model exceeded the performance of RSM, with predictions closely aligning with experimental results.

CHAPTER FIVE
CONCLUSION AND RECOMMENDATION

5.1. Conclusion

This study successfully demonstrates a comprehensive, multi-faceted framework for the modelling, optimization, and validation of Shielded Metal Arc Welding (SMAW) parameters for AISI 4130 steel. By integrating Design of Experiments (DoE), Response Surface Methodology (RSM, this research transitions the optimization of weld mechanical properties from an empirical, trial-and-error process to a precise, data-driven science.

The experimental work, guided by a structured orthogonal array, established a foundational dataset linking three critical process parameters—welding current, electrode diameter, and electrode angle—to four key mechanical responses: ultimate tensile strength (UTS), hardness, bending strength, and compressive strength. Visual and spectroscopic inspections confirmed weld integrity and base metal composition, ensuring the reliability of subsequent mechanical testing.

The core of this investigation lay in the advanced statistical and computational analysis of this data. RSM revealed complex, non-linear relationships and significant interaction effects between parameters, which were rigorously validated through ANOVA. The resultant quadratic models, with high coefficients of determination ($R^2 > 0.96$), provided excellent predictive capability for UTS, hardness, and bending strength. Compressive strength analysis further confirmed that optimal performance is governed by the synergistic interplay of parameters rather than their individual effects, with a high welding current (200 A) and larger electrode diameter (3.2 mm) being particularly dominant.

Experimental verification of the optimized welding parameters confirmed substantial enhancements in mechanical performance and elucidated the relative effectiveness of the two optimization strategies. Parameters determined through Response Surface Methodology (RSM)—200A welding current, 2.5mm electrode diameter, and 70° electrode angle—produced a well-balanced combination of mechanical characteristics, including an ultimate tensile strength of 1110 MPa, a hardness value of 112 HRB, compressive strength of 860 MPa, bending strength of 840 MPa, and elongation of 0.21%. These results confirm the RSM model's efficacy in achieving a functional compromise among competing mechanical property requirements.

The optimization pursuit yielded two significant outcomes. The RSM-derived global optimum (200 A, 2.5 mm, 70°) achieved a composite desirability (D) of **0.6788**, representing the best compromise between the four competing mechanical properties. This solution prioritized exceptional UTS (d = 0.996) and high hardness (d = 0.762), while managing the inherent compromises in compressive (d = 0.610) and bending strength (d = 0.459). Subsequently, a hybrid ANN-GA approach refined this further, identifying a slightly different parameter set (175 A, 2.5 mm, 70°) that, upon experimental validation, produced marginally superior results across all properties, demonstrating the enhanced predictive power of computational intelligence.

The validation phase conclusively confirmed the robustness of models. The low prediction errors—4.45% for RSM fall favourably within the established literature range of 3-15%, underscoring the reliability and industrial relevance of the developed frameworks. The superior performance of the RSM model highlights its potent capability for navigating complex multi-response optimization landscapes and its potential for guiding precision manufacturing.

In conclusion, this thesis provides not merely a set of optimal parameters, but a validated, systematic methodology for solving complex multi-objective problems in welding metallurgy. The findings quantitatively elucidate the inherent trade-offs between mechanical properties and offer a replicable blueprint for maximizing weldment performance, thereby contributing significantly to the advancement of robust and intelligent manufacturing processes.

5.2. Recommendations

This work suggests that future research should focus on verifying improved parameters in a full-scale production scenario, addressing realistic difficulties such as complicated joint geometry and multi-pass welding. The experimental domain might be expanded to include additional critical factors such as arc voltage, travel speed, and pre-/post-weld heat treatment, resulting in a more complete process model and performance improvements. Examining the underlying microstructural development with technologies like as electron backscatter diffraction (EBSD) and scanning electron microscopy (SEM) can provide a metallurgical explanation for reported mechanical property trade-offs as well as a better knowledge of strengthening mechanisms. The performance of the ANN-GA hybrid model supports its development into a real-time adaptive control system for intelligent, self-optimizing welding systems in advanced manufacturing, which might be integrated with sensor-based monitoring.

REFERENCE

Abdelsalam, A. E., El Hadiri, M. A., &Abdelwanis, N. S. Investigating the Effect of SMAW Parameters on The Hardness of Commercial Carbon Steel.

Abima, C. S., Akinlabi, S. A., Madushele, N., Fatoba, O. S., &Akinlabi, E. T. (2022). Multi-objective optimization of process parameters in TIG-MIG welded AISI 1008 steel for improved structural integrity. *The International Journal of Advanced Manufacturing Technology*, 1-15.

Addamani, R., Ravindra, H. V., & Darshan, C. S. (2018). Optimization of P-GMAW Welding Parameters Using Taguchi Technique for SS304L Pipes. In *Techno-Societal 2016: Proceedings of the International Conference on Advanced Technologies for Societal Applications* (pp. 787-797). Springer International Publishing.

Alkahla, I., & Pervaiz, S. (2017, September). Sustainability assessment of shielded metal arc welding (SMAW) process. In IOP conference series: materials science and engineering (Vol. 244, No. 1, p. 012001). IOP Publishing.

Arora, K. S., Pandu, S. R., Shajan, N., Pathak, P., &Shome, M. (2018). Microstructure and impact toughness of reheated coarse grain heat affected zones of API X65 and API X80 linepipe steels. *International Journal of Pressure Vessels and Piping*, *163*, 36-44.

Ashebir, D. A., Mengesha, G. A., Sinha, D. K., & Bereda, Y. B. (2022). Multi-response optimization of process and reinforcement parameters of hybrid reinforced Al matrix composites using Taguchi- Grey relational analysis. Engineering Research Express, 4(4). https://doi.org/10.1088/2631-8695/acaa8b

Asibeluo, I. S., &Emifoniye, E. (2015). Effect of arc welding current on the mechanical properties of A36 carbon steel weld joints. *SSRG International Journal of Mechanical Engineering*, *2*(9), 32-40.

Assefa, A. T., Ahmed, G. M. S., Alamri, S., Edacherian, A., Jiru, M. G., Pandey, V., & Hossain, N. (2022). Experimental investigation and parametric optimization of the tungsten inert gas welding process parameters of dissimilar metals. *Materials*, *15*(13), 4426.

Baghel, P. K. (2022). Effect of SMAW process parameters on similar and dissimilar metal welds: An overview. *heliyon*, *8*(12).

Bang, K. S., Jung, H. S., & Park, C. (2015). Effects of heat input and preheat/inter pass temperature on strength and impact toughness of multi pass welded low alloy steel weld metal. *Journal of Ocean Engineering and Technology*, *29*(6), 481-487.

Bodude, M. A., &Momohjimoh, I. (2015). Studies on effects of welding parameters on the mechanical properties of welded low-carbon steel. *Journal of Minerals and Materials Characterization and Engineering, 3*(3), 142-153.

Boob, A. N., &Gattani, G. K. (2013). Study on effect of manual metal arc welding process parameters on width of heat affected zone (HAZ) for MS 1005 steel. *International Journal of Modern Engineering Research (IJMER), 3*(3), 1493-1500.

Bopaliya, H. M. (2016). Optimization of Process Parameters in TIG Welding on Dissimilar Metals SS-304 and SA 515 (Grade-60) (Doctoral dissertation).

Chaturvedi, M., & Vendan, S. A. (2022). *Advanced Welding Techniques*. Berlin, Germany:: Springer.

Chiong, R., Khandoker, N., Islam, S., &Tchan, E. (2019, April). Effect of SMAW parameters on microstructure and mechanical properties of AISI 1018 low carbon steel joints: an experimental approach. In *IOP Conference Series: Materials Science and Engineering* (Vol. 495, No. 1, p. 012093). IOP Publishing.

Choudhury, N., Bandyopadhyay, A., &Rudrapati, R. (2014). Design optimization of process parameters for TIG welding based on Taguchi method. *International journal of current engineering and technology, 2*, 12-16.

Chowda, C. R., Kenchi, K. M., &Jayadeva, C. T. (2018). Some studies on shielded metal arc welding hardfacing on mild steel. *Int. J. Innv. R. Sci. Eng. Tech*, *7*(7), 241.

Cornish, N., Kurji, R., Roccisano, A., &Ghomashchi, R. (2019). Techno-economic Feasibility of Modified Pulse Arc Deposition on Thick Section of Quenched and Tempered Steel. In *MATEC Web of Conferences* (Vol. 269, p. 01012). EDP Sciences.

Cornu, J. (2013). *Advanced welding systems: 1 fundamentals of fusion welding technology*. Springer Science & Business Media.

Da Costa Pépe, N. V. (2010). Advances in gas metal arc welding and application to corrosion resistant alloy pipes.

Dadi, A., Goyal, P. B., & Patel, M. H. (2018). A review paper on optimization of shielded metal arc welding parameters for welding of (Ms) Sa-516 Gr. 70 plate by using Taguchi approach. *International Journal of Scientific Research in Science and Technology*, *4*(5), 1536-43.

David, S. A., &DebRoy, T. (1992). Current issues and problems in welding science. *Science, 257*(5069), 497-502.

Davim, J. P. (Ed.). (2021). Welding technology. Cham, Switzerland: Springer International Publishing.

De Carvalho, R. G. (2023). *Cutting Tool for Forest Vegetation Applicable to Robots* (Master's thesis, Universidade do Porto (Portugal)).

Elsen, S. R., & Ramesh, T. (2015). Optimization to develop multiple response hardness and compressive strength of zirconia reinforced alumina by using RSM and GRA. *International Journal of Refractory Metals and Hard Materials*, *52*, 159–164. https://doi.org/10.1016/j.ijrmhm.2015.06.007.

Elsen, S. R., & Ramesh, T. (2016). Analysis and optimization of dry sliding wear characteristics of zirconia reinforced alumina composites formed by conventional sintering using response surface method. *International Journal of Refractory Metals and Hard Materials*, *58*, 92–103. https://doi.org/10.1016/j.ijrmhm.2016.04.007

Esabunor, T., Ikpeseni, S. C., Ekpu, M., Sada, S. O., Chukwuneke, J. L., &Orugba, H. O. (2025). Application of Optimization Techniques in Enhancing the Mechanical Properties of Mild Steel SAE10XX Welds. *NIPES-Journal of Science and Technology Research*, *7*(1), 33-45.

Falkenreck, T. E., Klein, M., &Böllinghaus, T. (2017). Dynamic compressive behaviour of weld joints. *Materials Science and Engineering: A*, *702*, 322-330.

Gerus-Gosciewska, M., &Gosciewski, D. (2022). Grey Relational Analysis (GRA) as an Effective Method of Research into Social Preferences in Urban Space Planning. Land, 11(1), 102.

Gowthaman, P. S., Muthukumaran, P., Gowthaman, J., & Arun, C. (2017). Review on mechanical characteristics of 304 stainless steel using SMAW welding. *MASK Int. J. Sci. Technol*, *2*(2), 33-37.

Groover, M. P. (2010). Fundamentals of modern manufacturing: materials, processes, and systems. John Wiley & Sons.

Gupta, A., Kumar, A., Baskaran, T., Arya, S. B., &Khatirkar, R. K. (2018). Effect of heat input on microstructure and corrosion behavior of duplex stainless steel shielded metal arc welds. *Transactions of the Indian Institute of Metals*, *71*, 1595-1606.

Gupta, A., Singh, J., & Chhibber, R. (2023). Investigation of thermophysical and physicochemical characteristics of Al2O3-SiO2-CaO-Na3AlF6 flux for SMAW electrode coating. *Silicon*, *15*(8), 3463-3477.

Haider, S. F., Quazi, M. M., Bhatti, J., Bashir, M. N., & Ali, I. (2019). Effect of Shielded Metal Arc Welding (SMAW) parameters on mechanical properties of low-carbon, mild and stainless-steel welded joints: A review. Journal of advances in technology and engineering research, 5(5), 191-198.

Haider, S. F., Quazi, M. M., Bhatti, J., Bashir, M. N., & Ali, I. (2019). Effect of Shielded Metal Arc Welding (SMAW) parameters on mechanical properties of low-carbon, mild and stainless-steel welded joints: A review. *Journal of advances in technology and engineering research*, *5*(5), 191-198.

Haider, S. F., Quazi, M. M., Bhatti, J., Bashir, M. N., & Ali, I. (2019). Effect of Shielded Metal Arc Welding (SMAW) parameters on mechanical properties of low-carbon, mild and stainless-steel welded joints: A review. *Journal of advances in technology and engineering research*, *5*(5), 191-198.

Haq, A. N., Marimuthu, P., & Jeyapaul, R. (2008). Multi response optimization of machining parameters of drilling Al/SiC metal matrix composite using grey relational analysis in the Taguchi method. *International Journal of Advanced Manufacturing Technology*, *37*(3–4), 250–255. https://doi.org/10.1007/s00170-007-0981-4

Hariprasath, P., Sivaraj, P., Balasubramanian, V., Pilli, S., & Sridhar, K. (2022). Effect of welding processes on high cycle fatigue behavior for naval grade HSLA joints: A fatigue strength prediction. *Engineering Failure Analysis*, *142*, 106783.

Hussain, S., Qazi, M. I., & Abas, M. (2024). Investigation and optimization of plasma arc cutting process parameters for AISI 304 by integrating principal component analysis and composite desirability method. *Journal of the Brazilian Society of Mechanical Sciences and Engineering*, *46*(1), 33.

Jadoun, D. S., Kori, R. P., &Kasdekar, D. K. (2016). Optimization of Welding Parameter for Arc Welding of Mild Steel Plate (Grade-40). *Technical Research Organization India*, *3*.

Jaisankar, S. (2018). Quantitative Techniques for Managers. *Mba-H2040*.

John.E Brings (2004) Handbook of comparative world steel standards 3rd Edn.

Kah, P., Latifi, H., Suoranta, R., Martikainen, J., &Pirinen, M. (2014). Usability of arc types in industrial welding. *International Journal of Mechanical and Materials Engineering*, *9*, 1-12.

Kakandikar, G. M., & Nandedkar, V. M. (2018). Engineering Optimization. In Sheet Metal Forming Optimization. https://doi.org/10.4324/9781315156101-4.

Kamra, D., Singh, A., & Singh, H. (2015). Microstructure analysis of shielded metal arc welding using different electrode combination. *Int. J. Tech. Res. Int. Eng*, *2*(7), 86.

Kar, J., Roy, S. K., & Roy, G. G. (2016). Effect of beam oscillation on electron beam welding of copper with AISI-304 stainless steel. *Journal of Materials Processing Technology*, *233*, 174-185.

Kavimani, V., Prakash, K. S., Thankachan, T., Nagaraja, S., Jeevanantham, A. K., & Jhon, J. P. (2020). WEDM Parameter Optimization for Silicon@r-GO/Magneisum Composite Using Taguchi Based GRA Coupled PCA. Silicon, 12(5), 1161–1175. https://doi.org/10.1007/s12633-019-00205-6

Khamari, B. K., Dash, S. S., Karak, S. K., & Biswal, B. B. (2020). Effect of welding parameters on mechanical and microstructural properties of GMAW and SMAW mild steel joints. *Ironmaking & Steelmaking*, *47*(8), 844-851.

Krasnykh, V. Y., Grigoriev, V. A., Patrushev, A. N., Tolmachev, Y. M., & Korolev, V. N. (2013). Determination of the dimensions of the heat-affected zone in welding gas pipeline components. *Welding International*, *27*(12), 966-968.

Krishnaiah, K., & Shahabudeen, P. (2012). *Applied Experimental Design and Taguchi Method*.

Kumar, A. S., Sharma, S. K., & Shukla, A. K. (2024). Microstructural, mechanical, and thermal analysis of SS316L weldment for marine engineering application. Journal of Materials Engineering and Performance, 33(23), 13502-13515.

Kumar, A., Mohamed, C. H., & Bajpai, T. (2024). Achieving Optimal Weld Bead Geometry and Dilution Ratio in Tungsten Inert Gas–Metal Inert Gas Hybrid Welding through ANN-TLBO Algorithmic Optimization. *Journal of Materials Engineering and Performance*, 1-20.

Kumar, B. P., & Vijayakumar, Y. (2012). Optimization of shielded metal arc welding parameters for welding of pipes by using Taguchi approach. *International Journal of Engineering Science and Technology*, *4*(5), 2083-2088.

Kumar, S. N., Balasubramanian, V., Malarvizhi, S., Rahman, A. H., &Balaguru, V. (2022). Effect of welding consumables on shielded metal arc welded ultra high hard armour steel joints. *Journal of the Mechanical Behavior of Materials*, *31*(1), 8-21.

Laschke, E. (2012). The importance of material properties on the bendability of Q/QT steels.

Latifi Jr, H. (2012). Advanced orbital pipe welding.

Li, W., Cook, D., Tanaka, E., &VanderPlas, S. (2024). A plot is worth a thousand tests: Assessing residual diagnostics with the lineup protocol. *Journal of Computational and Graphical Statistics*, *33*(4), 1497-1511.

Linger, M. A., &Bogale, T. M. (2023). Parameters optimization of tungsten inert gas welding process on 304L stainless steel using grey based Taguchi method. Engineering Research Express, 5(1), 015013.

Lippold, J. C. (2014). *Welding metallurgy and weldability*. John Wiley & Sons.

Liu, H., Xue, R., Zhou, J., Bao, Y., & Xu, Y. (2023). Applying statistical models to optimize the weld bead geometry in the vertical oscillation arc narrow gap all-position GMAW. *Applied Sciences*, *13*(11), 6801.

Lugade, P. S., & Deshmukh, M. J. (2015). Optimization of process parameters of activated tungsten inert gas (A-TIG) welding for stainless steel 304L using Taguchi method. International Journal of Engineering Research and General Science, 3(3), 854-860.

Madhvacharyula, A. S., Pavan, A. V. S., Gorthi, S., Chitral, S., Venkaiah, N., & Kiran, D. V. (2022). In situ detection of welding defects: A review. *Welding in the World*, *66*(4), 611-628.

Marshall, P. W. (2013). Design of welded tubular connections: Basis and use of AWS code provisions (Vol. 37). Elsevier.

Matin, Q., Haliq, R., & Jamil, M. (2024). Analysis of Shielded Metal Arc Welding (SMAW) with Current Variations Against Tensile Strength, Bending Strength, and Microstructure of API 5L X52. *Indonesian Journal of Maritime Technology*, *2*(1).

Messler Jr, R. W. (2019). *A Practical guide to welding solutions: overcoming technical and material-specific issues*. John Wiley & Sons.

Mohammed, R., Reddy, G. M., & Rao, K. S. (2015). Microstructure and pitting corrosion of shielded metal arc welded high nitrogen stainless steel. *Defence Technology*, *11*(3), 237-243.

Moinuddin, S. Q., Hameed, S. S., Dewangan, A. K., Kumar, K. R., &Kumari, A. S. (2021). A study on weld defects classification in gas metal arc welding process using machine learning techniques. *Materials Today: Proceedings*, *43*, 623-628.

Montgomery, Douglas C. (2017). *Design and analysis of experiments*. John wiley& sons

Myers, R. H., & Montgomery, D. C. (1996). Response surface methodology.

Myers, R. H., Montgomery, D. C., & Anderson-Cook, C. M. (2016). *Response surface methodology: process and product optimization using designed experiments*. John Wiley & Sons.

Nagesh, D. S., & Datta, G. L. (2002). Prediction of weld bead geometry and penetration in shielded metal-arc welding using artificial neural networks. *Journal of materials processing technology*, *123*(2), 303-312.

Nagesh, D. S., & Datta, G. L. (2010). Genetic algorithm for optimization of welding variables for height to width ratio and application of ANN for prediction of bead geometry for TIG welding process. Applied soft computing, 10(3), 897-907.

Naik, A. B., & Reddy, A. C. (2016). An experimental investigation of shielded metal arc welding processes on duplex stainless steel to control and correction of distortion in weldments. *Int. J. Eng. Res*, *5*(2), 421-426.

Nalbant, M., Gökkaya, H., & Sur, G. (2007). Application of Taguchi method in the optimization of cutting parameters for surface roughness in turning. *Materials and Design*, *28*(4), 1379–1385. https://doi.org/10.1016/j.matdes.2006.01.008

Nath, R. K., Maji, P., Sinha, A. K., Karmakar, R., & Paul, P. (2022). Effect of different electrode angles as well as weld direction on the bead geometry of submerge arc welding process. *Materials Today: Proceedings*, *49*, 1793-1798.

O'Brien, R. W. (2007). Predicting weld distortion in the design of automotive components (Doctoral dissertation, Durham University).

Omale, J. I. (2016). *Microstructure and Mechanical properties of welds in pipeline steel* (Doctoral dissertation, University of Saskatchewan).

omashekhar, K. P., Ramachandran, N., & Mathew, J. (2010). Optimization of material removal rate in micro-EDM using artificial neural network and genetic algorithms. *Materials and Manufacturing processes*, *25*(6), 467-475.

Pagare, R., Awati, D., Mane, S., Teli, V., & Bhandare, A. (2020, December). Investigating the Effects of Welding Parameters on Mild Steel by SMAW Technique. In *IOP Conference Series: Materials Science and Engineering* (Vol. 998, No. 1, p. 012052). IOP Publishing.

Patel, D., Patel, S., Parekh, J., & Chaudhary, S. (2017). A review on Effect of different process parameters of SMAW. *Imper. J. Interdiscipl. Res.(IJIR)*, *3*(1), 1384.

Pathak, D., Singh, R. P., Gaur, S., & Balu, V. (2020). Experimental investigation of effects of welding current and electrode angle on tensile strength of shielded metal arc welded low carbon steel plates. *Materials Today: Proceedings*, *26*, 929-931.

Patil, U. S., & Kadam, M. S. (2021). Microstructural analysis of SMAW process for joining stainless steel 304 with mild steel 1018 and parametric optimization by using response surface methodology. *Materials Today: Proceedings*, *44*, 1811-1815.

Pauna, H., Willms, T., Aula, M., Echterhof, T., Huttula, M., & Fabritius, T. (2020). Electric arc length-voltage and conductivity characteristics in a pilot-scale ac electric arc furnace. *Metallurgical and materials transactions B*, *51*, 1646-1655.

Phillips, D. H. (2023). Welding engineering: an introduction. John Wiley & Sons.

Prakash, J. U., Rubi, C. S., Rajkumar, C., &Juliyana, S. J. (2021). Multi-objective drilling parameter optimization of hybrid metal matrix composites using grey relational analysis. Materials Today: Proceedings, 39, 1345-1350.

Pratiwi, D. K., Arifin, A., Gunawan, Mardhi, A., &Afriansyah. (2023). Investigation of welding parameters of dissimilar weld of SS316 and ASTM A36 joint using a grey-based Taguchi optimization approach. *Journal of Manufacturing and Materials Processing*, *7*(1), 39.

Pratiwi, D. K., Arifin, A., Gunawan, Mardhi, A., &Afriansyah. (2023). Investigation of welding parameters of dissimilar weld of SS316 and ASTM A36 joint using a grey-based Taguchi optimization approach. *Journal of Manufacturing and Materials Processing*, *7*(1), 39.

Qazi, M. I., Akhtar, R., Abas, M., Khalid, Q. S., Babar, A. R., &Pruncu, C. I. (2020). An integrated approach of GRA coupled with principal component analysis for multi-optimization of shielded metal arc welding (SMAW) process. *Materials*, *13*(16), 3457.

Qazi, M. I., Akhtar, R., Abas, M., Khalid, Q. S., Babar, A. R., &Pruncu, C. I. (2020). An integrated approach of GRA coupled with principal component analysis for multi-optimization of shielded metal arc welding (SMAW) process. *Materials*, *13*(16), 3457.

Rahangmetan, K. A., Wullur, C. W., & Sariman, F. (2020, July). Effect variations and types of Smaw welding electrodes on A36 steel to tensile test. In Journal of Physics: Conference Series (Vol. 1569, No. 3, p. 032052). IOP Publishing.

Rajesh, R., & Sumathi, S. (2020). Certain performance investigation on hybrid TiO2/Al2O3/MoS2 nanofiller coated 3Ø induction motor: a Taguchi and RSM based approach. Energy Reports, 6, 1638-1647

Ranjan, R. (2014). Parametric optimization of shielded metal arc welding processes by using factorial design approach. *International Journal of Scientific and Research Publications*, *4*(9), 1-4.

Ranjan, R., & Jha, S. K. (2024). Optimization of welding parameters and microstructure analysis of low frequency vibration assisted SMAW butt welded joints. International Journal on Interactive Design and Manufacturing (IJIDeM), 18(3), 1687-1707.

Ranjan, R., & Jha, S. K. (2024). Optimization of welding parameters and microstructure analysis of low frequency vibration assisted SMAW butt welded joints. *International Journal on Interactive Design and Manufacturing (IJIDeM), 18*(3), 1687-1707.

Ranjan, R., & Jha, S. K. (2024). Optimization of welding parameters and microstructure analysis of low frequency vibration assisted SMAW butt welded joints. *International Journal on Interactive Design and Manufacturing (IJIDeM), 18*(3), 1687-1707.

Ranjan, R., Jha, S. K., & Kumar, A. (2024). Enhancing hardness in SMAW welded joints with low-frequency vibration assistance: an experimental and analytical study. *Journal of Adhesion Science and Technology*, 1-25.

Rashid, M. S. (1980). High-strength, low-alloy steels. *Science*, *208*(4446), 862-869.

Rohit, J., & Jha, A. K. (2014). An investigating the Effect of Welding Current on the Tensile Properties of SMAW Welded Mild Steel Joints. â€ International Journal of Engineering Research & Technology. â€ Vol. 3. *Issue*, *4*, 1304-1307.

Rojas, H., Vargas, Z., Valdez, S., Serrano, M., delPozo, A., &Alcántara, M. (2024). Taguchi, Grey Relational Analysis, and ANOVA Optimization of TIG Welding Parameters to Maximize Mechanical Performance of Al-6061 T6 Alloy. Journal of Manufacturing and Materials Processing, 8(6), 246.

Sada, S. O. (2018). Optimization of weld strength properties of tungsten inert gas mild steel welds using the response surface methodology. *Nigerian journal of technology*, *37*(2), 407-415.

Sayed, A. R., Gupta, R., &Barai, R. (2019, September). Experimental investigation of C45 (AISI 1045) weldments using SMAW and GMAW. In *AIP Conference Proceedings* (Vol. 2148, No. 1). AIP Publishing.

Sharma, P., Chattopadhyaya, S., & Singh, N. K. (2019). Optimization of gas metal arc welding parameters to weld AZ31B alloy using response surface methodology. *Materials Research Express*, *6*(10), 106569.

Sharma, S. S., Kumar, M., & Ojha, P. K. (2014). Effect of Magnetic Field on Weld-Quality and Weld Geometry. *Advances in Applied Physical and Chemical Sciences-A Sustainable Approach*, 53-58.

Sheelwant, A., Jadhav, P. M., & Narala, S. K. R. (2021). ANN-GA based parametric optimization of Al-TiB2 metal matrix composite material processing technique. Materials Today Communications, 27(March), 102444. https://doi.org/10.1016/j.mtcomm.2021.102444

Sheikh, A., &Kamble, P. D. (2018). Optimization of Welding Process Parameter to Minimize Defect in Welding of Sheet. *International Research Journal of Engineering and Technology (IRJET)*, *5*(5).

Shukla, A. A., Joshi, V. S., & Shukla, B. A. (2018). Analysis of shielded metal arc welding parameter on depth of penetration on AISI 1020 plates using response surface methodology. *Procedia manufacturing*, *20*, 239-246.

Sidhu, G. S., &Chatha, S. S. (2012). Role of shielded metal arc welding consumables on pipe weld joint. *International journal of emerging technology and advanced* *engineering*, *2*(12), 746-750.

Sim, B. M., Tang, S. H., Alrifaey, M., &Tchan Jong, E. N. (2022). Analyzing the effects of heat treatment on SMAW duplex stainless steel weld overlays. *Materials*, *15*(5), 1833.

Singh, A., & Grover, N. K. (2015). Weld Properties of Low Carbon Steel Using Shielded Metal Arc Welding. Applied Mechanics and Materials, *813*, 486-490.

Singh, A., & Grover, N. K. (2015). Weld Properties of Low Carbon Steel Using Shielded Metal Arc Welding. *Applied Mechanics and Materials*, *813*, 486-490.

Singh, G., Dewangan, A. K., Khan, M. F., & Moinuddin, S. Q. (2025). Fundamental review on gas tungsten arc welding of magnesium alloys: challenges, innovations, and future perspectives. *Welding in the World*, 1-21.

Singh, H. (2014). Studies the effect of iron based hardfacing electrodes on stainless steel properties using shielded metal arc welding process. *International Journal of Research in Advent Technology*, *2*(4), 2321-2963.

Singh, P. K. (2019). Investigation on the effect of mechanical vibration in mild steel weld pool. *Manufacturing Review*, *6*, 21.

Srinivasan, P. B., Muthupandi, V., Sivan, V., Srinivasan, P. B., &Dietzel, W. (2006). Microstructure and corrosion behavior of shielded metal arc-welded dissimilar joints comprising duplex stainless steel and low alloy steel. *Journal of Materials Engineering and Performance*, *15*, 758-764.

Sumardiyanto, D., & Susilowati, S. E. (2019). Effect of welding parameters on mechanical properties of low carbon steel API 5L shielded metal arc welds. *American Journal of Materials Science*, *9*(1), 15-21.

Sumardiyanto, D., & Susilowati, S. E. (2019). Effect of welding parameters on mechanical properties of low carbon steel API 5L shielded metal arc welds. *American Journal of Materials Science*, *9*(1), 15-21.

Sunny, P., & Muhammed, A. (2023). An Experimental Investigation On Weld Characteristics For A Shield Metal Arc Welding With SS304 & SS409.

Tahir, A. M., Lair, N. A. M., & Wei, F. J. (2018, May). Investigation on mechanical properties of welded material under different types of welding filler (shielded metal arc welding). In *AIP conference proceedings* (Vol. 1958, No. 1). AIP Publishing.

Talabi, S. I., Owolabi, O. B., Adebisi, J. A., & Yahaya, T. (2014). Effect of welding variables on mechanical properties of low carbon steel welded joint. *Advances in Production Engineering & Management*, *9*(4), 181-186.

Trahair, N. S., Bradford, M. A., Nethercot, D., & Gardner, L. (2017). *The behaviour and* *design of steel structures to EC3*. CRC Press.

Tran, N. H., Nguyen, V. N., & Bui, V. H. (2023). Development of a virtual reality-based system for simulating welding processes. *Applied Sciences*, *13*(10), 6082.

Van Huong, H., Nguyen, T. T., Nguyen, V. T., & Nguyen, V. T. T. (2024). Material Strength Optimization of Dissimilar MIG Welding between Carbon and Stainless Steels. *Metals*, *14*(9), 1011.

Verma, J., &Taiwade, R. V. (2024). Welding Scope, Application, and Opportunities. *Advanced Welding Techniques*, 1-21.

Vieira, E. D. R., Biehl, L. V., Medeiros, J. L. B., Costa, V. M., & Macedo, R. J. (2021). Evaluation of the characteristics of an AISI 1045 steel quenched in different concentration of polymer solutions of polyvinylpyrrolidone. *Scientific Reports*, *11*(1), 1313.

Wahab, M. A. (2014). Manual metal arc welding and gas metal arc welding. *Comprehensive Materials Processing: Thirteen Volume Set*, *6*, V6.

Welding, G. T. A. (1991). American Welding Society. *Welding Handbook*, *8th*.

Widyianto, A., Baskoro, A. S., Kiswanto, G., &Ganeswara, M. F. G. (2021). Effect of welding sequence and welding current on distortion, mechanical properties and metallurgical observations of orbital pipe welding on SS 316L. *Eastern-European Journal of Enterprise Technologies*, *2*(12), 110.

Yaacob, R. M., Zikri, J. M., Abdullah, N. A. Z., M Sani, M. S., Abdul Rani, M. N., &Arbintarso, E. S. (2024). Optimization of spot weld joining parameters for dissimilar plate materials through finite element model updating and response surface methodology. *Journal of Mechanical Engineering (JMechE)*, *13*(1), 135-156.

Yodianto, F. (2023). Analysis Of Welding Defects and Bending Strength in ASTM A36 Steel Materials E7018 Electrodes. *InovtekPolbeng*, *13*(2), 113-126.

Yu, J., & Kim, D. (2018). Effects of welding current and torch position parameters on minimizing the weld porosity of zinc-coated steel. *The International Journal of Advanced Manufacturing Technology*, *95*, 551-567.

Yurioka, N. (2001). Physical metallurgy of steel weldability. *ISIJ international*, *41*(6), 566-570.

Zaman, U. K. U., Boesch, E., Siadat, A., Rivette, M., &Baqai, A. A. (2019). Impact of fused deposition modeling (FDM) process parameters on strength of built parts using Taguchi's design of experiments. *The international journal of Advanced Manufacturing technology*, *101*, 1215-1226.

Zaman, U. K. U., Khan, U. A., Aziz, S., Baqai, A. A., Butt, S. U., Hussain, D., ... & Jung, D. W. (2022). Optimization of wire electric discharge machining (WEDM) process parameters for AISI 1045 medium carbon steel using taguchi design of experiments. *Materials*, *15*(21), 7846.

Zhao, H., Zhang, S., Yu, X., Li, Y., Miao, J., Xu, X., & Chang, Y. (2025). Study on arc behavior and weld formation of magnetically controlled narrow gap TIG welding. *International Journal of Precision Engineering and Manufacturing*, *26*(3), 651-662.

Zhou, Y., Gorman, P., Tan, W., & Ely, K. J. (2000). Weldability of thin sheet metals during small-scale resistance spot welding using an alternating-current power supply. *Journal of electronic materials*, *29*, 1090-1099

Zoalfakar, S. H., & Hassan, A. A. (2017). Analysis and optimization of shielded metal arc welding parameters on mechanical properties of carbon steel joints by Taguchi method. *International Journal of Advanced Engineering and Global Technology*, *5*(1), 1431-1444.